

A STUDY ON THE USE OF GEOPOLYMER COMPOSITES  
FOR NITROGEN AND PHOSPHORUS REMOVAL  
FROM POULTRY LITTER

By

GIZEM GUL TOPAL

Bachelor of Science in Environmental Engineering  
Middle East Technical University  
Ankara, Turkey  
2014

Submitted to the Faculty of the  
Graduate College of the  
Oklahoma State University  
in partial fulfillment of  
the requirements for  
the Degree of  
MASTER OF SCIENCE  
December, 2020

A STUDY ON THE USE OF GEOPOLYMER COMPOSITES  
FOR NITROGEN AND PHOSPHORUS REMOVAL  
FROM POULTRY LITTER

Thesis Approved:

Dr. Pankaj Sarin

---

Thesis Adviser

Dr. Raman P. Singh

---

Dr. Mark Krzmarzick

---

## ACKNOWLEDGEMENTS

This journey would not have been possible without the support of many people. To my dear mother and my brother, your presence is my blessing, and thank you for everything you have done to make my dreams possible. My dear cousins, Ilgu Ozler and Ozge Topal, I am so lucky to have you in my life and I can't thank you enough for your support and encouragement.

I owe my finest gratitude and appreciation to my advisor, Dr. Pankaj Sarin, who guided me through my graduate education. I am grateful for the opportunity to join his research group and have my Master's in Materials Science and Engineering at Oklahoma State University. This work would not have been accomplished without his guidance and endless support. His patience and valuable mentorship taught me how to approach difficulties I've faced during my work which shaped me into a better researcher and for that, I will always be grateful.

I would like to extend my thanks to my committee members, Dr. Raman P. Singh and Dr. Mark Krzmarzick, thank you for helping guide me through this experience.

To my friends and colleagues in the Helmerich Research Center for their kindness, help and friendship. To Dr. Sarin's research group members, Christine, Rohit and Stephen, this has been a great experience because of your friendship, thanks for making me laugh all the time.

This research was supported by the College of Engineering, Architecture and Technology (CEAT) at Oklahoma State University under the CEAT Dean's Grand Challenges of Engineering Initiative. The facilities at the Helmerich Research Center, Oklahoma State University at Tulsa were used for the reported studies.

Name: GIZEM GUL TOPAL

Date of Degree: DECEMBER, 2020

Title of Study: A STUDY ON THE USE OF GEOPOLYMER COMPOSITES FOR NITROGEN AND PHOSPHORUS REMOVAL FROM POULTRY LITTER

Major Field: MATERIALS SCIENCE AND ENGINEERING

**Abstract:** With the growing world population, animal agriculture demand in the following years will increase substantially to meet nutritional needs for humankind. An inevitable increase in demand is strongly interconnected with the meat production industry. Meeting the need creates a paradox for not bringing further stress on the environment where natural resources.

The poultry industry is one of the major meat production branches for the meat industry and Oklahoma is one of the biggest poultry contributors of the United States. Nonjudicious disposal of chicken litter or use as manure can result in leaching of nitrates and phosphates causing contamination in aquifers, a primary source of clean water. Current practices of waste management are not feasible in the long term while they majorly depend on disposal. Harvesting the waste through engineered materials and treatment on-site without additional costs is necessary to take this problem under control.

Adsorbent materials offer answers to this problem by their ion-selective structure. Their performance depends on environmental conditions and majorly on the exchangeable ions in their structure. Although most adsorbent materials are applicable for nutrient control, there are still limitations to full-scale waste management. Geopolymers, non-crystalline aluminosilicate materials on the other hand promise several advantages, including higher nutrient removal capacity, their low-cost requirements and most importantly their high adaptation into diverse applications. Hence, their promise is considered valuable for waste management.

This study is a beginning effort on developing geopolymer composites for nutrient removal in complex environmental systems like poultry houses. Composites were processed using geopolymer as binder phase and natural zeolites and metal oxides powders as additives to increase nutrient removal capacity and nutrient uptake speed of the adsorbent products. Geopolymer composites are characterized by their microstructural and mechanical properties. Adsorbent performances are evaluated for their nutrient removal efficiencies from model solutions. In addition to their use in simultaneous nutrient removal was investigated to observe matrix effects created by the environment. This study provides a proof of concept on the development of novel geopolymer composites as adsorbents.



## TABLE OF CONTENTS

Chapter	Page
I. MOTIVATION.....	1
1.1.Poultry Industry .....	2
1.2.Waste Management in Poultry Farming .....	3
1.2.1. Current Practices and Environmental Impacts .....	7
1.2.2. Nutrient Content and Environmental Impacts of Poultry Litter .....	8
1.3.Adsorbents for Nitrogen and Phosphorus Removal.....	10
1.4.Geopolymers.....	14
1.5.Opportunities for Geopolymer Based Adsorbents for Poultry Farming.....	16
II.OBJECTIVES .....	18
III.MATERIALS AND METHODS.....	20
3.1.Materials .....	20
3.1.1.Geopolymer.....	21
3.1.2.Clinoptilolite .....	23
3.1.3.Magnesium Oxide (MgO).....	25
3.2.Processing .....	26
3.3.Materials Characterization and Analytical Methods.....	30
3.3.1.Microscopy .....	30

Chapter	Page
3.3.2. Analytical Chemistry methods.....	34
3.3.3. Macroscopic Testing.....	37
3.3.4. Mechanical Testing.....	41
IV. PHYSICOCHEMICAL ANALYSIS OF VIRGIN ADSORBENTS .....	43
4.1. Microstructural and mechanical properties of geopolymer composites .....	44
4.1.1. Mechanical strength.....	45
4.1.2. Optical microscopy .....	49
4.1.3. Density – Pycnometry.....	51
4.1.4. Porosity and Permeability .....	53
4.1.5. Scanning Electron Microscopy (SEM) .....	59
4.2. Elemental Composition.....	62
4.2.1. Wavelength Dispersive X-Ray Fluorescence (WDXRF) .....	62
4.3. Summary.....	64
V. AMMONIUM REMOVAL BY PURE GEOPOLYMER AND CLINOPTILOLITE- GEOPOLYMER COMPOSITES .....	66
5.1. Composite Processing.....	68
5.2. Model Solutions .....	68
5.3. Batch Adsorption Study.....	68
5.4. pH Evolution.....	70
5.5. Ammonium Removal.....	73
5.6. Summary.....	83

Chapter	Page
VI.PHOSPHORUS SEQUESTRATION BY PURE GEOPOLYMER AND CLINOPTILOLITE-GEOPOLYMER COMPOSITES.....	85
6.1.Model Solutions.....	87
6.2.Batch Adsorption Study.....	87
6.3.pH Evolution.....	88
6.4.Phosphorus Removal.....	90
6.5.Summary.....	100
VII.SIMULTANEOUS SEQUESTRATION OF NUTRIENTS BY PURE GEOPOLYMER AND GEOPOLYMER COMPOSITES.....	101
7.1.Model Solutions.....	103
7.2.Batch Adsorption Study.....	103
7.3.pH Evolution.....	104
7.4.Nitrogen and Phosphate removal.....	105
7.5.Summary.....	127
VIII. CONCLUSIONS AND FUTURE WORK.....	129
8.1. Conclusions.....	130
8.2. Future Work.....	132
REFERENCES.....	134
APPENDICES.....	144
APPENDIX A.....	144
APPENDIX B.....	148
APPENDIX C.....	152

## LIST OF TABLES

Table	Page
1. 1. Nutrient content of poultry litter on an as-is basis .....	10
1. 2. Ammonium removal technologies and efficiencies.[24]–[29] .....	12
1. 3. Phosphorus removal technologies and efficiencies. ....	13
3. 1. Poly(sialate-siloxo) networks constitutes geopolymers[48] .....	22
3. 2. Chemical analysis of commercial zeolite .....	25
3. 3. Chemical composition and Physical properties of MgO powder .....	26
4. 1. Compressive strength test results from cylindrical geopolymer samples .....	48
4. 2. Data retrieved from AccuPyc II runs for the absolute density of virgin adsorbents and raw materials (*) .....	52
4. 3. BET surface area values of virgin samples .....	55
4. 4. Porosity and permeability results obtained from mercury intrusion porosimetry experiments .....	58
4. 5. Elemental composition of geopolymer adsorbents measured by WDXRF .....	63
5. 1. Mass of adsorbents used in each replicate of batch adsorption study .....	73
5. 2. Average ammonium nitrogen removal from model solutions by percentage .....	76
6. 1. Mass of adsorbents used in each replicate of batch adsorption study .....	91
6. 2. Average phosphorus removal from model solutions by percentage .....	93

Table	Page
6. 3. Normalized elemental composition obtained from EDS mapping of selected area.	99
7. 1. Mass of adsorbent used in batch adsorption studies on phosphate removal.....	106
7. 2. Average ammonium nitrogen and phosphate removal from model solutions by percentage. ....	109
7. 3. AutoID results of overall EDS map analysis and normalized values for elemental distribution. ....	118
7. 4. AutoID results of overall EDS map analysis of CGP5, normalized values for elemental distribution .....	121
7. 5. Normalized elemental distribution for Spectrum 1 point on CGP5.....	121
7. 6. Map spectrum results of CGP20, normalized values for elemental distribution ....	124
C. 1. Water quality testing results for pure geopolymer on phosphorus removal .....	153
C. 2. Water quality testing results for pure geopolymer on nitrogen removal.....	154
C. 3. Water quality testing results of CPG5 on nitrogen removal. ....	155
C. 4. Water quality testing results for CGP10 on nitrogen removal .....	156
C. 5. Water quality testing results for CGP15 on nitrogen removal .....	157
C. 6. Water quality testing results for CGP20 on nitrogen removal .....	158
C. 7. Water quality testing results for CGP5 on phosphorus removal.....	159
C. 8. Water quality testing results for CGP20 on phosphorus removal .....	160
C. 9. Water quality testing results for pure geopolymer on simultaneous removal of nitrogen and phosphorus .....	161
C. 10. Water quality testing results for CGP5 on simultaneous removal of nitrogen and phosphorus .....	162

Table	Page
C. 11. Water quality testing results for CGP20 on simultaneous removal of nitrogen and phosphorus .....	163
C. 12. Water quality testing results for MGP5 on simultaneous removal of nitrogen and phosphorus .....	164

## LIST OF FIGURES

Figure	Page
1. 1. Waste handling and utilization flow scheme in poultry farming .....	4
1. 2. Uncontrolled waste pathways in a poultry farming facility.....	6
3. 1. Schematics of geopolymerization reaction .....	22
3. 2. Steps involved in geopolymer and geopolymer composite processing .....	28
3. 3. Molding geopolymer slurry into half-inch diameter spheres.....	29
3. 4. Carl Zeiss' AxioLab A1 Modular, upright Optical Microscope for Materials Science (Carl Zeiss Microscopy, LLC, White Plains, NY).....	31
3. 5. Hitachi S-4800 field emission scanning electron microscope (FE-SEM) coupled with an Oxford Instruments (Tubney Woods, Abingdon, Oxon, UK) energy dispersive spectroscopy (EDS) silicon drift detector. ....	32
3. 6. Rigaku Primus IV Wavelength Dispersive X-ray Fluorescence (WDXRF) spectrometer (Rigaku, Tokyo, Japan) in the Helmerich Research Center, Core Laboratories .....	33
3. 7. SevenCompact pH meter S220 used for pH and ionic strength measurements.....	34

Figure	Page
3. 8. Oakton Con 700 Total Dissolved Solid (TDS) meter (Oakton Instruments, Vernon Hills, IL).....	36
3. 9. Hach DR4000 UV-Visible Spectrometer (HACH, Loveland, CO).....	37
3. 10. Gas displacement pycnometry system, AccuPyc II 1340 (Micromeritics, Atlanta, GA) .....	38
3. 11. 3 Flex Surface Characterization Analyzer (Micromeritics, Norcross, GA).....	40
3. 12. Autopore V, Mercury Intrusion Porosimetry (MIP) (Micromeritics, Norcross, GA) .....	41
3. 13. Instron 5582 Universal Testing System.....	42
4. 1. Cylindrical and ball shaped samples presented together .....	46
4. 2. Schematic of Typical Fracture Patterns according to ASTM standard C39/C39M-18 .....	47
4. 3. Compressive test performed on cylindrical geopolymer samples, Type 3 fracture is observed on failed samples. ....	48
4. 4. Pure geopolymer (a), MgO incorporated geopolymer (MGP5) (b), Clinoptilolite incorporated geopolymer given increasing order of additive in terms of volume percentage, CGP5 (a), CGP10 (b), CGP15 (c) and CGP20 (d) .....	50
4. 5. Comparison of cumulative pore volume ( $\text{cm}^3/\text{g}$ ) and pore radius ( $\text{\AA}$ ) for all geopolymer types.....	56
4. 6. Cumulative pore area ( $\text{cm}^3/\text{g} \cdot \text{\AA}$ ) and pore radius ( $\text{\AA}$ ) comparison for all geopolymer types .....	56



Figure	Page
4. 7. Incremental intrusion (mL/g) and Pore Diameter (Å) comparison for all composite types.....	57
4. 8. (a) Clinoptilolite at low magnification, (b) Clinoptilolite at x25k.....	60
4. 9. Metakaolin powder x20k (left) and x45k (right) .....	61
4. 10. SEM image of pure geopolymer taken at x25.0k, 15.0kV.....	61
5. 1. Agitator setup of six having triplicate solutions of each batch adsorption test. Two sets of adsorption experiments can be run at the same time. (Velp Scientifica, Bohemia, NY) .....	67
5. 2. Change of pH over time when pure geopolymer soaked in DI water for 8 hours. ....	71
5. 3. Change in pH over time when CGP composite is soaked in DI water for 8 hours... ..	72
5. 4. Change in pH over time when CGP composite is used as an adsorbent in model solutions with nitrogen.....	72
5. 5. Remaining nitrogen concentration in all studies performed by CGP and PGP (top), by CGP composites only (bottom).....	74
5. 6. Percent removal of nitrogen in model solutions over time. ....	77
5. 7. Sampling points in linescan of PGP before and after the experiment (top), nitrogen presence in PGP before and after nitrogen removal study (bottom).....	79
5. 8. Sampling points in linescan of CGP5 before and after the experiment (top), nitrogen presence in CGP5 before and after nitrogen removal study (bottom) .....	80
5. 9. Sampling points in linescan of CGP10 before and after the experiment (top), nitrogen presence in CGP10 before and after nitrogen removal study (bottom) .....	81

Figure	Page
5. 10. Sampling points in linescan of CGP20 before and after the experiment (top), nitrogen presence in CGP20 before and after nitrogen removal study (bottom) .....	82
6. 1. Change in pH over time when test composites are soaked in DI for 8 hours. ....	89
6. 2. Change in pH over time when PGP, CGP5 and CGP 20 composites are used as an adsorbent in model solutions with phosphorus.....	90
6. 3. Remaining phosphorus concentration in all studies performed by PGP, CGP5 and CGP20.....	92
6. 4. Remaining phosphorus concentration studies performed by CGP5 and CGP20.....	92
6. 5. Percent removal of nitrogen in model solutions over time. ....	94
6. 6. Sampling points in linescan of PGP before and after the experiment (top), phosphorus presence in PGP before and after phosphorus removal study (bottom).....	95
6. 7. Sampling points in linescan of CGP5 before and after the experiment (top), phosphorus presence in CGP5 before and after phosphorus removal study (bottom).....	96
6. 8. Sampling points in linescan of CGP20 before and after the experiment (top), phosphorus presence in CGP20 before and after phosphorus removal study (bottom)....	97
6. 9. Pure geopolymer image captured at x1.0k magnification (right) and major elements reported by EDS mapping auto identification. ....	98
7. 1. pH evolution over time with geopolymer composites used in simultaneous nutrient removal studies .....	105
7. 2. Phosphorus (top) and nitrogen (bottom) concentrations remaining in model solutions over time .....	108

Figure	Page
7. 3. Ammonium and phosphate removal amounts from model solutions. ....	110
7. 4. Sampling points in linescan of PGP before and after the experiment (top), nitrogen and phosphorus presence in PGP before and after phosphorus removal study (bottom)	111
7. 5. Sampling points in linescan of CGP5 before and after the experiment (top), nitrogen and phosphorus presence in CGP5 before and after phosphorus removal study (bottom) .....	112
7. 6. Sampling points in linescan of CGP20 before and after the experiment (top), nitrogen and phosphorus presence in CGP20 before and after phosphorus removal study (bottom) .....	113
7. 7. Sampling points in linescan of MGP5 before and after the experiment (top), nitrogen and phosphorus presence in MGP5 before and after phosphorus removal study (bottom) .....	114
7. 8. Layered EDS image showing P, Al and Si distribution in PGP after simultaneous removal .....	115
7. 9. Layered EDS image showing nitrogen distribution in PGP after simultaneous removal .....	116
7. 10. Line Scan performed on PGP after simultaneous study, Al, Si, P and N from the surface (right) to inner structure (left) .....	117
7. 11. EDS image of CGP5 and scanned the area with selected line scans in CGP5 after simultaneous removal .....	119
7. 12. Line Scan performed on CGP5 after simultaneous study, Al, Si, P and N from the surface (right) to inner structure (left) .....	120

Figure	Page
7. 13. EDS image of CGP20 and scanned area with selected line scans in CGP5 after simultaneous removal .....	122
7. 14. Line Scan performed on CGP20 after simultaneous study, Al, Si, P and N from the surface (left) to inner structure (right) .....	123
7. 15. EDS image of MGP5 and scanned area with selected line scans in CGP5 after simultaneous removal .....	125
7. 16. EDS image layers showing Al, Si, Mg, N, P and K distribution in MGP5 after simultaneous removal. ....	125
7. 17. Line Scan performed on MGP5 after simultaneous study, Al, Si, Mg, P and N from the surface (right) to inner structure (left).....	126
A. 1. Compressive strength and strain diagram of pure geopolymer samples. Testing repeated three times with three separate samples. Compressive strength reported as 37.84 MPa at maximum and average is reported as 27.63 MPa.....	145
A. 2. Compressive strength and strain diagram of clinoptilolite-geopolymer composite samples with 5% clinoptilolite by volume. Testing repeated three times with three separate samples with compressive strength reported as 55.73 MPa at maximum and average is reported as 47.96 MPa .....	145
A. 3. Compressive strength and strain diagram of clinoptilolite-geopolymer composite samples with 10% clinoptilolite by volume. Testing repeated three times with three separate samples with compressive strength reported as 104.96 MPa at maximum and average is reported as 66.36 MPa .....	146

Figure	Page
A. 4. Compressive strength and strain diagram of clinoptilolite-geopolymer composite samples with 15% clinoptilolite by volume. Testing repeated three times with three separate samples with compressive strength reported as 30.52 MPa at maximum and average is reported as 28.54 MPa .....	146
A. 5. Compressive strength and strain diagram of clinoptilolite-geopolymer composite samples with 20% clinoptilolite by volume. Testing repeated three times with three separate samples with compressive strength reported as 20.46 MPa at maximum and average is reported as 14.19 MPa .....	147
A. 6. Compressive strength and strain diagram of clinoptilolite-geopolymer composite samples with 5% MgO by volume. Testing repeated three times with three separate samples with compressive strength reported as 39.69 MPa at maximum and average is reported as 32.23 MPa.....	147
B. 1. Cumulative adsorption graph of corresponding geopolymer composites obtained by gas adsorption (BJH analysis for pore size and volume distribution) .....	149
B. 2. Cumulative desorption graph of corresponding geopolymer composites obtained by gas adsorption (BJH analysis for pore size and volume distribution) .....	149
B. 3. Cumulative adsorption graph of corresponding geopolymer composites obtained by gas adsorption (BJH analysis for pore size and volume distribution) .....	150
B. 4. Cumulative desorption graph of corresponding geopolymer composites obtained by gas adsorption (BJH analysis for pore size and volume distribution) .....	150

Figure	Page
B. 5. Pore area corresponding to pore radius obtained by gas adsorption for geopolymer and geopolymer composites.....	151

## **CHAPTER I**

### **MOTIVATION**

With the growing world population, animal agriculture demand in the following years will increase substantially in order to meet the nutritional needs of humankind. An inevitable increase in demand is strongly interconnected with the meat production industry. Meeting the need creates a paradox of not bringing further stress on the environment where natural resources will be vastly used.

The extent of physical resources exploited leads natural food, energy and water (FEW) systems to go under stress unavoidably. [1] The poultry industry is one of the most localized translations of this problem in southern states of the US, affecting natural water systems in particular by non-point nutrient pollution. As a consequence of the lack of handling poultry litter, the mechanism that sparks the problem is mainly the excess discharge of nutrients such as nitrogen and phosphorus. This research is focused on handling this issue by developing materials that are easy to fabricate as well as easy to be disposed of without causing further damage to environmental systems they are in.

## **1.1.Poultry Industry**

In the United States, poultry production is the biggest contributor to the overall livestock industry. According to the North American Meat Institute, in 2017 there are 9 billion chickens produced which corresponds to 95% of the total meat production in the US with respect to 9.4 billion animals produced in total.[2]

Oklahoma is one of the biggest contributors to the poultry industry in the states, ranking eleventh in the nation for chicken production.[3] Poultry review report published by United States Department of Agriculture (USDA) including 2017 and 2018 data for all poultry types including production, eggs and slaughter shows that 2018 broiler production in Oklahoma decreased by 8 million with respect to numbers published in 2017, ended having 197 million head produced corresponding \$773 million market value. Chicken excluding broilers ended the 2018 marketing year with \$33.6 million.[4]–[6] Total value for the poultry industry (broilers, turkeys, chickens and eggs) reported as \$46 billion.[6] The Poultry Federation summarized statistics published by the National Agricultural Statistics Service (NASS) of the USDA in Oklahoma in 2020 as;

- The broiler industry in Oklahoma creates approximately twenty-five thousand jobs
- The industry made about \$6 billion in total economic activity
- Total of 700 million eggs produced valued at \$82 million
- There are over 77,000 farms in Oklahoma, having %13.5 of them related to poultry.[3] (Numbers are based on the Census of Agriculture conducted every 5 years)



Although data being very localized and a small fraction of the overall state, the poultry industry is an ever-growing branch of animal agriculture that is in great balance with economic growth and supplying the demand of people. Moreover, it is adding nutritional quality and diversity to the human diet as well as converting some plant materials that are not preferred by humans into consumables. On the other hand, the impact of global food production on natural systems cannot be underestimated.[7], [8] Stressors on natural resources caused by the poultry industry are explained further in the following chapters.

## **1.2.Waste Management in Poultry Farming**

As reviewed in the previous section, poultry production is a major contributor to animal agriculture and showing a great increase every year despite its widespread negative effects on natural systems.

Raising chickens, ducks, turkeys for their meat and egg production capabilities is the gross content of poultry production. Poultry litter is defined as the materials used for bedding including sawdust, wood shavings, rice hulls, etc. Manure is also mixed in bedding material during production, therefore the waste that is being handled is the mixture of these two. [9], [10] Hence, it is appropriate to use “poultry litter” when defining the major waste material of the poultry industry.

Although manure constituents (nitrogen, phosphorus and organic matter) are known to provide natural fertilizer and increase the quality of soil, it affects air and water quality unless they are managed properly. [10] Production, collection, transfer are the first three keys of poultry production. Storage, treatment and utilization are secondary steps of waste

handling [11], [12]. According to this flow; the ideal design of poultry housing, manure handling and storage/disposal practices adopted in the US is illustrated in Figure 1. 1.

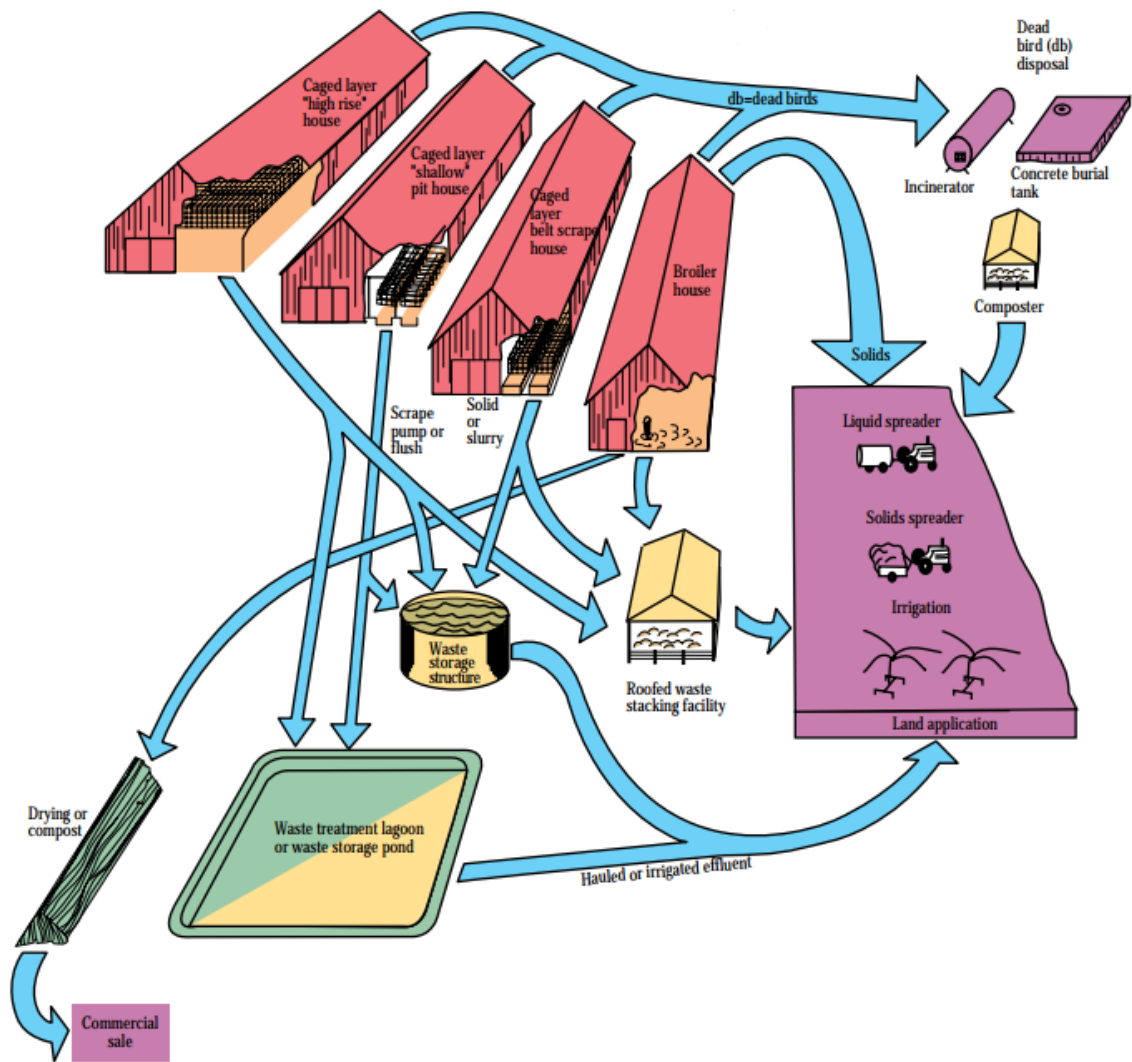


Figure 1. 1. Waste handling and utilization flow scheme in poultry farming (Image is adapted from [12])

In ideal practices, waste is characterized and collected in separate lines as solid and liquid/slurry manure. Solid manure is handled by mechanical scrapers. On the other hand, liquid and slurry manure is usually handled by pumping or by flushing it with water. Besides handling the waste by the content, collection interval varies by the type and the operation of poultry houses. It can be daily or weekly flushing, 20 minutes once a day being the most common means of operation and it is sent to storage lagoons or anaerobic treatment tanks when available.[13] Solid manure is usually handled once a year by simply scraping and directly applying to the land. Waste being handled is recorded to be;

- Used in livestock feeding
- Soil amendment
- Applied as fertilizer
- Used in bioenergy production
- Recycled as bedding material

The main problem of handling the waste is that a small portion of it is treated before it is used for land application, biogas production and composting for alternative uses. How it is being handled in terms of disposal methods of manure is affecting water, soil and air systems directly and indirectly. Eutrophication is one of the most concerning impacts on freshwater bodies where excess plant growth and oxygen depletion takes place with nutrient enrichment. It can result in algal blooms, mass fish kills, taste and odor problems. Air pollution is a considerable part of pollution created by poultry farming where dust arises from manure, feed, feathers. Also, liquid aerosols contribute since they are arising from bird respiration, high-pressure washing of buildings.

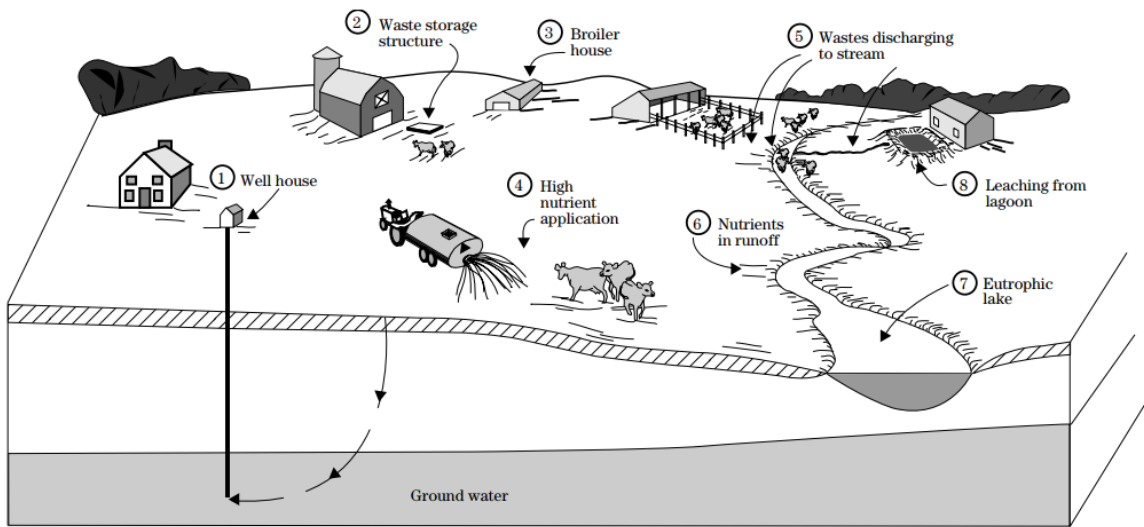


Figure 1. 2. Uncontrolled waste pathways in a poultry farming facility. [14]

The amount and scale of pollution depend on the type of poultry farming and waste handling methods. In Figure 1. 2 all possible ways of environmental pollution caused by poultry farming can be observed. Those highlighted points of contamination can be summarized as,

- Well water can be contaminated by bacteria and nitrates leaching
- Explosive gases can accumulate in storage houses
- Ammonia gas accumulation can take place in poorly ventilated poultry houses and harm the animals.
- The waste application can easily elevate nitrate toxicity, therefore leaching of  $\text{NO}_3$  and microorganisms
- Discharging lagoon is an open source for leaching of nutrients; depending on the location it can create creating toxic conditions for fish in terms of  $\text{NH}_3$  production, organic matter content in waste leads to low dissolved oxygen levels

Runoff and leaching of nutrients is always the main threat for contamination where it can be caused by land application, poultry housing, discharging lagoons and other direct and indirect contributions. [14]

Great care has to be taken when deciding how much of the manure should be applied to the land because of these concerns. However great care of waste comes with a price; requires higher initial cost due to making the farm leach proof, construction costs for waste handling facilities, need for larger land to govern those facilities, ventilation installment for poultry houses. Besides, the nitrogen and phosphorus need of the plants should be the main indicator of the amount of fertilizer applied. [10], [15]

### **1.2.1. Current Practices and Environmental Impacts**

The poultry industry is a great contributor to Oklahoma's economy despite the questions and concerns being raised related to its contribution to environmental issues that increased over the years. Save the Illinois Watershed, a non-profit organization is engaged specifically for the preservation of the upper and lower Illinois river, remarking the importance of non-point nutrient pollution caused by excess nutrient runoff caused by concentrated poultry farming in Oklahoma and Arkansas. They are very engaged in the problem-solving process and have been active since the early 1980s. Over the years they held an important role in decision making for Oklahoma water regulators to take action on water quality monitoring. [16] In the spring of 1998, the Oklahoma legislature passed Oklahoma Registered Poultry Feeding Operations Act followed by the Oklahoma Poultry Waste Applicators Certification Act. According to those, individuals applying more than

10 tons of poultry waste per year are subject to taking necessary measures when making land applications. [17]

Most current and resounding problems emerged from the poultry industry are taken place in eastern Oklahoma. Although The Oklahoma Department of Agriculture, Food and Forestry is tracking the number of licensed chicken farms and new legislations are being discussed, nuisance caused by farming activities is not likely to decrease. Concerns about air and water pollution are reported by locals. Also, the smell caused by farming along with the sound of fans and increased dust content cannot be overlooked. [16], [18] Following sections will focus on nutrient types of concern arising from uncontrolled poultry litter management.

### **1.2.2. Nutrient Content and Environmental Impacts of Poultry Litter**

Waste material is named poultry litter and it contains essential plant nutrients used by plants. These nutrients are considered to be originated from the feed, medication, water used by chicken, supplements, etc. Nitrogen, phosphorus, potassium, calcium, sulfur, manganese, copper, zinc, chlorine, iron is known to be some of these nutrients. In most cases, litter is used as fertilizer which can be a great potential in indirect pollution source that is emerged by stormwater runoff.

Of all nutrients mentioned, nitrogen and phosphorus have significant importance due to their various effects on the environment. Despite their necessity for plant growth, they hold an important role due to their negative impact on surface water when they exceed environmentally tolerable limits.

Inorganic forms of nitrogen are readily available for plant uptake (approximately 14%) where this number varies around 10% (corresponds to almost all inorganic forms of phosphorus) for phosphorus upon mineralization. [17] Besides plant uptake and manure's potential use in the environment, it has to be taken into consideration that with some pathways excess nutrients can harm environmental systems. Those pathways can be listed as; solution/suspension, sorption onto soil particles and particulate forms of the pollutants. Solution/suspension is a path that has mostly organic nitrogen, soluble phosphorus, nitrate ( $\text{NO}_3$ ) and ammonium ( $\text{NH}_4$ ). Sorption of ammonium and P may soil particles can be followed by erosion where transport in particulate form is also possible for organic N and P. [9], [19], [20]. Recalling that, excess nitrogen and phosphorus are linked closely to eutrophication,  $\text{NO}_3$  can be harmful to both humans and animals, also  $\text{NH}_3$  being toxic to aquatic life, necessary measures have to be taken to prevent uncontrolled disposal of manure.

Table 1. 1. Nutrient content of poultry litter on an as-is basis

<b>Pollutant</b>	<b>Mean Weight (g/kg)</b>
<b>pH</b>	5.6-9.4
<b>Total N</b>	17-72
<b>NH<sub>4</sub>-N</b>	0.1-30
<b>NO<sub>3</sub>-N</b>	0.03-1.5
<b>Total P</b>	0.15-34
<b>P</b>	15
<b>P<sub>2</sub>O<sub>5</sub></b>	26.5 - 36
<b>K</b>	25
<b>K<sub>2</sub>O</b>	30
<b>Total Ca</b>	25
<b>Total C</b>	252
<b>WEP10</b>	0.95

*\*Values gathered from analyses based on both as-is (wet) and dry basis [9], [10], [15], [16], [21], [22]*

### 1.3. Adsorbents for Nitrogen and Phosphorus Removal

Selective ion exchange is a physical process that provides an alternative to biological treatment systems. If waste material is not conveyed and handled in a waste treatment facility, ion exchanger materials, named as adsorbents, are the most feasible options. They provide on-site treatment of the waste, doesn't require transportation costs also they don't require a large land. Also, poultry farms are not following a full waste treatment practice. Waste is handled on-site which means on-site treatment is the most cost-effective option in these terms. For this reason, selective ion exchange is offering a cost-effective, easy operation option.



Nitrogen control through adsorbents usually takes place by the exchange of ammonium ( $\text{NH}_4^+$ ), an exchangeable cation. The potential use of nitrogen removing adsorbents as fertilizers is making ion exchange technologies more interesting. Similarly, there is a wide range of methods and technologies for phosphorus removal from water. These methods usually include chemical processes to remove phosphorus as a precipitate.[23] Ion exchangers for phosphorus removal is an area that has been researched, however, it has not come to a breakthrough as other technologies that are very effective on phosphorus removal. Its ability to precipitate with ammonium ions on the other hand is a promising way of handling waste streams and recovery of these nutrients together for future use. Removal efficiencies and methods for nitrogen and phosphorus removal are summarized in Table 1. 2 and Table 1. 3. Listed methods are predominantly used in water and wastewater treatment facilities which often require initial installation investments, and usually require wastewater to be conveyed to treatment facilities. Ion exchangers and adsorbents, on the other hand, offer on-site treatment practices that will be effective on poultry litter handling.

Table 1. 2. Ammonium removal technologies and efficiencies.[24]–[29]

Removal/Recovery Technology	Materials	Removal Efficiency	Advantages	Disadvantages
Ion exchange / Adsorption by natural zeolites	Natural Zeolites: Zeolite, clinoptilolite, Mordenite, Chabazite, Mesolite	Ranges for each zeolite type, contact time, dosed concentration and pH ( 55 - 97 %)	Easy operation, Low cost, low TDS yield	Fails at lower pH
Ion exchange / Adsorption by synthetic zeolites	Synthetic Zeolites: NaCl modified zeolite, NaCl modified clinoptilolite, MgO modified zeolite, Geopolymer, magnetic zeolite.	75 - 100 %		
Ion exchange / Adsorption by synthetic zeolites by polymeric ion exchangers	Dowex, Purolite C160H, Amberjet 1200 Na	70 – 96.4 %		
Ion exchange / Adsorption by carbon-based adsorbents.	Combination of powdered activated carbon (PAC) and powdered zeolite, organic acid modified AC, Na+ impregnated AC, peanut shells, rusk husk biochar, multiwall carbon nanotube	30 – 97 %		
Ion exchange / Adsorption by industrial wastes	Fly ash, slag, red mud,	50 – 80 %		
Biological Methods	-	70 - 95 %	Most commonly used method, high efficiency	High cost, high energy use, requires certain climate conditions
Air Stripping	-	50 – 90 %	Commonly used in the pretreatment of wastewater, simple equipment	Requires certain pH, temperature, time and energy-consuming
Chlorination		80 - 95 %	Adaptable technology, high efficiency	pH sensitivity, disinfection byproducts
Oxidation			Organic waste removal produces molecular nitrogen	High cost, temperature and pressure, salt precipitation

Table 1. 3. Phosphorus removal technologies and efficiencies.

<b>Removal/Recovery Technology</b>	<b>Removal Efficiency</b>
Immobilized Algae	62 - 90 %
Suspended growth photo-bioreactors	61 %
MBR-UCT  (Membrane bioreactor integrated into a continuous-flow enhanced biological phosphorus removal (EBPR))	88 %
Granular Sludge	87 %
Active filter media  (Naturally occurring or man-made materials that remove P through precipitation or absorption)	77 – 95 %
Ion exchange	80 – 90 %

*\*Adapted from [30]. Only pilot and full-scale applications are reported in this table.*

Natural clays, low-cost materials due to their abundance in nature, are preferable ion exchange materials. [23] Also, tailoring novel materials based on natural clay are a promising way to achieve low-cost, on-site waste handling in the future. One major advantage is for using zeolites as ion exchange materials is, after reaching their nutrient uptake capacity they can be harvested as fertilizers [23] On the other hand, phosphorus removal through the ion exchange process is ongoing research with highly assuring results. Removal of both ammonium and phosphorus with natural clays or novel materials at the same time showed promised results [31] Especially, the lesser need for chemical addition into treatment systems to precipitate phosphorus is more convenient as it doesn't require additional handling of by-products. They are cheap and easy to process materials, therefore using them as the basis for creating cost-efficient adsorbents is anticipated to be a breakthrough in nutrient removal technologies.

The use of adsorbents outdoors such as poultry houses requires special care. A material that is going to be used in poultry farms should be tailored in a way that they can later be harvested on the soil. Deep cleaning or changing the bedding material is not performed more than once or twice a year. Also, daily or weekly handling is limited to washing and scraping the waste from the surface. Considering this fact, recollection should be easy during the cleaning of the bedding material. Applying a raw adsorbent material with very small particle sizes will make waste handling harder than it's before. However, natural clay-based adsorbent materials can be tailored for specific functions like their use in poultry farming applications.

#### **1.4. Geopolymers**

Geopolymer is a clay-based inorganic cementitious material with a long-range three-dimensional network having a mixed microstructure. [32] “Geo” in the name stands for natural material, as the name itself means “relating to earth”. They are classified as aluminosilicate materials which can be fabricated from natural or synthetic aluminosilicate natural minerals [33]–[35] Fabrication of geopolymers refer to mixing natural and synthetic aluminosilicates (metakaolin, fly ash, biochar, rice husk, perlite, or any combination) with aqueous solutions having reactive ingredients such as sodium, potassium hydroxide/silicate, phosphoric acid, etc. [36]–[38] Geopolymers draw attention because of their flexibility to be adapted into a wide range of applications, such as being used as membranes, adsorbents or filters, catalysts, thermal insulators, toxic pollutant encapsulators. [37]

As summarized in earlier sections, there have been numerous methods and adsorbent materials discovered in the search for the optimal pollutant removal efficiency. Materials like activated carbon, zeolite, resin, biochar and have been researched for many years and many of them showed high removal efficiency of certain pollutants. [28], [39], [40] Some had the flexibility for alterations for specific use and tailoring opportunities. However, the same adsorbents showed limitations like low adsorption capacities, high production costs, failing at low pH environments, low performance on regeneration, and such. A look for alternative lead researchers gives another take on geopolymers as adsorbents. There are several features of geopolymers which made them preferable;[41]

- Low-cost raw materials,
- The abundance of raw materials in nature
- Low curing temperature requirements a
- The flexibility of being synthesized with using waste materials
- High adsorption capacities
- Being easy to be tailored to increase porosity and surface modification.
- Easy processing for including [39][36]

Geopolymers have gained interest in adsorption studies along with distinct application opportunities. Along with other novel cementitious types, geopolymers reportedly have lower CO<sub>2</sub> emissions (169 kg CO<sub>2</sub>/m<sup>3</sup>) and energy consumption which can positively affect the environment if widespread production is encouraged. [42] For all the mentioned reasons, geopolymers are found to be suitable for the binder phase to accommodate different adsorbents while they were also explored for their adsorptive characteristics.

## **1.5. Opportunities for Geopolymer Based Adsorbents for Poultry Farming**

Facilitating sustainable operation of poultry farming requires reducing the adverse impacts on the environment. Current practices cause degradation of groundwater and surface water qualities due to excess nutrient runoff, degradation of air quality in poultry houses due to ammonia gas generation, increase in energy costs due to heating and ventilation and affecting animal health due to toxic levels of ammonia production.

It was found essential that healthy poultry farm operations should include smart handling of the waste. Therefore, the need for an adsorbent material with high nutrient removal capacity is addressed as a result of a natural material search. In addition to being efficient new adsorbent materials should be tailored in a way to be used for longer periods, lowering maintenance and cleaning activities. Also, having this as a potential fertilizer when it reaches up to its adsorption capacity was one of the driving motives to meet sustainability goals.

As stated in the previous section, geopolymers found to be a good fit as a waste management tool in poultry farming. First of all, geopolymers are easy to manufacture structures with low energy requirements and low carbon dioxide emission. This makes this material a low-cost alternative for waste handling. Secondly, they have proven efficiency on nitrogen removal which is one of the most problematic nutrients found in poultry litter. Last and most importantly, their adaptability in various uses gives room for the addition of other materials into the geopolymeric binder phase. Therefore, an ion exchanger that is manufactured by using the geopolymer phase is found to be the most optimal solution. In addition to this, adsorbent material can be tailored in certain shapes and sizes since the

initial geopolymeric phase is a gel that is to be cured into a solid. This makes it a material that is to be collected easily after they reach their adsorption capacity.

The content covered in the previous sections has lead this research to focus on nitrogen and phosphorus removal, main pollutants contributing to eutrophication and water quality degradation, via adsorbents tailored using natural raw materials like clinoptilolite. Geopolymers are found to be the best serving materials for this purpose due to their easy fabrication and adaptability.

To understand and observe geopolymer efficiency in a complex environment like poultry farms, there will be certain approaches followed in this research. The adapted approach will employ; developing geopolymers and geopolymer composites to sequester nitrogen and phosphorus from aqueous solutions, optimizing the composition of these novel adsorbents. Also, the composition of these novel clay-based adsorbents will be optimized based on rigorous testing to maximize N and P removal in complex environments. Lastly, removal efficiency will be determined for short and long-term nutrient uptake performances.

## CHAPTER II

### OBJECTIVES

The overall aim of this research is to investigate the sequestration of nitrogen and phosphorus, contaminants commonly present in poultry litter, by adsorption from aqueous solutions using inexpensive novel clay-based composites. Towards this goal, a proof of concept study was devised with the following three objectives.

**Objective 1.** Processing and characterization of the physicochemical microstructure of geopolymer and select geopolymer composite adsorbents.

Optimization of geopolymer and geopolymer composite adsorbent processing was the focus of this objective. It involved rigorous characterization of physical and chemical properties of the adsorbents using state of the art tools. Paramount was the requirement to understand the porosity, surface area, permeability, microstructure and mechanical strength of the adsorbents processed as half-inch spheres for application.

**Objective 2.** Assess individual efficiencies of removal of nitrogen and phosphorus from aqueous solutions by pure geopolymer and geopolymer composites.

Towards this objective three-tiered experimental approach was defined;



- Stability of adsorbents in aqueous solutions – Physical integrity and modification of pH of aqueous solutions was the primary focus of this study. Information on leaching of any unreacted soluble species from the adsorbents together with pH change was used to interpret nutrient removal mechanisms.
- Ammonium removal - Pure geopolymer and four different clinoptilolite incorporated geopolymer composites are tested by batch adsorption studies where adsorbents are immersed in aqueous solutions having ammonium ions only.
- Phosphorus removal - Pure geopolymer and clinoptilolite incorporated geopolymer composites with lowest and highest clinoptilolite concentration are tested through the same experimental procedure with the only difference of aqueous solutions having phosphorus ions alone.

**Objective 3:** Investigate the simultaneous removal of nutrients by geopolymer and geopolymer composites

In this objective, candidate adsorbents were evaluated for their nitrogen and phosphorus removal efficiencies when both ions co-existed in aqueous solutions. A sample solution having predefined amounts of nitrogen and phosphorus was prepared. These studies were designed to explore any matrix effect on individual nutrient removal.

## CHAPTER III

### MATERIALS AND METHODS

This chapter delivers the materials and methods used for this research. Materials used in this study are explained in detail to give familiarity. It is followed by the instrumentation and methods utilized to obtain the results presented in the following chapters. Details set for experimental conditions for each method are presented in the respective chapters.

#### 3.1. Materials

Inexpensive natural clay-based composites were processed with the addition of clinoptilolite and MgO into the geopolymer matrix. Geopolymer and clinoptilolite are both aluminosilicate materials with tetrahedral  $\text{SiO}_4$  and  $\text{AlO}_4$  units where they are linked by an oxygen atom. The difference between the two materials is the crystallinity where geopolymers are namely amorphous materials, unlike clinoptilolite. Adsorbents are preferred to be modified physically and chemically to increase their adsorption capacities. In this research clinoptilolite and MgO is also used as an addition to the geopolymer matrix in order to evaluate their capacity for nitrogen and phosphorus removal from aqueous solutions.

### 3.1.1. Geopolymer

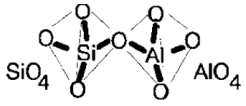
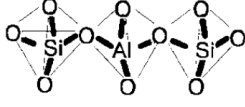
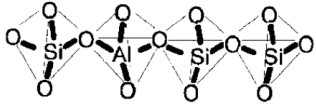
The term “geopolymer” was brought into literature by French materials scientist Joseph Davidovits in 1978.[43] Rock-forming minerals of geological origin are often used as raw materials in the synthesis of these aluminosilicate polymers and hence including “geo” in the name can be explained by this. Although, the name is frequently associated with other terms, such as low-temperature aluminosilicate glass, alkali-activated cement, geocement, inorganic polymer concrete, etc., a broader term “inorganic polymer is an appropriate use [42], [44], [45]

Geopolymerization reaction is the fundamental reaction that takes place to create these materials and it is what defines geopolymers as a new category of inorganic polymers.[39], [46] These materials polycondense as organic polymers in ambient temperatures, diminishes the need for high-temperature techniques. It involves a chemical reaction of aluminosilicate oxides ( $Al^{3+}$  with IV-fold coordination) with alkali polysilicates, yielding polymeric Si – O – Al bonds which is a three-dimensional structure with a shared oxygen atom. [32], [45]Geopolymers can be named as polysialates where the term sialate stands for silicon-aluminate. It is assumed that synthesis through oligomers (dimers and trimers) is the reaction providing the three-dimensional structure.[32]

Amorphous and semi-crystalline structures that produce polysialates are given in Table 3.

1. Terminology has been set and was presented to scientific community at IUPAC conference in 1976 by Joseph Davidovits himself, as; Si:Al = 0, siloxo, Si:Al = 1, sialate (acronym for silicon-oxo-aluminate of Na, K, Ca, Li), Si:Al = 2, sialate-siloxo, Si:Al = 3, sialate-disiloxo, Si:Al > 3, sialate link.[47]

Table 3. 1. Poly(sialate-siloxo) networks constitutes geopolymers[48]

Poly(sialate)	(-Si-O-Al-O-)	
Poly(sialate – siloxo)	(-Si-O-Al-O-Si-O-)	
Poly(sialate – disiloxo)	(-Si-O-Al-O-Si-O-Si-O-)	

The aforementioned term for use of sialates refers to sharing an oxygen atom. At the same time, the framework has to have positive ions, such as  $\text{Na}^+$ ,  $\text{K}^+$ ,  $\text{Li}^+$ ,  $\text{Ca}^{2+}$ ,  $\text{Ba}^{2+}$ ,  $\text{NH}_4^+$ ,  $\text{H}_3\text{O}^+$ , in order to balance the negative charge created by  $\text{Al}^{3+}$ . This yields the empirical formula for geopolymers;

$$M_n \{-(\text{SiO}_2)_z-\text{AlO}_2\} \cdot w\text{H}_2\text{O} \quad [32], [49]$$

Where M is a cation ( $\text{K}^+$ ,  $\text{Na}^+$ ,  $\text{Ca}^{2+}$ ), n is the degree of polycondensation, z is the degree of polymerization 1, 2, 3 and w is the amount of binding water. According to the information given, a simplified geopolymers reaction process for K based geopolymers are given in Figure 3. 1.

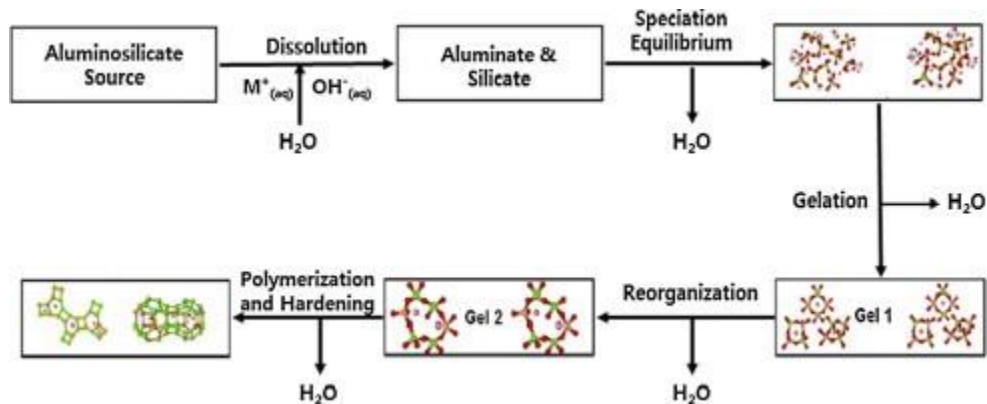


Figure 3. 1. Schematics of geopolymers reaction [46]

According to the suggested geopolymerization reaction, dissolution of aluminosilicate sources by highly alkaline solutions reduces the system into aluminate and silicate groups. The alkaline solution used for this process may also contain silicates, as is going to be mentioned in the following subsections. Dissolution reaction takes place at high pH and immediately creates a saturated solution, leading to gel formation. It should be noted that geopolymerization is an exothermic process and water is rapidly consumed. The system continues to rearrange until the three-dimensional network is attained. [44], [50], [51]

In this research metakaolin based geopolymers were processed by mixing solid precursors with potassium silicate solution. A variety of aluminosilicate materials can be used as raw materials in geopolymer processing. Metakaolin (MetaMax®, Ludwigshafen, Germany), calcined kaolin at temperatures 650 – 750° C, used as solid aluminosilicate precursor for this study. It is a widely used material for geopolymer synthesis.

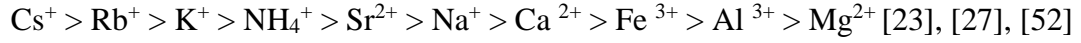
Processing details of geopolymers and geopolymer composites are given later in this chapter. Besides, structural details of processed geopolymers are shared geopolymers and represented in Chapter4 of this document.

### **3.1.2. Clinoptilolite**

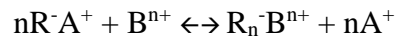
Clinoptilolite, a natural zeolite used as an additive material for geopolymer processing for this research. They are microporous, aluminosilicate materials and commonly used as adsorbents and catalysts. Clinoptilolite is one of the cheapest zeolite materials due to its abundance. In addition to being used as adsorbents, it has been applied in the

manufacturing of building materials, soil modifiers, dietary supplements, dryers, deodorizers, etc. [52]

Their negatively-charged framework is compensated by weakly bounded exchangeable cations. [53] Their cation affinity is reported as follows;



Cation exchange equilibrium between a solution containing the cation and zeolite can be written as;



where A and B are exchange ions, R<sup>-</sup> is an anionic group attached on zeolite surface and A<sup>+</sup> and B<sup>n+</sup> are ions in solution. [23]

For this research, commercially available clinoptilolite (KMI Zeolite, Amargosa Valley, NV) with the chemical formula Na<sub>6</sub>[Al<sub>6</sub>Si<sub>130</sub>O<sub>72</sub>]24H<sub>2</sub>O. The chemical composition provided from the vendor and XRF analysis done in Core Labs are given in Table 3. 2

Table 3. 2. Chemical analysis of commercial zeolite

<b>Component</b>	<b>KMI Product Catalog(%)</b>	<b>XRF (%)</b>
<b>SiO<sub>2</sub></b>	66.70	58.70
<b>Al<sub>2</sub>O<sub>3</sub></b>	11.48	10.10
<b>Fe<sub>2</sub>O<sub>3</sub></b>	0.90	4.29
<b>CaO</b>	1.33	11.30
<b>MgO</b>	0.27	0.82
<b>Na<sub>2</sub>O</b>	3.96	3.14
<b>K<sub>2</sub>O</b>	3.42	9.56
<b>MnO</b>	0.03	0.22
<b>TiO<sub>2</sub></b>	0.13	0.46

### 3.1.3. Magnesium Oxide (MgO)

Magnesium oxide (MgO) is an inorganic material that occurs in nature as a periclase mineral. It is used extensively in soil and groundwater remediation and waste treatment industries and as plant fertilizers. In the form of magnesium hydroxide slurry, also referred to as “the milk of magnesia” for wastewater treatment, has been widely utilized for heavy metal precipitation and acid neutralization. [54]

In this study, MgO (MAGCHEM50, Martin Marietta, Baltimore, MD) is used as an additive material in geopolymer processing due to its adaptive use in ion exchange. MgO addition into geopolymers reportedly enhanced reaction rate and mechanical properties[55]

Chemical composition and physical properties obtained from the vendor is given in Table 3. 3.

Table 3. 3. Chemical composition and Physical properties of MgO powder

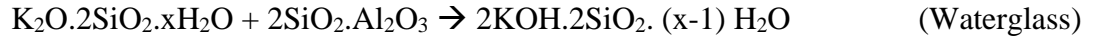
<b>Composition</b>	Magnesium Oxide (MgO), % ignited basis	98.2
	Calcium Oxide (CaO), %	0.8
	Silicon Oxide (SiO <sub>2</sub> ), %	0.35
	Iron Oxide (Fe <sub>2</sub> O <sub>3</sub> ), %	0.15
	Aluminum Oxide (Al <sub>2</sub> O <sub>3</sub> ), %	0.1
	Chloride (Cl), %	0.3
	Sulfate (SO <sub>3</sub> ), %	0.05
	Loss on Ignition, %	4.5
<b>Physical Properties</b>	Loose Bulk Density, lb/ft <sup>3</sup> (g/cm <sup>3</sup> )	24 (0.38)
	Median Particle Size, micron	3-8
	Surface Area, m <sup>2</sup> /g	60
	Activity Index, seconds	8
	% Passing 100 mesh	100
	% Passing 325 mesh	99.5

### 3.2.Processing

Geopolymers and geopolymer composites were prepared to have a stoichiometric relation of  $4\text{SiO}_2 \cdot \text{Al}_2\text{O}_3 \cdot \text{K}_2\text{O} \cdot x\text{H}_2\text{O}$  by mixing; metakaolin ( $\text{Al}_2\text{O}_3 \cdot 2\text{SiO}_2$ ) and reactive alkali solution named water glass, prepared with potassium hydroxide (KOH), silica fume ( $\text{SiO}_2$ )



and water, resulting  $K_2O \cdot 2SiO_2 \cdot xH_2O$ . Mixing reaction of metakaolin and waterglass solution follows;



where x is moles of water used. Dissolution of KOH will yield 1 mole of water, therefore the waterglass formula presents water content as (x-1). The reaction yields stoichiometric ratios of  $SiO_2/Al_2O_3=2$  and  $K_2O/Al_2O_3=1$ .

Mixing of reagents done by using planetary centrifugal mixer “THINKY” (ARE-310 Thinky, CA). Mixing is set to 5 minutes at 1100 rpm followed by defoaming for 3 minutes at 1300 rpm. Mixing took place at room temperature until obtaining a homogeneous slurry. In order to have correct stoichiometric ratios mixing should be kept until all powdered media is incorporated in the slurry.

For this research clinoptilolite and MgO were decided as additives. Mixing should be done any time an additive material is used to make geopolymer composites. When composites are made, additives are weighed carefully and mixed into a slurry. This process was followed by additional mixing for 5 minutes at 1100 rpm.

There are six geopolymer composites prepared by the addition of clinoptilolite and MgO. First, geopolymer is processed as is and no additive material was used. This type will be referred to as pure geopolymer (PGP) in the following chapters. There were four composites processed by clinoptilolite addition into geopolymer slurry. Fine clinoptilolite with particle size between 106-212 $\mu$ m was added by 5, 10, 15 and 20 volume %.

Abbreviations that are going to be used for these composites are CGP5, CGP10, CGP15 and CGP20. The last composite type was magnesium oxide incorporated geopolymers, referred to as MGP5, by the addition of MgO by 5 volume %. The process flow is given in Figure 3. 2

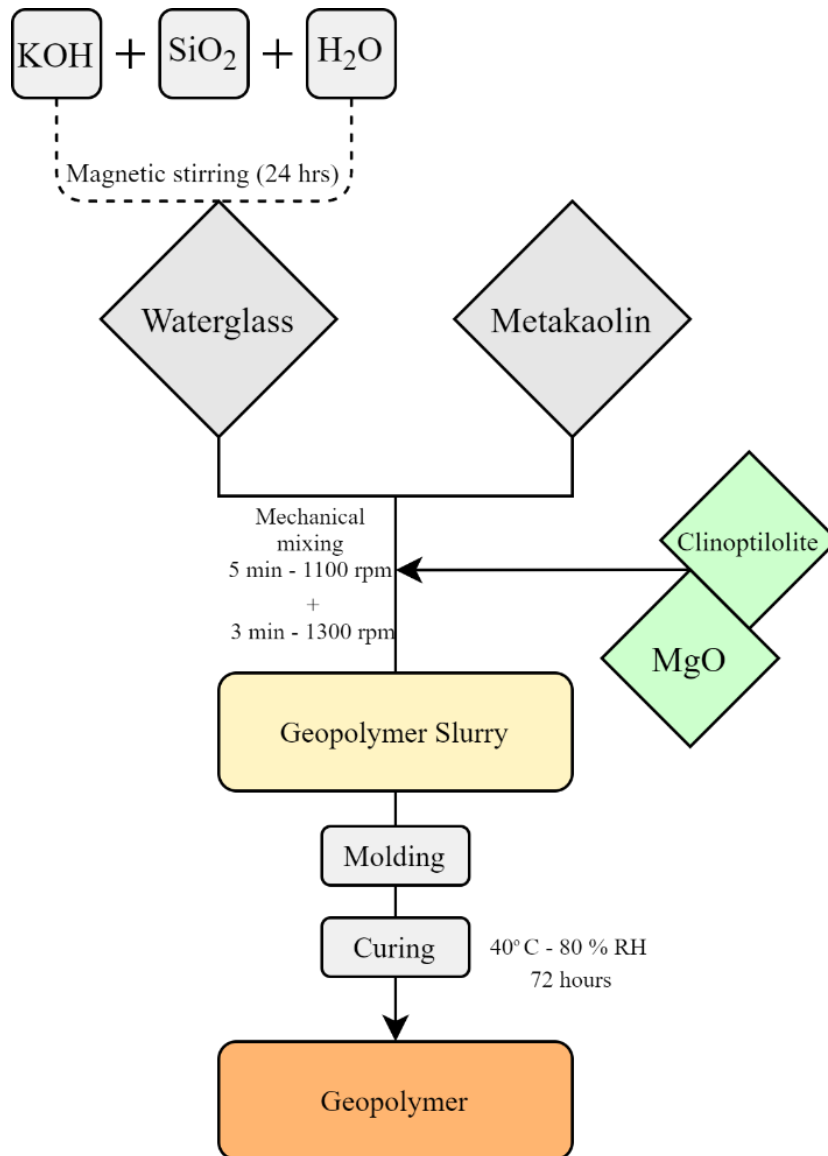


Figure 3. 2. Steps involved in geopolymer and geopolymer composite processing

After mechanical mixing was finalized, the slurry was vibrated using Syntron Paper Jogger (J-1 Flat Deck; D.L. Williams Company, Bluefield, VA) until all trapped air was removed before it was transferred into silicon molds. Molds used for this study had sphere shapes of 0.5 inch diameters Figure 3. 3. Another set of samples was prepared following the same steps, but they were molded in cylindrical plastic cups in order to have samples for compressive testing.



Figure 3. 3. Molding geopolymer slurry into half-inch diameter spheres

Transferred samples are covered with plastic wrap and stacked in sealed bags to cut the contact with the atmosphere. Samples then cured in Controlled Temperature and Humidity Chamber (TestEquity 123H Controlled Temperature and Humidity Chamber, TestEquity,

CA) at 40° and 80 relative humidity (RH%) for 72 hours to prevent cracking and rapid water loss from the samples. With the climatic conditions set for curing, cracking is prevented and structure has consolidated.

### **3.3. Materials Characterization and Analytical Methods**

Characterization tools are utilized to observe structural, morphological and chemical properties of geopolymer composites before and after being used in adsorption studies. Utilizing the characterization tools are useful to interpret the physicochemical properties of samples. Since the information about the ion-exchange mechanism is the key for this research the positive values of these tools cannot be undermined. The following sections have information about each instrument and further details will be given in related chapters.

#### **3.3.1. Microscopy**

##### **Optical Microscopy (OM)**

The microstructure of the processed geopolymer composite membranes was studied using an optical microscope. Digital images were acquired using the Carl Zeiss' AxioLab A1 Modular, upright Optical Microscope for Materials Science (Carl Zeiss Microscopy, LLC, White Plains, NY) with 5X, 20X magnifying lenses. Optical microscope was used to observe the porosity and filler phase distribution on the surface of the geopolymer and geopolymer composites. The samples used for these measurements were half-inch adsorbent balls cut using the slow action diamond saw. The sample surface was not polished.



Figure 3. 4. Carl Zeiss' AxioLab A1 Modular, upright Optical Microscope for Materials Science (Carl Zeiss Microscopy, LLC, White Plains, NY)

#### **Scanning Electron Microscopy (SEM) and Energy Dispersive Spectroscopy (EDS)**

A Hitachi S-4800 field emission scanning electron microscope (FE-SEM) coupled with an Oxford Instruments (Tubney Woods, Abingdon, Oxon, UK) energy dispersive spectroscopy (EDS) silicon drift detector was used to characterize the microstructure and determine the elemental composition and distribution of the samples. These included solid adsorbent ball samples.

The post-evaluation samples are embedded in epoxy. The top surface of these samples (where separation occurs) was coated with carbon to prevent charging of the surface during SEM studies. Elemental distribution on the surface was carefully examined to observe the residual particles that were retained by the filter. Elemental maps were acquired using an accelerating voltage of 20 keV at a working distance of 15mm.

The pre-test or virgin filter samples were at first vacuum impregnated (using Citovac, Struers Inc., Cleveland, OH) with epoxy (Epothin, Buehler, Lake Bluff, IL), and polished surface finish using Struers LaboPol-35 Polishing/Grinding System, (Struers Inc., Cleveland, OH) and SiC polishing papers of different grades. Subsequently, these samples were cleaned with DI water, dried overnight in a vacuum oven (VWR Symphony, VWR International, LLC., Radnor, PA) at 60°C, and then coated with carbon for 2 seconds. The SEM investigations on these samples were primarily focused on evaluating the bonding between the filler phase (i.e. clinoptilolite) and the matrix (geopolymer) at high magnifications. Also, geopolymer composites that are used in batch adsorption studies have been studied by EDS mapping to observe the adsorption localization on composite surfaces.

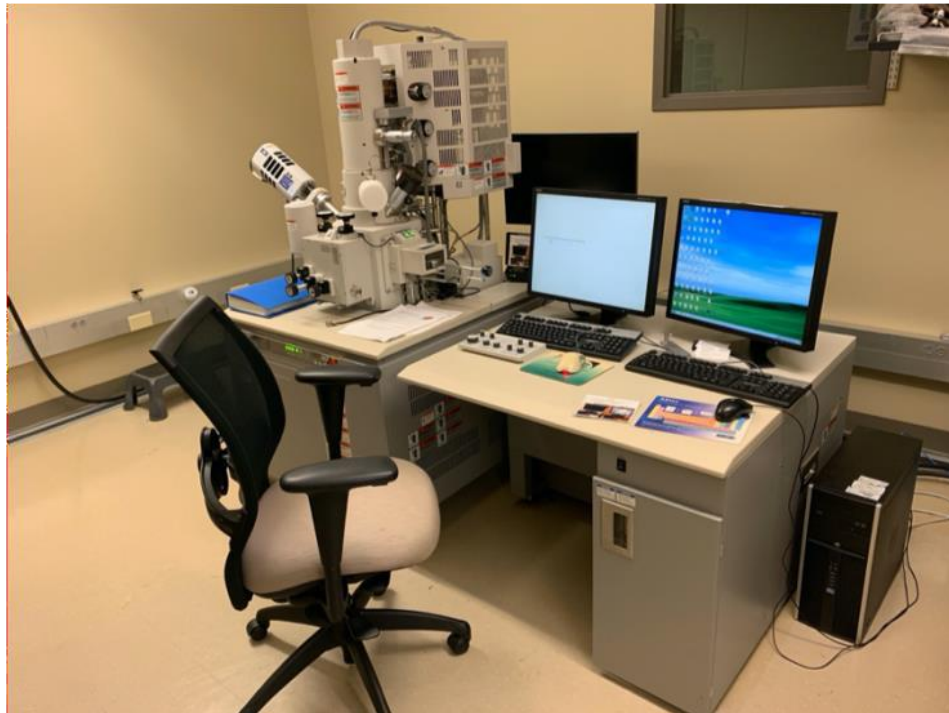


Figure 3. 5. Hitachi S-4800 field emission scanning electron microscope (FE-SEM) coupled with an Oxford Instruments (Tubney Woods, Abingdon, Oxon, UK) energy dispersive spectroscopy (EDS) silicon drift detector.

### **X-ray: Wavelength dispersive X-ray spectroscopy (WDX, WDS)**

Chemical composition of pure geopolymer and geopolymer composites characterized by the Rigaku Primus IV Wavelength Dispersive X-ray Fluorescence (WDXRF) spectrometer (Rigaku, Tokyo, Japan) (shown in Figure 3.19). Samples were studied as intact solid half-inch adsorbent balls that were mounted in epoxy. Samples were not covered with a film. Mapping analysis is done to detect nutrient localization after the adsorption process.

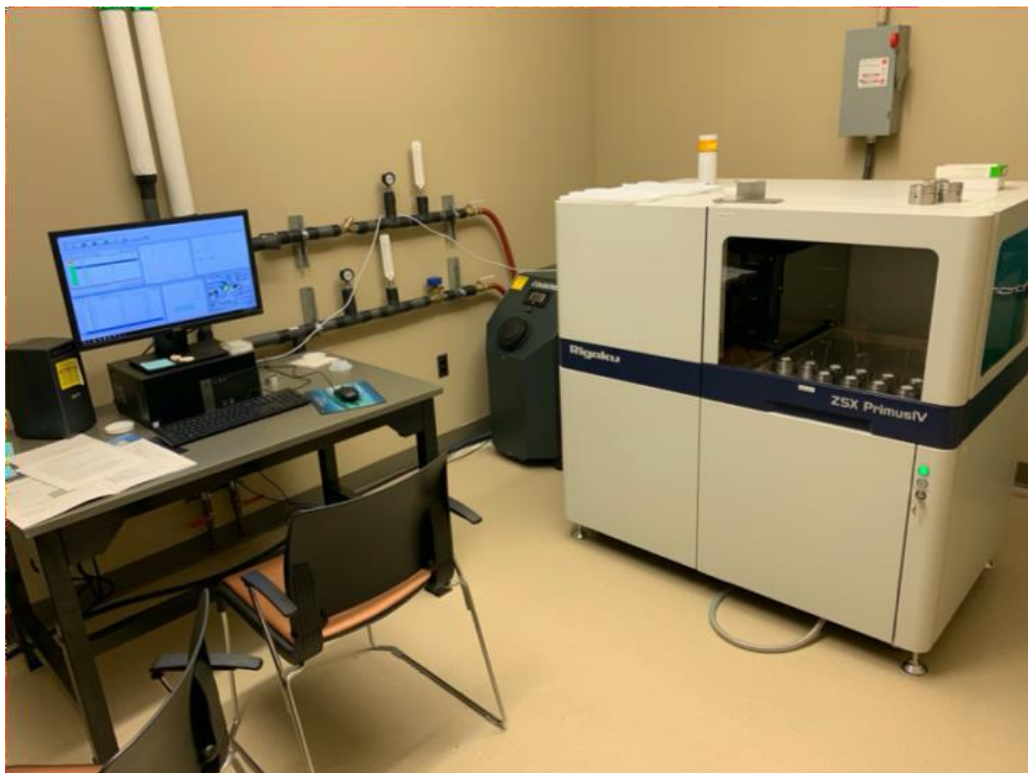


Figure 3. 6. Rigaku Primus IV Wavelength Dispersive X-ray Fluorescence (WDXRF) spectrometer (Rigaku, Tokyo, Japan) in the Helmerich Research Center, Core Laboratories

### 3.3.2. Analytical Chemistry methods

#### pH

The water quality of model solutions was monitored constantly throughout the adsorption studies. They were characterized by a pH meter (SevenCompact pH meter S220, Mettler-Toledo, LLC, Columbus, OH) to verify the water during the tests. The instrument was calibrated regularly, as per the instrument manual using standard buffer solutions.



Figure 3. 7. SevenCompact pH meter S220 used for pH and ionic strength measurements

#### TDS/Conductivity

Total dissolved solids (TDS) is a measure of the dissolved combined content of all inorganic and organic substances present in a liquid in molecular, ionized, or micro-granular (colloidal sol) suspended form. Generally, the operational definition is that the



solids must be small enough to survive filtration through a filter with 2-micrometer (nominal size, or smaller) pores.

The two principal methods of measuring total dissolved solids are gravimetric analysis and conductivity (EPA Method 160.1). Gravimetric methods are the most accurate and involve evaporating the liquid solvent and measuring the mass of residues left. This method is generally the best despite its time consuming measurement.

The electrical conductivity of water is directly related to the concentration of dissolved ionized solids in the water. Ions from the dissolved solids in water create the ability for that water to conduct an electric current, which can be measured using a conventional conductivity meter or TDS meter. When correlated with laboratory TDS measurements, conductivity provides an approximate value for the TDS concentration, usually to within ten-percent accuracy. The relationship between TDS and specific conductance of groundwater can be approximated by the following equation:

$$\text{TDS} = k_e \text{EC}$$

where TDS is expressed in mg/L and EC is the electrical conductivity in micro siemens at 25 °C. The correlation factor  $k_e$  varies between 0.55 and 0.8. For this study, the Oakton Con 700 Total Dissolved Solid (TDS) meter (Oakton Instruments, Vernon Hills, IL) was used. The instrument was calibrated following the procedures outlined by the instrument manufacturer.

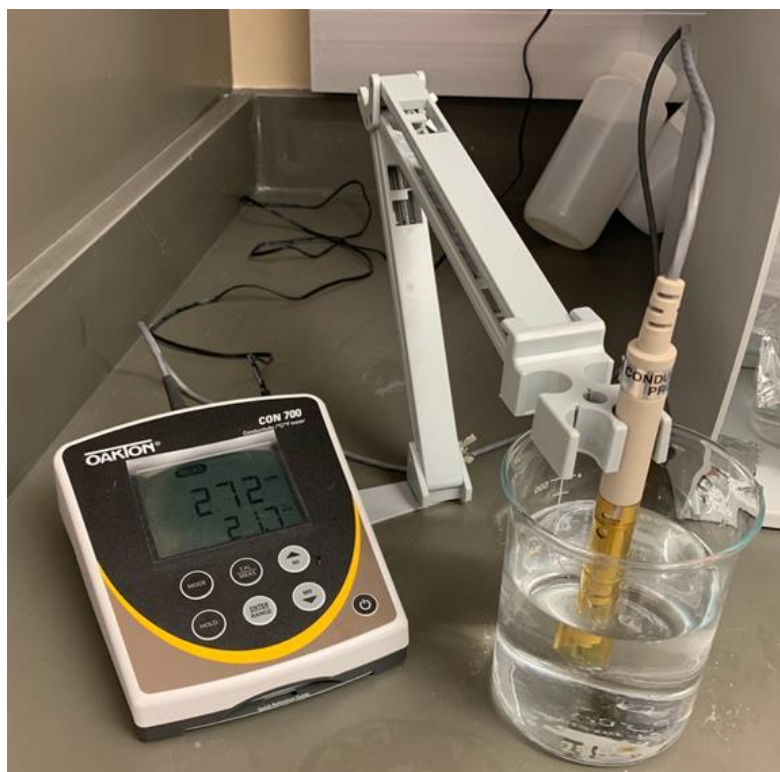


Figure 3. 8. Oakton Con 700 Total Dissolved Solid (TDS) meter (Oakton Instruments, Vernon Hills, IL).

### **Optical Spectrometry**

HACH DR/4000 Spectrophotometer (Loveland, CO) is used in this study to measure nutrient concentrations of the model solutions prepared for the experiments. It is a direct reading instrument. User-entered calibrations can be stored in the instrument, thus it was done for this research. The DR/4000 Spectrophotometer provides digital readouts indirect concentration units, absorbance, or percent transmittance. The instrument is capable of producing wavelengths 190 – 1100 nm when both tungsten and deuterium lamp installed.



Figure 3. 9. Hach DR4000 UV-Visible Spectrometer (HACH, Loveland, CO)

### 3.3.3. Macroscopic Testing

#### Pycnometry

Gas displacement pycnometer system, AccuPyc II 1340 (Micromeritics, Atlanta, GA) is used to analyze true volume and true density of solids and powders used in this study. This method is characterized as a reliable technique to obtain true, absolute, skeletal, apparent volume and density where sensitivity is subject to the type of samples used and instrument. It is a non-destructive test where product integrity can be maintained throughout the measurements.

It is important to note the preparation method of samples before performing the tests. Samples were oven dried briefly at 110 °C to eliminate moisture content in adsorbents and

produce more accurate results. After the drying procedure was completed, adsorbent balls were crushed and sieved through 500 $\mu$ m sieves to obtain uniformly sized particles. Crushed samples are placed in a chamber insert after being weighed carefully. A chamber insert of 1 cm<sup>3</sup> and 3.5 cm<sup>3</sup> volume was used which is in compliance with instrument instructions and the standard method. Helium is used as the inert gas to be displaced. Software is then set to 50 purges – 50 cycles where the purging process cleans the sample cell and expansion chambers before analysis begins and the cycle is defined as a series of functions equal to single volume measurement. The increased number of purges and the corresponding number of cycles helped measurements to be as precise as possible. Also, results are recorded after each purge-cycle sequence.



Figure 3. 10. Gas displacement pycnometry system, AccuPyc II 1340 (Micromeritics, Atlanta, GA)

## **Porosimetry and Permeability**

3 Flex Surface Characterization Analyzer (Micromeritics, Norcross, GA), a tool for obtaining high-resolution adsorption, desorption and isotherms are used. It is used in this study was mainly for understanding the microporous and mesoporous structures in MK based K-geopolymers. All six types of geopolymer structures are first tested with 3Flex It was then followed by tests held in Autopore V, Mercury Intrusion Porosimetry (Micromeritics, Norcross, GA) which was used to collect information about surface characteristics of the composites. Mercury intrusion into a porous structure in a pressure-controlled environment is the basis of mercury porosimetry analysis. Through the combination of these methods it was possible to obtain;

- Pore size distribution
- Total pore volume
- Total pore surface area
- Median pore diameter
- Bulk and skeletal sample densities

BET (Brunauer–Emmett–Teller) analysis applied to obtain data through multilayer gas adsorption and get a detailed surface area evaluation. The technique covers external and pore area evaluation in order to determine the total specific surface area (as  $\text{m}^2/\text{g}$ ). Barrett-Joyner-Halenda (BJH) analysis was also employed to calculate pore area and specific pore volumes through adsorption and desorption. Pore size distribution is then calculated independently from the external area with the help of the particle size of the sample. [56]

MIP analysis was applied to collect pore size distribution and porosity data by applying a wide range of pressure incrementally into a material that is immersed in mercury. External pressure is used for mercury to penetrate pores, understand pore structure via the information gathered with the help of the high contact angle of mercury with surfaces and its high surface tension. Calculations are based on the volume of mercury intrudes into sample material for each pressure change. The pressure is changed according to user-defined steps that define the resolution while the volume of mercury intruded into pores is measured by a mercury penetrometer that is an electrical capacitance dilatometer. Although the working pressure can be high to push mercury through pores and interconnected pore channels, using a liquid instead of gas is one results in physical limitations for gathering information about smaller pores.



Figure 3. 11. 3 Flex Surface Characterization Analyzer (Micromeritics, Norcross, GA)



Figure 3. 12. Autopore V, Mercury Intrusion Porosimetry (MIP) (Micromeritics, Norcross, GA)

### 3.3.4. Mechanical Testing

The compressive strength was measured using an Instron universal testing machine according to the ASTM C39/C39M-18. The test was on the Cylindrical samples with ~25mm diameter and 18-28 mm height. The diameter used for calculating the cross-sectional area of the test specimen was determined by measuring three samples at about a mid height of the specimen. Values are averaged to introduce the testing procedure to the software. For these measurements, the cylindrical sample was placed on the lower bearing block of the testing machine such that the axis of the specimen aligned with the center of thrust of the upper bearing block. Before testing the specimen, it was verified that the load indicator was set to zero. During the testing the load was applied continuously, without

shock. The load was applied at a rate of movement (platen to crosshead measurement) corresponding to a stress rate on the specimen of 160 N/s (equivalent to 0.25 MPa/s for the investigated samples). The designated rate of movement was maintained at least during the latter half of the anticipated loading phase. As the standard guideline, the compressive strength of the specimens was calculated with the following equation;

$$f_{cm} = \frac{4000P_{max}}{\pi D^2}$$

Where  $f_{cm}$  = compressive strength, MPa,  $P_{max}$  = maximum load, kN



Figure 3. 13. Instron 5582 Universal Testing System



## **CHAPTER IV**

### **PHYSICOCHEMICAL ANALYSIS OF VIRGIN ADSORBENTS**

This chapter is dedicated to the materials characterization methods used to evaluate micro and macrostructural properties of adsorbents that have not yet been used. Materials characterization tools are used extensively to interpret the microstructure and morphology of composites thoroughly.

Geopolymer composites investigated in this chapter are used after drying and curing processes. They are analyzed by various tools to understand the fundamental characteristics; surface morphology, porosity, mechanical strength, density, porosity and permeability. For this research there are six types of adsorbents were processed. As stated in earlier chapters, composites are all potassium based metakaolin geopolymers, one is being pure geopolymer, four clinoptilolite incorporated composites and one MgO powder incorporated composite Processing details and composition information mentioned in Chapter 3.

#### **4.1. Microstructural and mechanical properties of geopolymer composites**

From the definitions made in earlier chapters clinoptilolite and geopolymers, it can be summarized that geopolymers are very similar to natural zeolites in terms. The main difference can be addressed as geopolymers not having a fully crystalline structure. Instead, they are known to contain amorphous unreacted precursor, amorphous aluminosilicate gel which is the binder phase as well as few crystalline phases. The number of crystalline phases observed depends on the type of precursor and natural clay material have chosen.[57]–[59]

The microstructure is a small scale, the prepared surface of the material that is observed by a range of microscopy techniques. It is often a significant parameter to reveal certain properties of the materials. Arrangement of the phases, grain structure and distribution, defects and their compositions define the mechanical, physical and chemical properties of a material. [60], [61] Such as strength and hardness of materials, electrical and magnetic properties. It is important to discover one material's properties to understand the nature of that material. In this research, virgin samples have been tested by characterization tools available. Moreover, this subchapter is dedicated to discussing the morphology of geopolymer composites along with the results obtained from characterization techniques that were used.

The targeted composition of the geopolymer was  $4\text{SiO}_2 \cdot \text{Al}_2\text{O}_3 \cdot \text{K}_2\text{O} \cdot 11\text{H}_2\text{O}$ . Processing and curing conditions were important processes that give attention to due to their importance in defining geopolymer integrity. In earlier stages of this research, it has come to attention that geopolymer adsorbent balls were cracking when they were immersed in aqueous

solutions. Immersing them in DI water itself was sufficient to destroy the integrity of adsorbents. After altering conditions for curing they showed and increased integrity and cracking was not an issue after this. Initially, curing conditions were set to 60°C and 60 relative humidity for 5 days and it appeared that climatic conditions were leading to a sudden loss of water content. Updated curing conditions were 40°C and 80 relative humidity for 72 hours and composites cured under these circumstances showed increased integrity where approximately 5 out of 216 adsorbent balls have cracked after long hours of exposure to aqueous environments.

#### **4.1.1. Mechanical strength**

Mechanical strength stands for a material's ability to endure an applied load without failure of the material. In this study, mechanical strength is important due to the adsorbent material's area of use. Geopolymer adsorbents balls are aimed to use in broiler and chicken houses to encapsulate nutrients in the source of the pollution. They are planned to be laid on the ground and mixed with bedding material, therefore those materials need to keep their integrity and not fail immediately. For this purpose, their compressive strength is tested using Instron 5582 UTM following ASTM standard C39/C39M-18 [62]. Cylindrical samples are cast for this purpose and they are cured according to standard requirements (Figure 4. 1)



Figure 4. 1. Cylindrical and ball shaped samples presented together

Sample length varied according to the amount of geopolymer slurry poured into each plastic cup but the diameter was the same initially. Due to drying shrinkage and composite composition some samples had different diameters at the time of the compressive test. Additionally, length and diameter values are averaged of the same sample and its two other replicates. Figure 4. 3 shows the experiment set used for this study. Sample specimens presented Type 3 (columnar vertical cracking through both ends with no well-formed cones) and Type 5 (side fractures at the top or the bottom, occur commonly with unbonded caps) fracture patterns (Figure 4. 2)

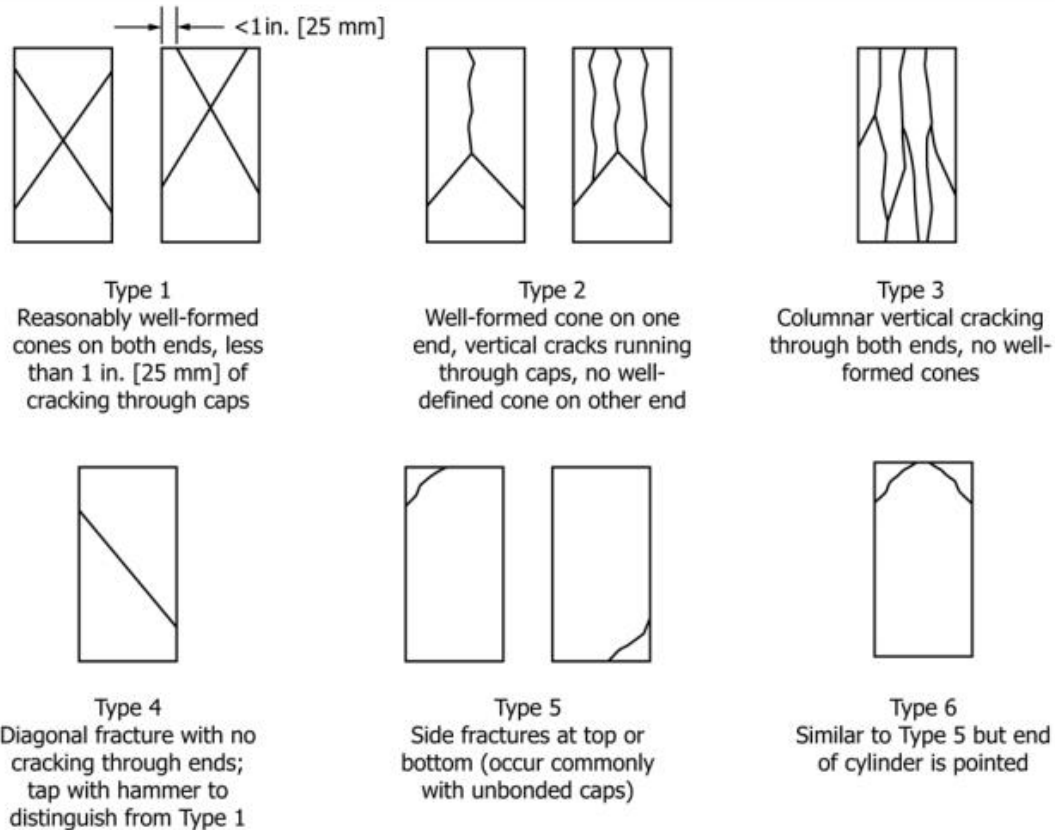


Figure 4. 2. Schematic of Typical Fracture Patterns according to ASTM standard C39/C39M-18

All six composites are tested as stated in the previous paragraphs. Results are reported in Table 4. 1, where sample diameter and length are averaged from three samples of the same type of composite. Compressive strength is reported as the true stress with units megapascals (MPa), similarly averaged from three tests utilized on the same type of composite. Standard error was identified by the standard deviation of the maximum values obtained from each compressive test run. Compressive strength of each sample type is reported in Appendix A., with graphs representing three samples of each type and their compressive strength corresponding to strain values.

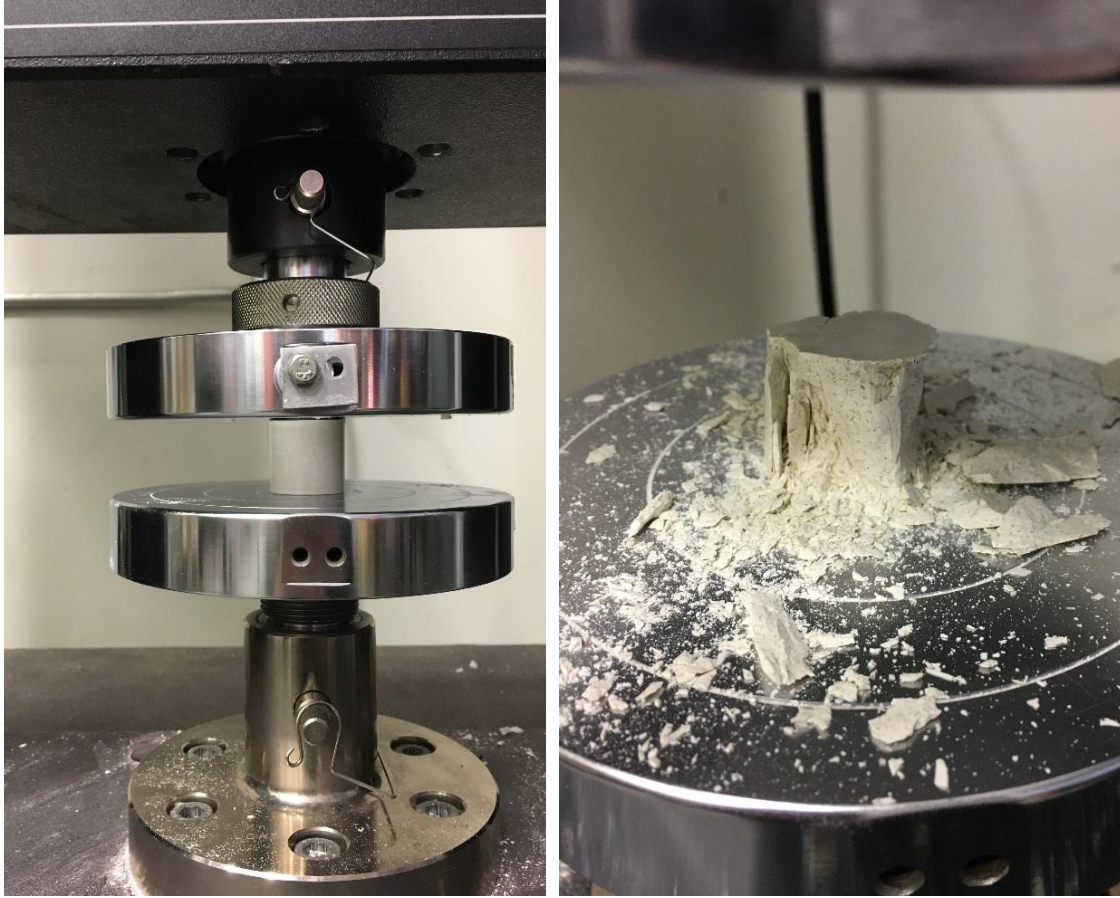


Figure 4. 3. Compressive test performed on cylindrical geopolymer samples, Type 3 fracture is observed on failed samples.

Table 4. 1. Compressive strength test results from cylindrical geopolymer samples

<b>Composite Type</b>	<b>Sample Length (mm)</b>	<b>Sample Diameter (mm)</b>	<b>Compressive Strength (MPa)</b>
<b>PGP</b>	21.08	25.10	27.63 ± 7.41
<b>CGP5</b>	23.50	24.03	47.96 ± 6.50
<b>CGP10</b>	18.17	25.10	66.36 ± 2.47
<b>CGP15</b>	26.33	25.00	28.54 ± 1.78
<b>CGP20</b>	22.90	23.50	14.19 ± 4.65
<b>MGP5</b>	19.17	24.83	28.10 ± 8.44

*\*Sample length and diameters are averaged from three samples of a related set of composites*

#### **4.1.2. Optical microscopy**

An optical microscope or light microscope has an important role in identifying phases and prevalent features of materials. It is a microscopy tool that uses visible light and a set of lenses to magnify the images of small features on a sample. An optical microscope used to capture surface properties of adsorbents uses reflected light. This method is to capture micrographs of opaque objects and usually works well with metals. It is not suitable for investigating nanocrystalline or submicron particles due to the limitation in resolution.[61] Although composites used in research are opaque, they are also non-conductive, amorphous materials; therefore, it created the challenge where different particles and phases were hard to identify. Creating contrast is one way to overcome this problem; thus it was used in this case. Although it was a challenging task to distinguish simple feature samples as PGP and MGP5 composites due to this issue (Figure 4. 4.)

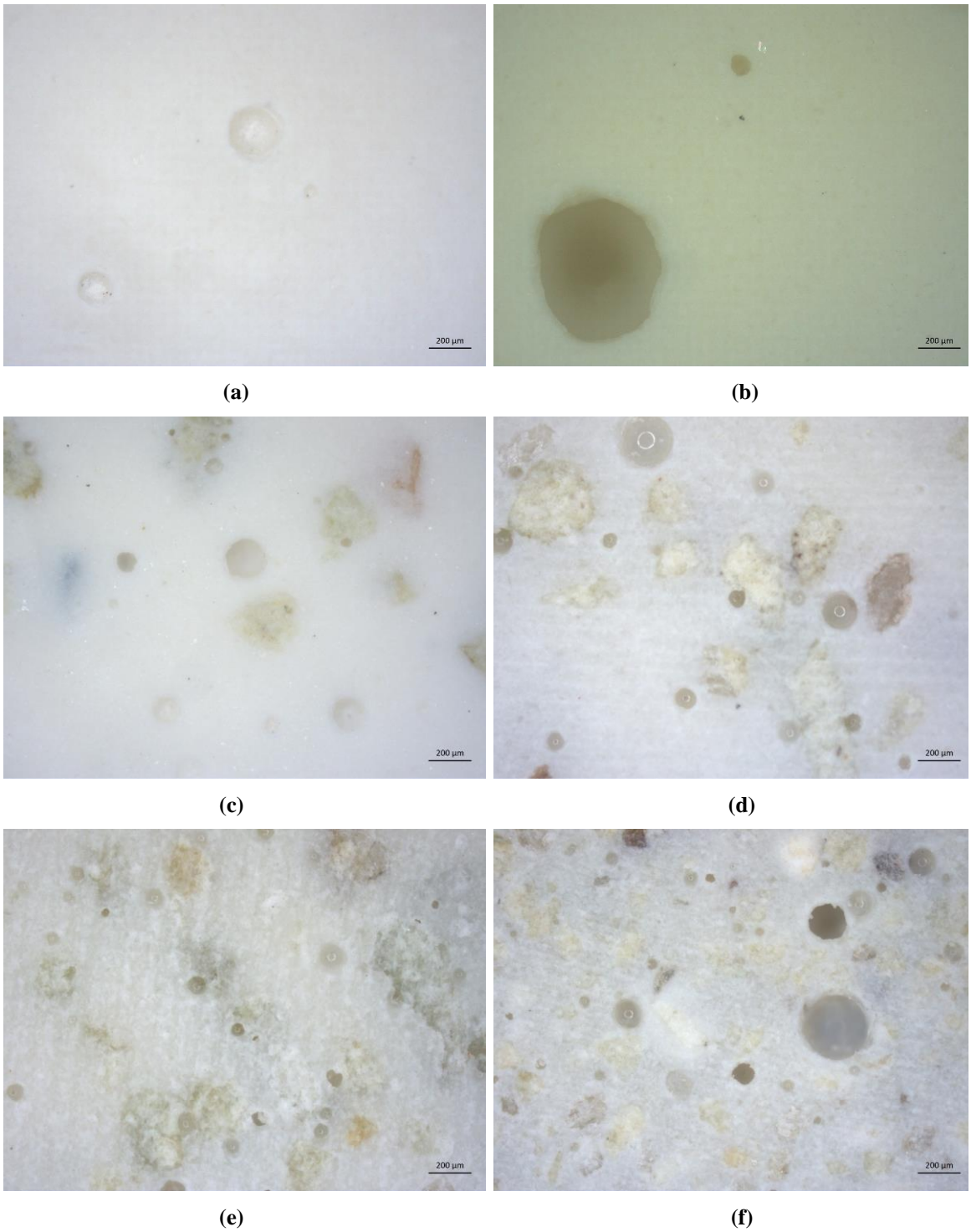


Figure 4. 4. Pure geopolymer (a), MgO incorporated geopolymer (MGP5) (b), Clinoptilolite incorporated geopolymer given increasing order of additive in terms of volume percentage, CGP5 (a), CGP10 (b), CGP15 (c) and CGP20 (d)



The initial observation gathered from the optical microscope is the macropores on the surfaces. It is not feasible to observe or interpret the structure of geopolymers only by optical microscopy, however, it can be seen from the images that pore distribution more apparent with increasing clinoptilolite content. The depth and interconnectivity of these cannot be interpreted from 2D images, yet other characterization tools such as Mercury Intrusion Porosimetry (MIP) is used mainly for this purpose and explained in the following section.

#### **4.1.3. Density – Pycnometry**

Gas displacement pycnometry system, AccuPyc II 1340 (Micromeritics, Atlanta, GA) is used to analyze true volume and true density of solids and powders used in this study. This method is characterized as a reliable technique to obtain true, absolute, skeletal, apparent volume and density where sensitivity is subject to the type of samples used and instrument. It is a non-destructive test where product integrity can be maintained throughout the measurements.

#### ***Sample Preparation and Operation***

It is important to note the preparation method of samples before performing the tests. Samples were oven dried briefly at 110 °C to eliminate moisture content in adsorbents and produce more accurate results. After the drying procedure was completed, adsorbent balls were crushed and sieved through 500µm sieves to obtain uniformly sized particles. According to ASTM standard D5550-06 [63], any size of particles is acceptable. Finally, crushed samples are placed in a chamber insert after being weighed carefully. A chamber insert of 1 cm<sup>3</sup> and 3.5 cm<sup>3</sup> volume was used which is in compliance with instrument

instructions and the standard method. Helium is used as the inert gas to be displaced. Software is then set to 50 purges – 50 cycles where the purging process cleans the sample cell and expansion chambers before analysis begins and the cycle is defined as a series of functions equal to single volume measurement. Increased number of purges and a corresponding number of cycles helped measurements to be precise as possible. Also, results are recorded after each purge-cycle sequence. Results of all pre-evaluation adsorbents are given in Table 4. 2 to represent the averaged values of total volume and density along with total pore volume.

Table 4. 2. Data retrieved from AccuPyc II runs for the absolute density of virgin adsorbents and raw materials (\*)

<b>Adsorbent Type</b>	<b>PGP</b>	<b>CGP5</b>	<b>CGP10</b>	<b>CGP15</b>	<b>CGP20</b>	<b>MGP5</b>	<b>FZ</b>	<b>MgO</b>
<b>Chamber Insert (cm<sup>3</sup>)</b>	3.5	3.5	1.0	1.0	1.0	3.5	3.5	3.5
<b>Sample Mass (g)</b>	2.56	2.30	0.68	0.867	0.37	2.95	-	1.66
<b>Volume (cm<sup>3</sup>)</b>	1.27	1.05	0.31	0.42	0.16	1.51	3.20	0.56
<b>Density (g/cm<sup>3</sup>)</b>	2.01	2.20	2.22	2.06	2.33	1.95	2.23	2.97
<b>Total Pore Volume (cm<sup>3</sup>/g)</b>	0.50	0.55	0.55	0.51	0.57	0.49	0.55	-
<b>Porosity (%)</b>	50.36	54.46	54.86	51.36	57.05	48.62	55.14	66.30

*\*Average values over 50-50 purge-cycle sequence.*

#### **4.1.4. Porosity and Permeability**

For porosity, 3 Flex Surface Characterization Analyzer (Micromeritics, Norcross, GA), a tool for obtaining high resolution adsorption, desorption and isotherms are used. It is used in this study was mainly for understanding the microporous and mesoporous structures in metakaolin based K-geopolymers. All six types of geopolymer structures are first tested with 3Flex It was combined with Autopore V, Mercury Intrusion Porosimetry (Micromeritics, Norcross, GA) which was used to investigate the complete range of pore sizes (micropores to macropores). Mercury intrusion into the porous structure in a pressure controlled environment is the basis of mercury porosimetry analysis, a method applied in porosity and permeability studies.

Porosity and surface area are physical properties that can alter the performance of the solid materials focused on this research. The porosity of the samples is the key variable to understand the surface area of the geopolymer composites which can help in tailoring the structure. Materials used in this research are going to be used as adsorbents, therefore having a porous structure and larger surface area is favored for this purpose.

BET (Brunauer–Emmett–Teller) analysis applied to obtain data through multilayer gas adsorption and get a detailed surface area evaluation. The technique covers external and pore area evaluation in order to determine the total specific surface area (as  $\text{m}^2/\text{g}$ ). Barrett-Joyner-Halenda (BJH) analysis was also employed to calculate pore area and specific pore volumes through adsorption and desorption. Pore size distribution is then calculated independently from the external area with the help of the particle size of the sample.

MIP analysis was performed to collect pore size distribution and porosity data by applying a wide range of pressure incrementally into a material that is immersed in mercury. External pressure is used for mercury to penetrate pores, understand pore structure via the information gathered with the help of the high contact angle of mercury with surfaces and its high surface tension. Calculations are based on the volume of mercury intrudes into sample material for each relative pressure increment. The pressure is changed according to user-defined steps that define the resolution while the volume of mercury intruded into pores is measured by a mercury penetrometer that is an electrical capacitance dilatometer. Although the working pressure can be high in order to allow mercury mobilization through pores and interconnected pores, using a liquid media instead of gas faces physical limitations for gathering information about smaller pores.

Before 3Flex analysis took place, samples are crushed and sieved into particle sizes ranging from 500 $\mu$ m to 1mm. Samples are weighed carefully and degassed by inert gases before analysis to remove any impurities. N<sub>2</sub> was used as an analysis of adsorptive gas with incremental pressure with a step size of 0.01. Adsorption isotherms are obtained at liquid nitrogen temperature 77 K. The equilibrium interval was set to 60 seconds.

For MIP analysis, fully intact adsorbent balls are placed in a penetrometer for degassing prior to the analysis. The analysis is held in two parts, low-pressure and high-pressure where the low pressure region is set to 1psi-50psi and the high-pressure region 50psi-60,000 psi. 50 psi is the transitioning pressure. Pressure increments are set in a way to collect 25 data points from 0 to 10 psi and 10 psi to 100 psi each.

Table 4. 3. BET surface area values of virgin samples

Sample	BET Surface Area (m <sup>2</sup> /g)	Average pore diameter (4V/A by BET) (Å)	
		Adsorption	Desorption
<b>PGP</b>	98.75	36.78	47.02
<b>CGP5</b>	69.78	44.16	58.82
<b>CGP10</b>	62.79	43.26	54.20
<b>CGP15</b>	51.01	43.25	56.83
<b>CGP20</b>	22.76	35.51	41.92
<b>MGP5</b>	170.63	20.78	22.46
<b>Fine Clinoptilolite</b>	15.30	29.08	46.72

From Table 4. 3, BET surface area is observed the highest was in MGP5 composites and It is followed by pure geopolymers. Clinoptilolite addition to geopolymeric structure resulted in lower surface area values.

Cumulative adsorption graph showing the pore size distribution of geopolymers are given in Figure 4. 5. A decrease in pore volume as increasing clinoptilolite addition is apparent in this figure. Differential pore volume on desorption given in Appendix B. indicate gas, giving more information about the dominant pore size throughout the related sample. Sharp peaks are an indicator of leaving gas. This graph is an indicator of a less cumulative pore volume for CGP20 samples.

CGP5, 10 and 15 are showing similar trends with decreasing cumulative pore volume although pore size corresponding to these values is similar. MGP5 has a similar cumulative pore volume to CGP10 composite where corresponding pore diameter is much lower, concentrated in micropore region. In mesopores region CGP composites show very similar characteristics except CGP20.

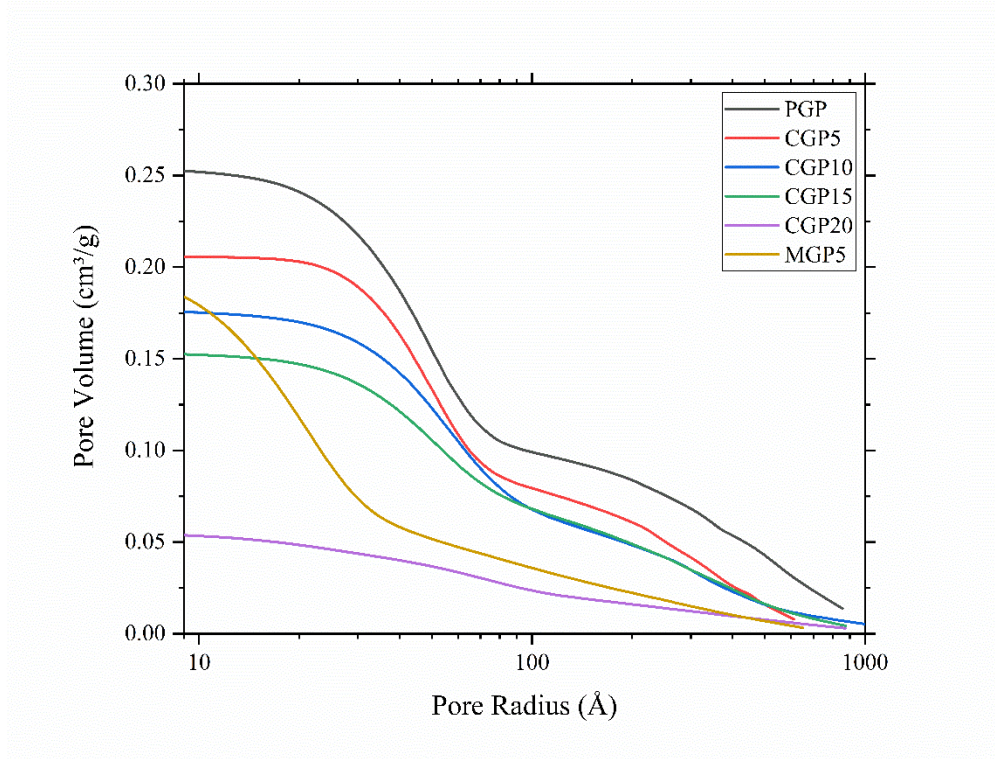


Figure 4. 5. Comparison of cumulative pore volume ( $\text{cm}^3/\text{g}$ ) and pore radius ( $\text{\AA}$ ) for all geopolymer types.

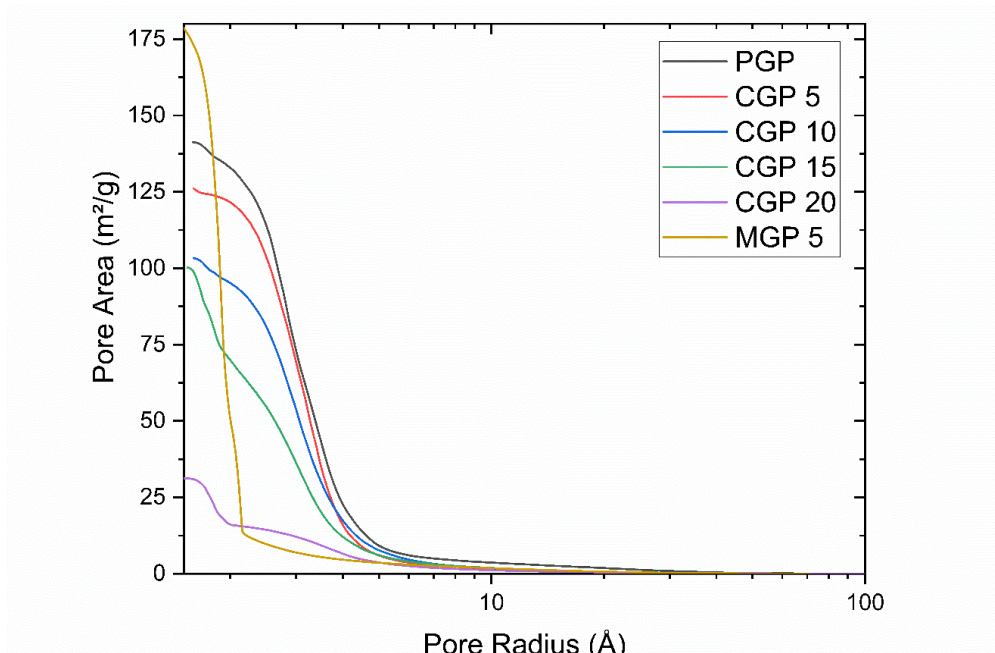


Figure 4. 6. Cumulative pore area ( $\text{cm}^3/\text{g} \cdot \text{\AA}$ ) and pore radius ( $\text{\AA}$ ) comparison for all geopolymer types

It is clear in Figure 4. 5that PGP has a larger cumulative pore area pore radius than every other type of composite. By looking at both adsorption and desorption cycles, pore size distribution can be interpreted as ranging between 2-10 nm for PGP samples. Although graphical representation gives information, visual interpretation can mislead in evaluating results. By looking at Table 4. 3, average pore diameter for PGP through adsorption and desorption cycles 3.7 and 4.7 nm, clinoptilolite geopolymer composite with 5 volume % 4.4 and 5.9 nm. Average pore diameter decreases as clinoptilolite is added in geopolymer composites.

MIP results are represented in Figure 4. 7 and Table 4. 4, where incremental intrusion compared to pore diameter (log scale). Permeability and porosity information obtained from mercury intrusion can help to interpret the information obtained from gas adsorption studies and vice versa.

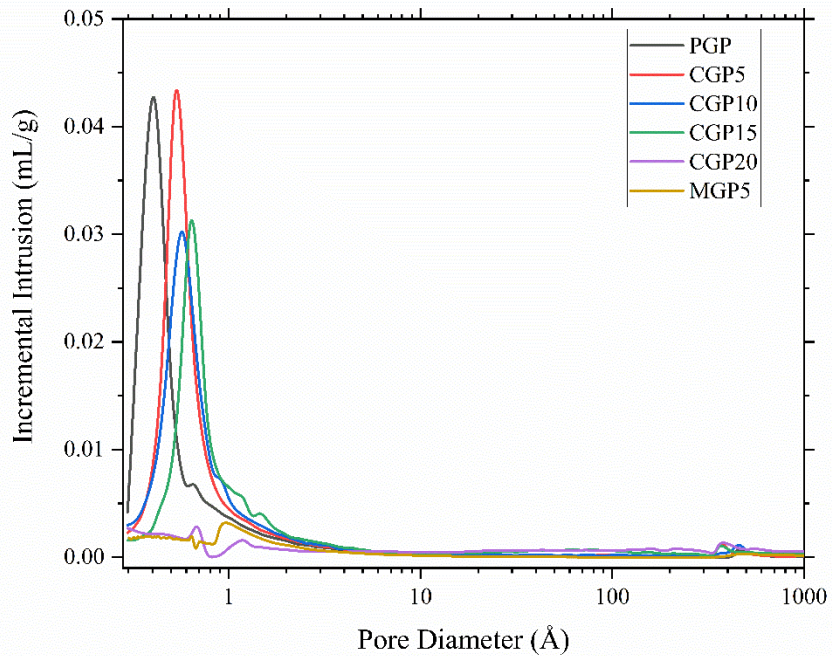


Figure 4. 7. Incremental intrusion (mL/g) and Pore Diameter (Å) comparison for all composite types.

It should be noted that the gas adsorption study in this research should be taken into account when interpreting a microporous structure. Moreover, mercury intrusion gives a broader understanding of the connectivity of the pore structure in adsorbents. Table 4. 4 summarizes the findings from mercury intrusion testing including permeability and tortuosity.

Table 4. 4. Porosity and permeability results obtained from mercury intrusion porosimetry experiments

<b>Sample</b>	<b>Porosity (%)</b>	<b>Permeability (mdarcy)</b>	<b>Tortuosity</b>
<b>PGP</b>	34.76	21.37	4.19
<b>CGP5</b>	34.56	53.24	3.82
<b>CGP10</b>	32.60	23.00	5.04
<b>CGP15</b>	32.02	76.58	4.03
<b>CGP20</b>	14.33	129.81	4.77
<b>MGP5</b>	14.83	2.65	6.88
<b>Fine Clinoptilolite</b>	50.30	1357.43	4.31

From Table 4. 4, the effect of clinoptilolite addition on overall porosity where it showed a notable decrease. On the other hand, permeability and tortuosity of adsorbents increased. CGP 10 can be taken as an outlier where it doesn't follow the increased permeability and tortuosity trend among clinoptilolite incorporated geopolymers where increasing clinoptilolite incorporation resulted in increased permeability and tortuosity. More detailed information can be gathered from the adsorption and desorption cycles for gas adsorption and MIP that are given in Appendix B



#### **4.1.5. Scanning Electron Microscopy (SEM)**

Not only for the chemistry of the materials, but scanning electron microscopy can also be used to investigate the microstructure as well. For this purpose, SEM (Hitachi S-4800/FE-SEM) is employed in the characterization of the surface of the adsorbents. While the sample surface is scanned by an electron beam, image is collected in a raster pattern. Imaging raw materials and virgin samples by SEM was very helpful during research in terms of identifying some of the features present in the adsorbent. Also, the method assisted to understand how geopolymerization took place before looking at the chemical composition of the samples.

In this subchapter SEM images of fine zeolites, metakaolin powder and all six types of virgin samples are represented to explain the main characteristics of metakaolin based geopolymers. It is important to point out the differences that can be observed in pure geopolymer samples and clinoptilolite and/or MgO geopolymer composites. The following paragraphs will be used to explain those features along with corresponding images.

##### ***Sample Preparation and Operation***

To analyze virgin adsorbents by SEM, they have to be impregnated with epoxy. CitoVac (Struers Inc., Cleveland, OH) is used to embed adsorbent balls. First, mounting cups having 25mm diameter were cleaned (degreased), then they are covered with Release Agent (Buehler, Lake Bluff, IL). After getting molds ready, adsorbents are placed in mounting cups where they are then filled with cold-setting epoxy resin. Resin is prepared by mixing EpoFix Resin with EpoFix Hardener with a mixing ratio of 25:3 by weight. Following the

molding step, samples are cured overnight at room temperature. Cured samples are cut with a slow action diamond saw (Minitom, Struers Inc., Cleveland, OH) to obtain samples that are short enough to fit in the sample chamber in SEM. As the final step of sample preparation for SEM imaging, mechanical polishing is done (started with SiC paper of 85 microns and finished with colloidal silica of 0.04 microns) to epoxy mounted adsorbents using LaboPol-35. For virgin samples, polishing is performed to the point where the surface had a mirror like appearance. Samples embedded in epoxy are then coated with carbon to make them electrically grounded and prevent charging. Coating thickness is estimated to be around 90nm according to profilometer measurements taken after 2 seconds of evaporation time.

Metakaolin and clinoptilolite samples are studied simply by pressing the sample stub with double-sided carbon tape on it into powders of raw materials. After purging the stubs with compressed air, samples are then coated with carbon the same way. Clinoptilolite with particle size smaller than  $45\mu\text{m}$  presented in Figure 4. 8, metakaolin powder is presented in Figure 4. 9 where images were captured in higher magnification to show its platy structure. Figure 4. 10 shows pure geopolymer structure identified through SEM imaging where effective incorporation of in geopolymer structure

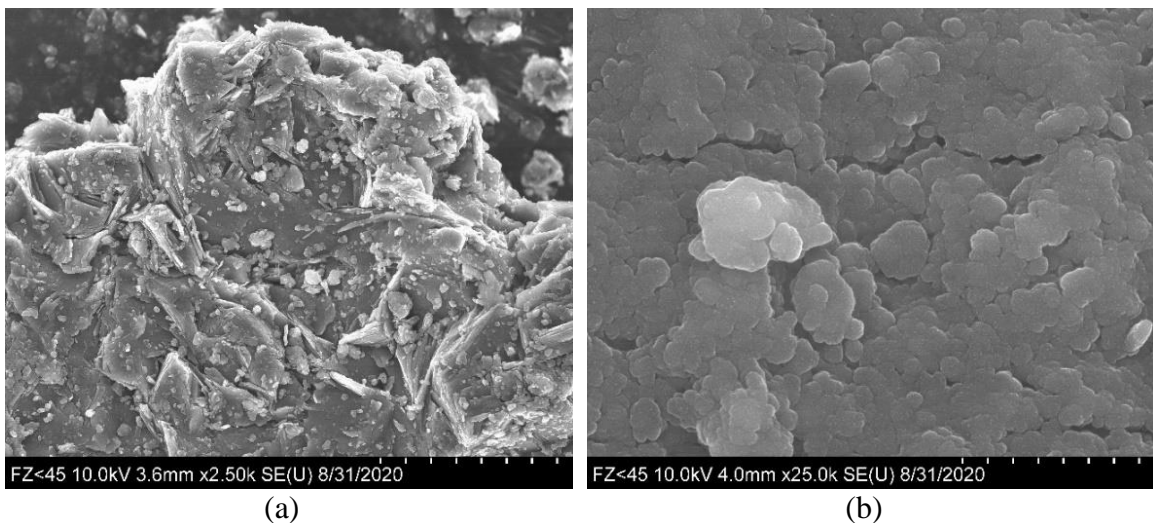


Figure 4. 8. (a) Clinoptilolite at low magnification, (b) Clinoptilolite at x25k

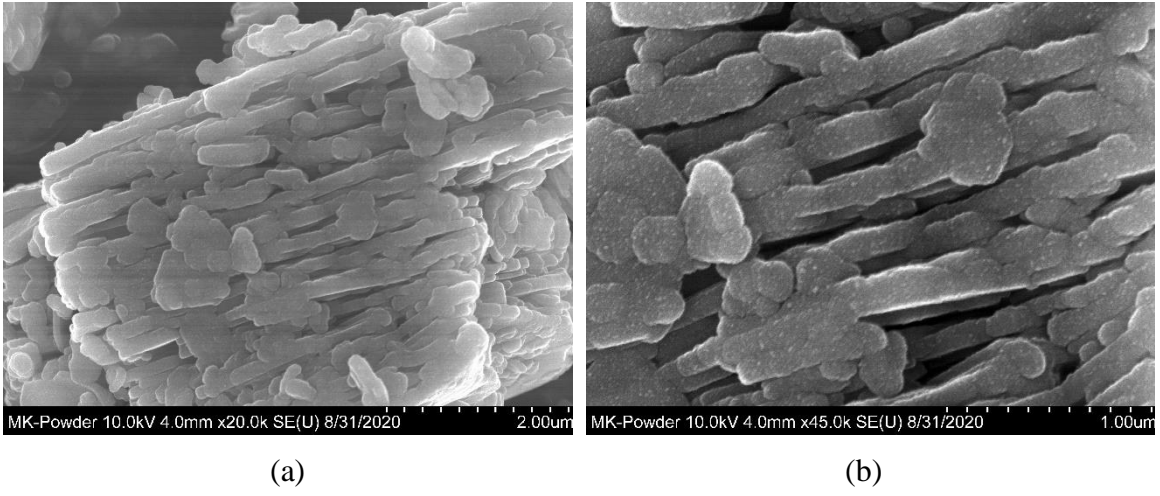


Figure 4. 9. Metakaolin powder x20k (left) and x45k (right)

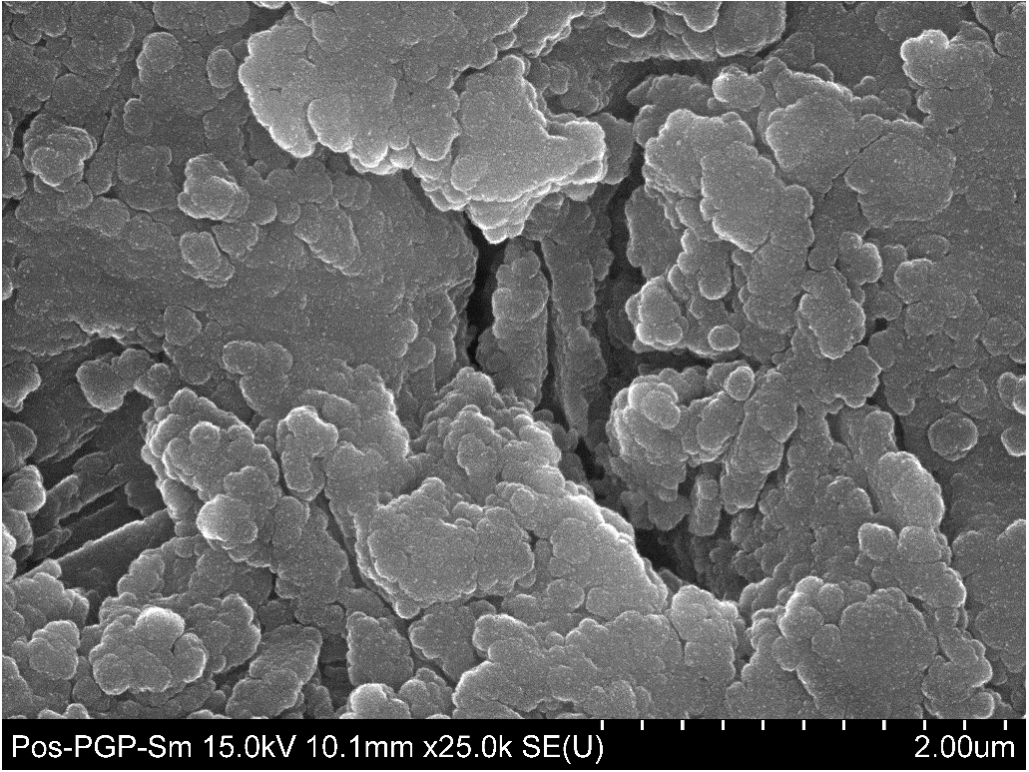


Figure 4. 10. SEM image of pure geopolymer taken at x25.0k, 15.0kV.

## **4.2. Elemental Composition**

### **4.2.1. Wavelength Dispersive X-Ray Fluorescence (WDXRF)**

Virgin samples are investigated in terms of their elemental composition with the help of Rigaku Primus IV Wavelength Dispersive X-Ray Fluorescence (WDXRF). Six virgin samples that already have been mounted with epoxy are used for this analysis. After polishing it into a flat, mirror like surface, they were analyzed by the EZ method. The method lets users scan an area defined by a user (selected by checking a mask that is used) for a wide range of elements (from B to U). Results are given in Table 4. 5 for virgin samples. Detailed analysis is done and will be presented in upcoming chapters to compare before and after use conditions on adsorbent samples. According to Table 4. 5, pure geopolymer and MGP5 is showing a very similar composition to the theoretical formulation of the composites. Since stoichiometric metakaolin and alkaline solution Targeted ratios for geopolymers were  $\text{Si/Al} = 2.0$  and  $\text{K/Al} = 1.0$ , therefore, results show satisfactory numbers

Table 4. 5. Elemental composition of geopolymer adsorbents measured by WDXRF

<b>Component</b>	<b>PGP</b>	<b>CGP5</b>	<b>CGP10</b>	<b>CGP15</b>	<b>CGP20</b>	<b>MGP5</b>
<b>SiO<sub>2</sub></b>	43.200	38.500	40.500	36.300	32.100	41.400
<b>Al<sub>2</sub>O<sub>3</sub></b>	20.800	18.100	17.800	13.300	12.700	20.100
<b>K<sub>2</sub>O</b>	17.400	15.800	14.000	19.000	16.300	16.600
<b>P<sub>2</sub>O<sub>5</sub></b>	0.025	0.024	0.022	0.027	0.021	0.024
<b>MgO</b>	Trace	0.045	0.079	0.088	0.095	8.210
<b>TiO<sub>2</sub></b>	0.748	0.563	0.574	0.448	0.420	0.677
<b>Fe<sub>2</sub>O<sub>3</sub></b>	0.174	0.211	0.268	0.296	0.345	0.175
<b>Na<sub>2</sub>O</b>	0.143	0.510	0.503	0.532	0.758	0.169
<b>CaO</b>	0.012	0.287	0.632	0.839	0.794	0.020
<b>Cl</b>	0.092	0.082	0.210	0.067	0.181	0.054
<b>SO<sub>3</sub></b>	0.073	0.117	0.084	0.053	0.038	0.061
<b>ZrO<sub>2</sub></b>	0.006	0.007	0.007	0.008	0.007	0.005
<b>Ga<sub>2</sub>O<sub>3</sub></b>	0.005	0.003	0.003	-	0.006	0.004
<b>SrO</b>	0.004	0.006	0.008	0.012	0.015	0.004
<b>Nb<sub>2</sub>O<sub>5</sub></b>	0.003	0.003	0.002	0.003	-	0.003
<b>Rb<sub>2</sub>O</b>	-	0.003	0.005	0.005	0.006	-

### 4.3. Summary

In this section, materials characterization tools utilizing the surface and subsurface structure of geopolymers. Geopolymer slurry having the formulation  $4\text{SiO}_2 \cdot \text{Al}_2\text{O}_3 \cdot \text{K}_2\text{O} \cdot 11\text{H}_2\text{O}$  is used to make pure geopolymer adsorbents, CGPs with adding clinoptilolite of 5, 10, 15, 20% by volume and MGP by adding MgO of 5% by volume. Those adsorbent types are investigated according to their mechanical strength, physical properties like density, appearance, porosity, permeability and surface areas.

Climate conditions have been set to 40°C and 80% relative humidity and duration set to 72 hours for curing. Revising and optimizing the curing conditions into stated numbers have resulted in increased integrity of the samples.

The structure is observed through optical microscopy to see geopolymer matrix and additive distribution. SEM imaging of pure geopolymer was observed to identify the metakaolin incorporation with the geopolymer phase. Platy appearance of geopolymers showed similarities to metakaolin which demonstrated that incorporation was achieved.

Porosity and permeability measurements performed by gas adsorption coupled with the mercury intrusion method. Results have shown the pore size distribution averages between 2 – 5nm. Porous structure was predominant for MGP according to the gas adsorption method, however, this wasn't supported with mercury intrusion porosimetry. CGP composites have shown larger pore diameters. However increasing clinoptilolite content decreased porosimetry in both techniques used. The surface area has decreased proportionally in clinoptilolite incorporated geopolymers from 69% to 22%. Pure

geopolymer is promising in terms of porosity. Considering smaller pore size is more preferable to achieve larger surface area on each adsorbent ball MGP was found to have the most desirable structure in terms of this issue, however, the finding wasn't supported by mercury intrusion porosimetry. Since the study itself didn't focus solely on tailoring fine details on adsorbent balls except for their endurance to stress and keeping their integrity, further research should conduct in the future.

An important detail, achieving the targeted stoichiometric composition of the final product. The preparation step is straightforward but the actual composition of geopolymer adsorbent may differ from what is expected. Hence this problem can affect the mechanical and chemical properties of the final product. From XRF and EDS results. it can be seen that desired ratios are achieved during processing.

## CHAPTER V

### AMMONIUM REMOVAL BY PURE GEOPOLYMER AND CLINOPTILOLITE- GEOPOLYMER COMPOSITES

The purpose of this study was to report the effect of the amount of clinoptilolite incorporated in geopolymers on removing nutrients from model solutions. Performance of pure geopolymer (geopolymer without any incorporation) and clinoptilolite added composites (CGP) were compared in terms of their removal efficiencies once they are used in batch adsorbent studies. The study held in two parts; examining pH evolution in model solutions once adsorbent material was used and testing the ammonium nitrogen removal by adsorption. Both cases are studied with PGP and CGP to detect the effect of additives on absorbance capacities. This stage of the research has been structured to reach the following objectives;

- Effect of PGP and CGP composites on the pH of the model solutions.
- Observing PGP behavior on nutrient removal
- Effect of clinoptilolite incorporation into geopolymers on their removal performances compared to pure geopolymers on nitrogen removal.

The aforementioned method in Chapter 3 is applied to make geopolymer composites having  $4\text{SiO}_2 \cdot \text{Al}_2\text{O}_3 \cdot \text{K}_2\text{O} \cdot n\text{H}_2\text{O}$  composition where n is 11. Later this composition was used as the matrix phase for clinoptilolite to be mixed in by 5%, 10%, 15% and 20% by



volume. Model solutions are prepared by dissolving an adequate amount of ammonium chloride ( $\text{NH}_4\text{Cl}$ ) in DI water, analytical tools are used to determine final concentrations and water quality measurements. Model solutions are prepared in 500 mL and mixed at a fixed speed in benchtop agitator set up shown in Figure 5. 1. Characterization tools, XRF, is adapted to observe and trace down the nutrients on the adsorbent body.



Figure 5. 1. Agitator setup of six having triplicate solutions of each batch adsorption test. Two sets of adsorption experiments can be run at the same time. (Velp Scientifica, Bohemia, NY)

### **5.1. Composite Processing**

Composites created are based on the geopolymer synthesis method that is shown earlier. Clinoptilolite particles that are sieved into particle sizes ranging from 106 to 212 $\mu$ m are incorporated by mixing. Four types of composites are processed by mixing clinoptilolite with 5, 10, 15 and 20% volume ratio. Larger amounts could be incorporated depending on several parameters such as molarity of waterglass solution used, mixing duration, mixing speed, etc. However, the amount of clinoptilolite was limited to 20% by volume due to workability issues.

### **5.2. Model Solutions**

Nutrient concentrations reported on chicken manure as a dry basis is used as the reference for deciding solution concentration. [15], [16], [22] To replicate the concentration  $\text{NH}_4\text{Cl}$  salt, with water solubility of 39.5 g/100 g  $\text{H}_2\text{O}$ , is dissolved in 500 ml of pure grade water.[64] Method for making model solutions are adapted from EPA Method 350.1, a calibration curve is also created for introducing user defined programs to UV-Vis instrument used in this study. With dissolving an adequate amount of  $\text{NH}_4\text{Cl}$ , a model solution having a concentration of 1 g/L as  $\text{NH}_3\text{-N}$  was prepared.  $\text{NH}_4\text{Cl}$  was kept in a drying oven set to 105  $^\circ\text{C}$  to remove any moisture content before dissolving. Solutions were prepared as triplicates to achieve reliable results.

### **5.3. Batch Adsorption Study**

In the previous sections, the preparation of model solutions and composite processing were mentioned. This section is to describe the experimental procedure that is followed and

explain reporting nitrogen removal from model solutions and to present the findings tested using the UV-Vis method.

To test adsorbent efficiencies on nutrient removal, model solutions are prepared in triplicates as described earlier. Prepared solutions are agitated for ten minutes in volumetric flasks, it was made sure that salt is completely dissolved. This procedure is followed by adding six adsorbent balls to each beaker and beakers are mixed at a fixed speed of 60 rpm. In batch adsorptions, studies only one concentration of the model solution is selected. Mass of adsorbent materials placed in flasks was ranging between 21-25 grams, changing according to composite composition. Adsorption experiment considered initialized as soon as adsorbent material placed in beakers.

Sampling was made in the first 10, 20, 30, 45 minutes and every hour after 60 minutes until the end of 8 hours of the experiment. Beakers left overnight at mixing conditions and another sampling is done at the end of 24 hours of the experiment. Consecutively, model solutions are tested for their water quality parameters; pH, total dissolved solids (TDS), conductivity, ionic strength and results are presented in Appendix C.

Samples are collected and tested for their final concentration by using UV-Vis (HACH DR/4000, Loveland, CO) with user defined program which was created earlier after creating and testing stock solutions and their dilutions. Results are also checked through default programs that are already defined by Hach. For this study Method 8038, Nessler Method with a detection limit of 0-2.5 mg/L NH<sub>3</sub>-N was found as suitable for this purpose. This method is also having major compliance with EPA Method 350.1, Determination of Ammonia Nitrogen by Semi-Automated Colorimetry. This is why collected samples are

first diluted into observable range to be able to take measurements through both programs and verified. In this chapter, there are five types of geopolymers tested, PGP and CGP composites for ammonium removal.

#### **5.4. pH Evolution**

pH adjustment was not done in any of the model solutions initially. One reason was to keep track of pH change to point out the leaching of ions. Also, adsorbents are soaked in DI water overnight before batch adsorption studies to observe the pH evolution of adsorbents to remove all soluble species. Figure 5. 2 is summarizing the pH evolution of model solutions when PGP is used as adsorbents for nitrogen, phosphorus and simultaneous removal studies. When PGP is soaked in DI water a day before batch adsorption tests show that there is an increase in pH mainly because of unreacted KOH leaching from geopolymer structure. On the contrary, there is a significant decrease in pH model solutions when PGP is used for adsorption studies where they are immersed in model solutions but the overall trend was in increasing order. Once it was immersed in a model solution where nitrogen and phosphorus ions co-exist, change in pH was relatively similar to individual nutrient removal studies. It has been observed that having nutrient ions in the solution is suppressing the rate of increase in pH. Another outcome of this study is that pH values are not coming stabilizing even after 24 hours.

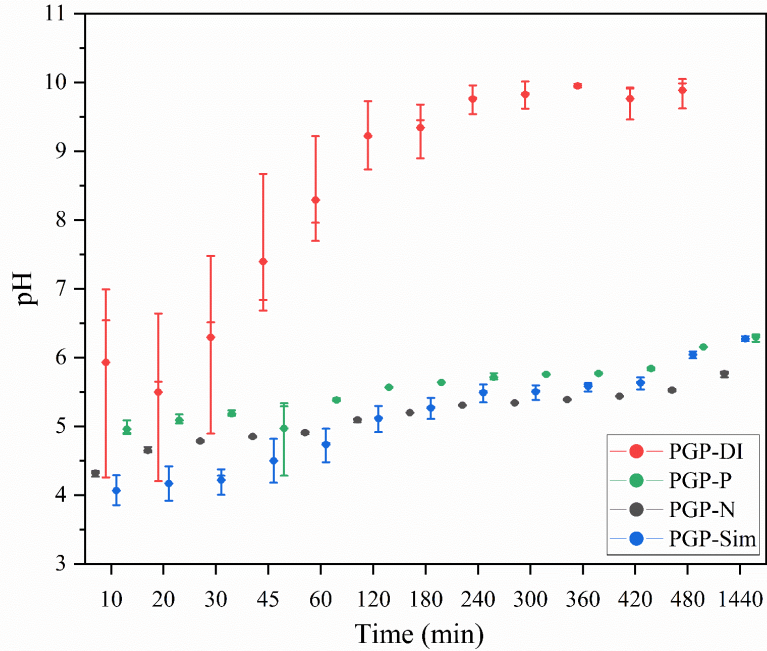


Figure 5. 2. Change of pH over time when pure geopolymer soaked in DI water for 8 hours.

In Figure 5. 3, CGP composites off all four compositions are observed in DI water for 8 hours. It is observed that increasing clinoptilolite addition pH shows more instability at the beginning. However, the rate of increase in pH decreases after the first hour. In Figure 5. 4 on the other hand, pH values are drastically lower than soaking experiments. In contrast to what had been observed during soaking in DI water, adsorbents that are tested in model solutions tend to have lower pH values once again. It can be concluded by looking at pH evolution, even after 24 hours of experimentation pH is not stabilizing in sets of experiments that are performed in model solutions. This is an indicator of ongoing ion exchange and there are ions still effective on decreasing solution pH.

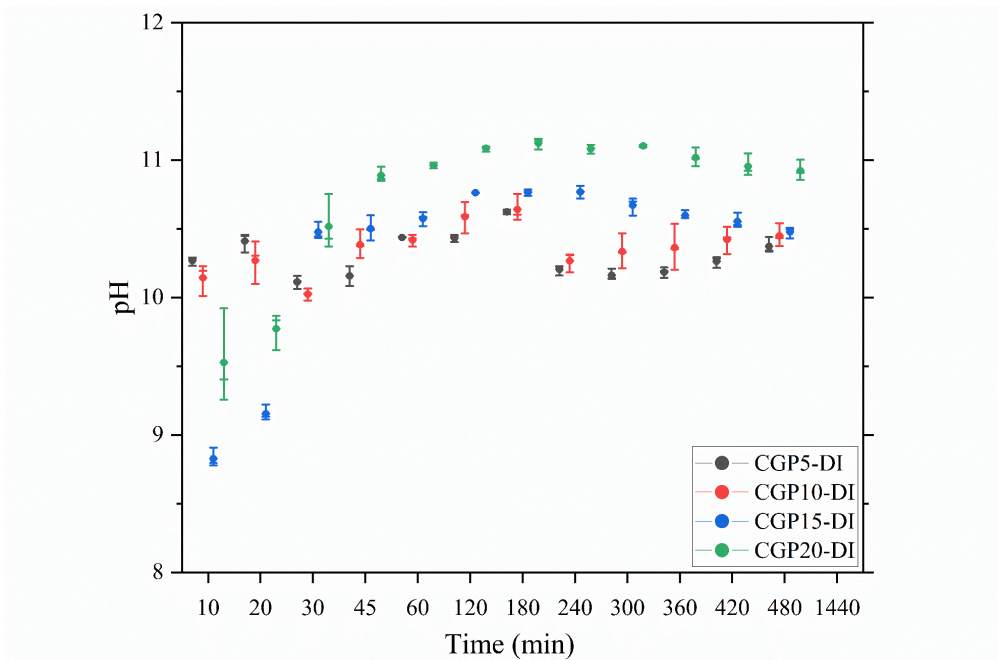


Figure 5. 3. Change in pH over time when CGP composite is soaked in DI water for 8 hours.

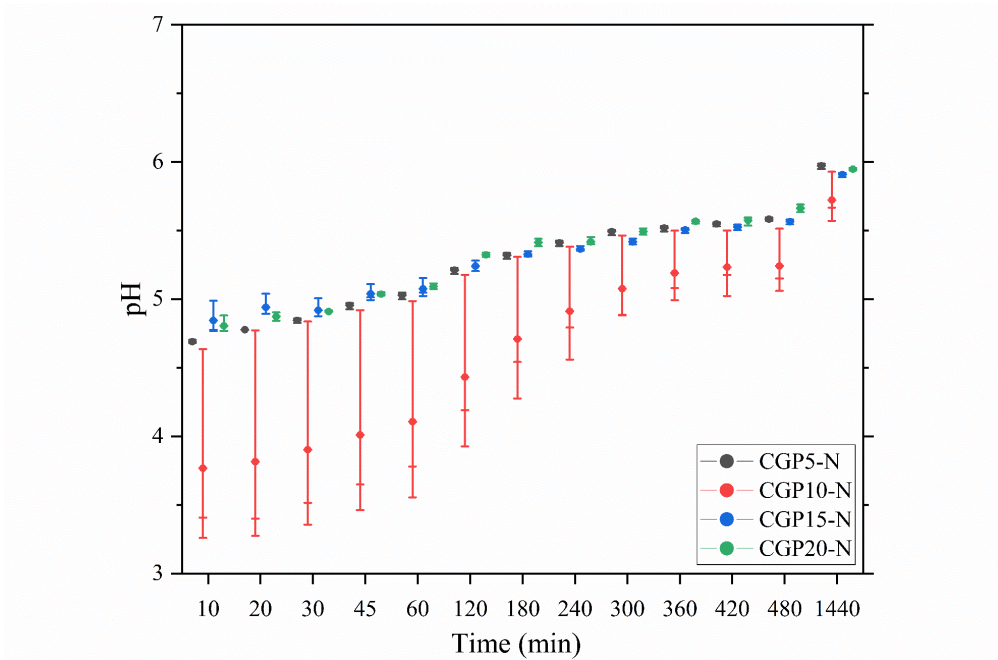


Figure 5. 4. Change in pH over time when CGP composite is used as an adsorbent in model solutions with nitrogen.

## 5.5. Ammonium Removal

Ammonium removal studies are performed as described at the beginning of this chapter. Model solutions are prepared with having nitrogen content as 1 g/L as  $\text{NH}_3\text{-N}$  at the beginning. Batch adsorption study started once all 6 adsorbent balls were immersed in homogeneously mixed solutions. Mass of adsorbents used is given in Table 5. 1. Additionally, beakers were kept in stirrer for 24 hours and samples have collected in intervals stated earlier. Figure 5. 5 shows the final nitrogen concentration in model solutions as  $\text{NH}_3\text{-N}$  at particular times.

Table 5. 1. Mass of adsorbents used in each replicate of batch adsorption study

	<b>PGP</b>	<b>CGP5</b>	<b>CGP10</b>	<b>CGP15</b>	<b>CGP20</b>
<b>Batch Adsorption Study I</b>	23.63	24.93	23.9	24.52	21.77
<b>Batch Adsorption Study II</b>	23.66	24.48	23.72	24	21.88
<b>Batch Adsorption Study III</b>	23.37	24.53	23.77	24.34	22.44
<b>Average Mass of Adsorbent (g)</b>	23.55	24.65	23.80	24.29	22.03

*\*Values for Batch Adsorption Study I-II-III are a total mass of 6 adsorbent balls*



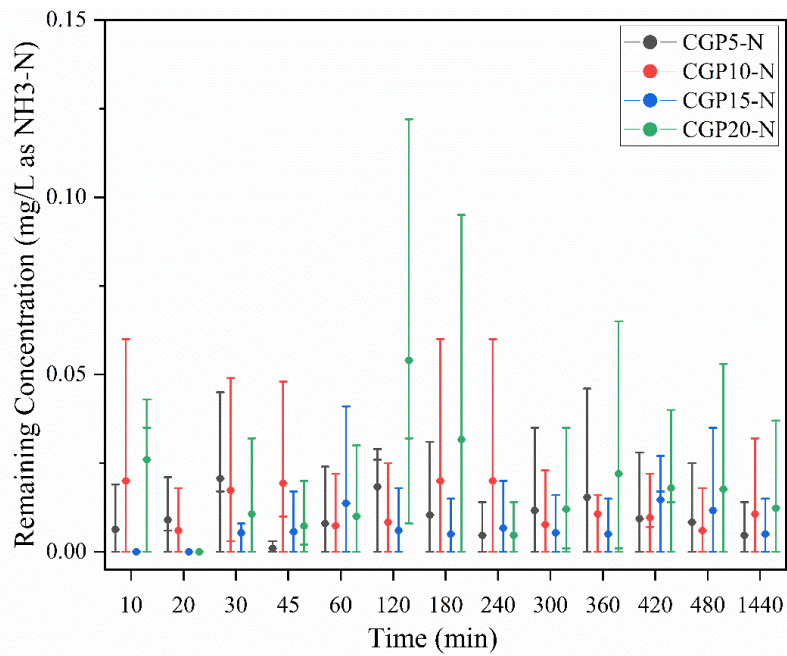
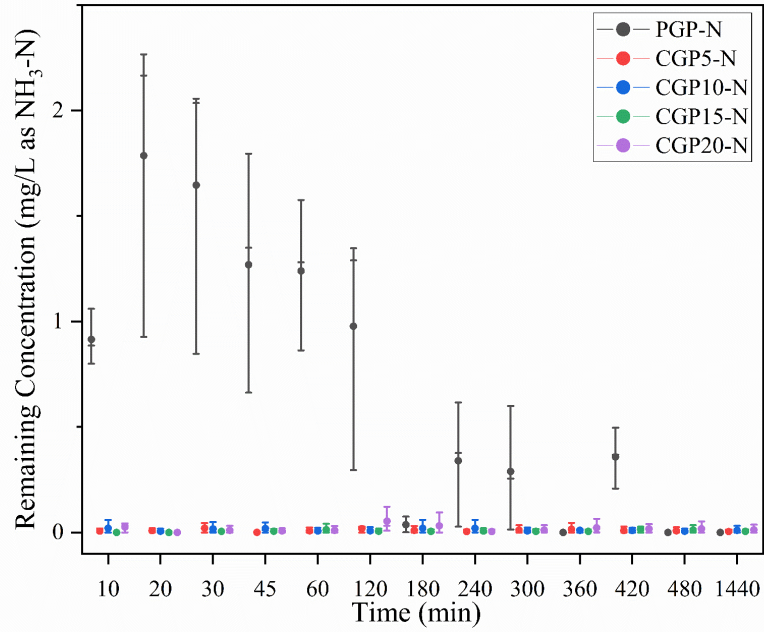


Figure 5. 5. Remaining nitrogen concentration in all studies performed by CGP and PGP (top), by CGP composites only (bottom)



By looking at Figure 5. 5 it can be interpreted that clinoptilolite has a significant effect on overall nitrogen removal. There can be seen some fluctuations, but it is not too significant considering more than 95% removal has been achieved in the first 10 minutes. Pure geopolymer on the other hand shows removal on a certain level after the third hour. That corresponds to its pH levels becoming close to other adsorbents' pH evolution trends. The first three hours in nitrogen removal studies take an important place in model solution pH evolution therefore in nitrogen removal. In Figure 5. 4, it can be seen that difference in pH is decreased in time with different CGP compositions. Likewise, stabilization can be observed in Figure 5. 2 where pH comes to a slower rate of increase when PGP was the adsorbent. Overall, CGP in all four compositions has given satisfactory results in terms of ammonium removal, up to %100 at times and the lowest being 5.1%. These numbers can be looked at in Table 5. 2 where removal percentages calculated according to the following equation and averaged for all three replicates;

$$\text{Removal efficiency \%} = \frac{(C_0 - C_t)}{C_0} \times 100$$

where  $C_0$  (mg/L) is the initial concentration and  $C_t$  (mg/L) is the concentration at time  $t$  (min).

Table 5. 2. Average ammonium nitrogen removal from model solutions by percentage

<b>Time (min)</b>	<b>PGP</b>	<b>CGP5</b>	<b>CGP10</b>	<b>CGP15</b>	<b>CGP20</b>
10	10.47	99.37	98.00	100.00	97.40
20	2.43	99.10	99.40	100.00	100.00
30	5.10	97.93	98.27	99.47	98.93
45	11.23	99.90	98.07	99.43	99.27
60	4.57	99.20	99.27	98.63	99.00
120	23.47	98.17	99.17	99.40	94.60
180	96.30	98.97	98.00	99.50	96.83
240	66.00	99.53	98.00	99.33	99.53
300	71.07	98.83	99.23	99.47	98.80
360	100.00	98.47	98.93	99.50	97.80
420	64.20	99.07	99.03	98.53	98.20
480	100.00	99.17	99.40	98.83	98.23
1440	100.00	99.53	99.37	99.50	98.77

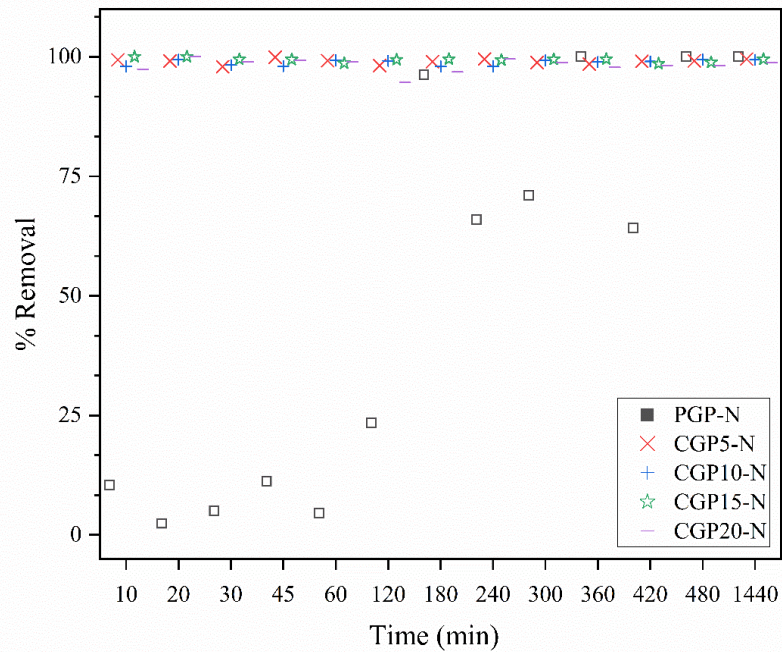


Figure 5. 6. Percent removal of nitrogen in model solutions over time.

XRF was used for investigating nitrogen presence on the geopolymer. It was assumed that adsorbed nitrogen is distributed evenly on all six balls in volumetric flasks. According to that assumption, mapping is performed using a line scan. To be able to perform it, samples are embedded in epoxy, cut and polished. Samples are dried in a vacuum oven prior to testing. Line scan is set to map the cross-section of adsorbent balls. Line scans obtained from virgin and post-evaluation composites are compared according to the measurement points and element concentration from the surface to the core of adsorbent balls.

None of the virgin samples have shown elemental nitrogen initially. Results are presented from Figure 5. 7 and Figure 5. 10

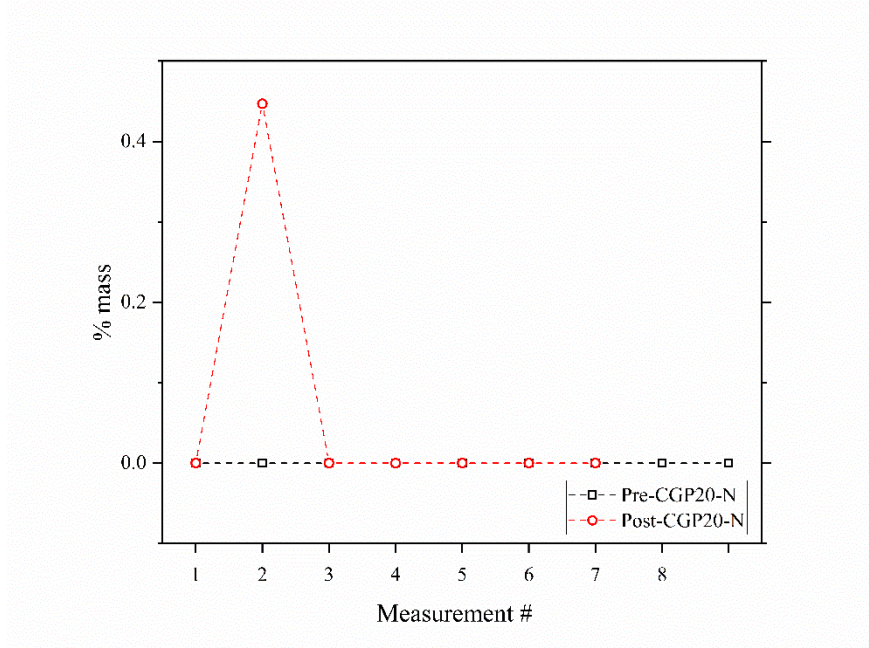
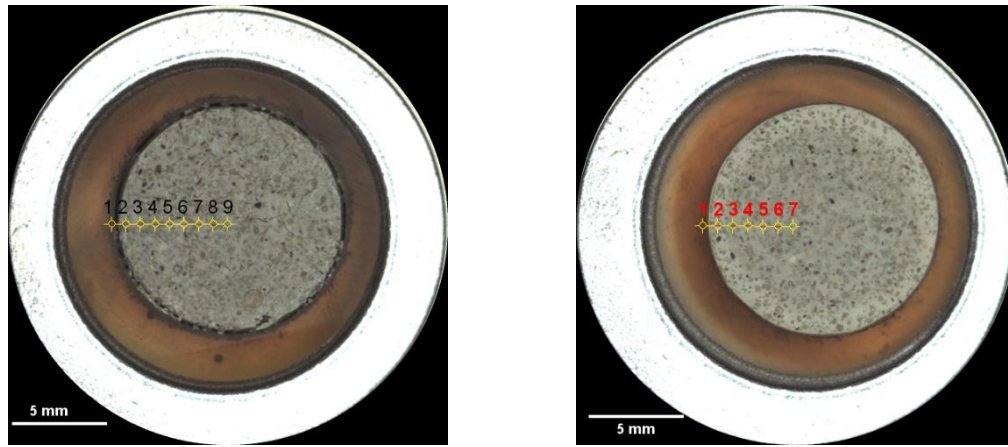


Figure 5. 10. Sampling points in linescan of CGP20 before and after the experiment (top), nitrogen presence in CGP20 before and after nitrogen removal study (bottom)

, the top row showing virgin and post-evaluation samples where the bottom row is showing the comparison of nitrogen content on both samples. It is reported that nitrogen is adsorbed on the surface of composites while in some cases sub-surface detection is also recorded. From observations made for this study, nitrogen is adsorbed on the contact surface of the geopolymer.

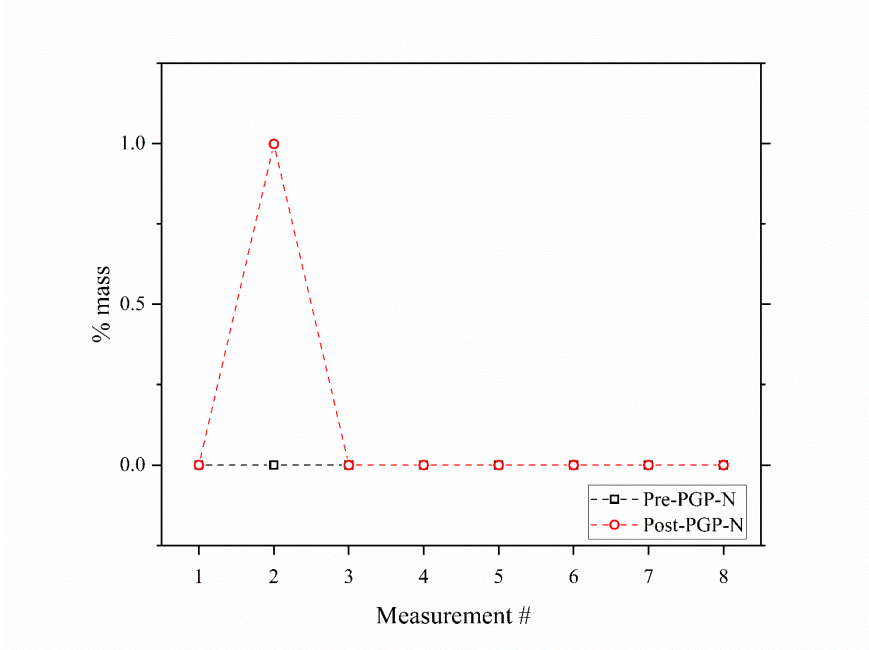
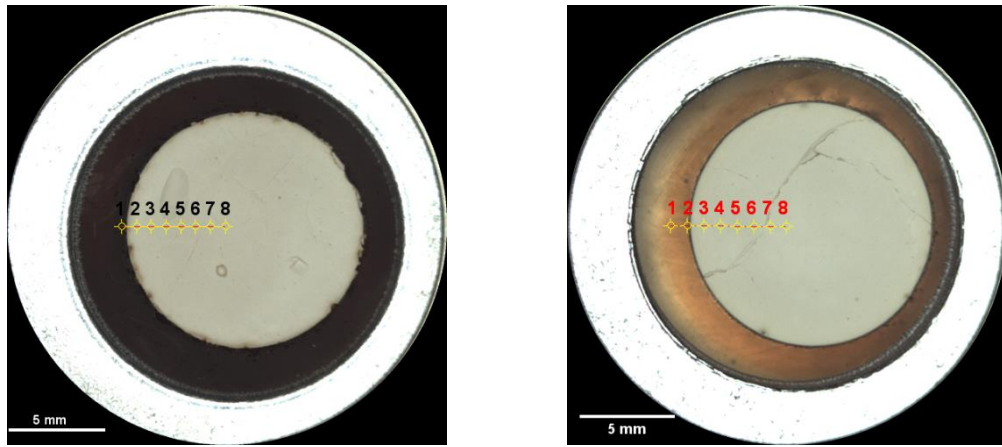


Figure 5. 7. Sampling points in linescan of PGP before and after the experiment (top), nitrogen presence in PGP before and after nitrogen removal study (bottom)



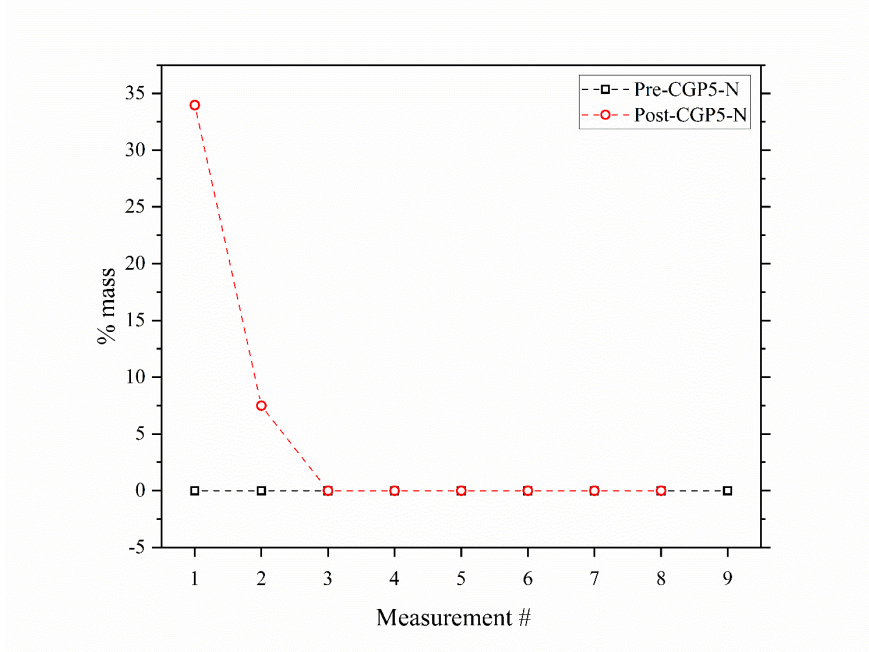
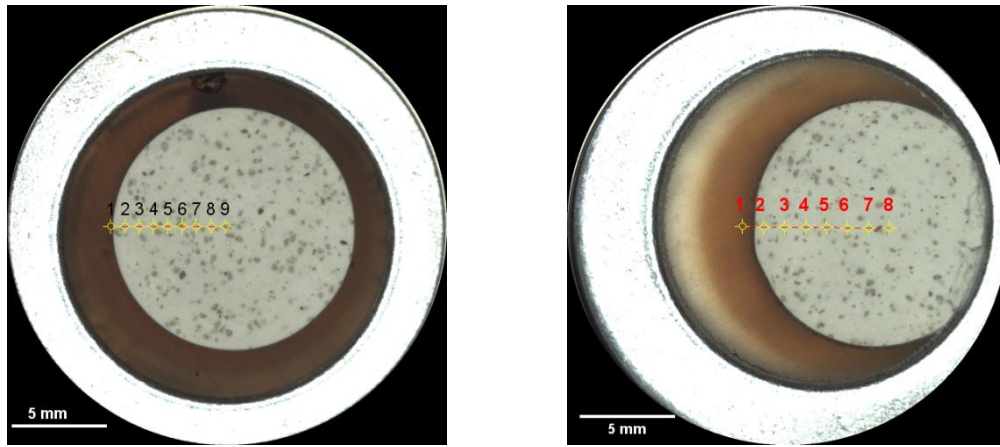


Figure 5. 8. Sampling points in linescan of CGP5 before and after the experiment (top), nitrogen presence in CGP5 before and after nitrogen removal study (bottom)

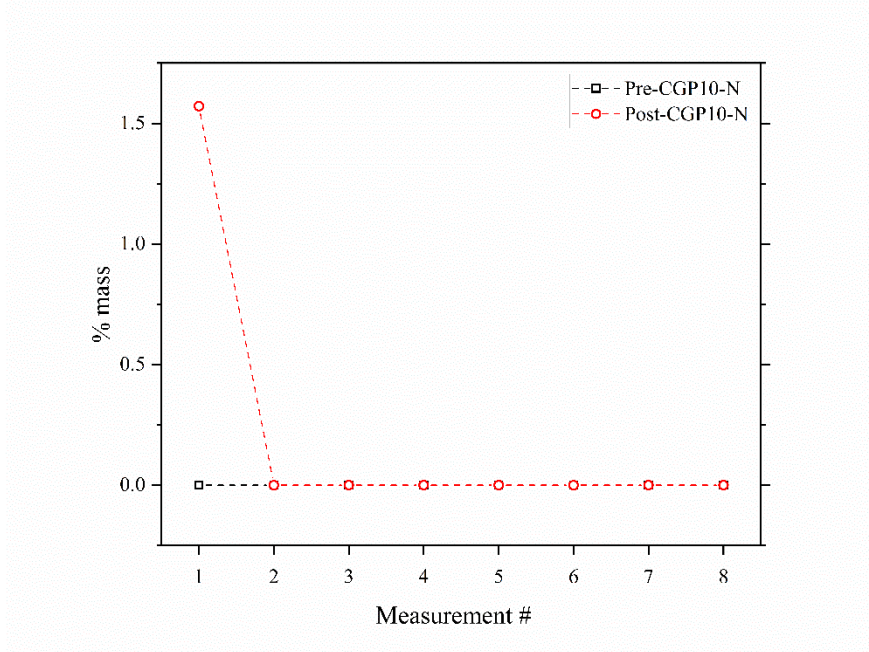
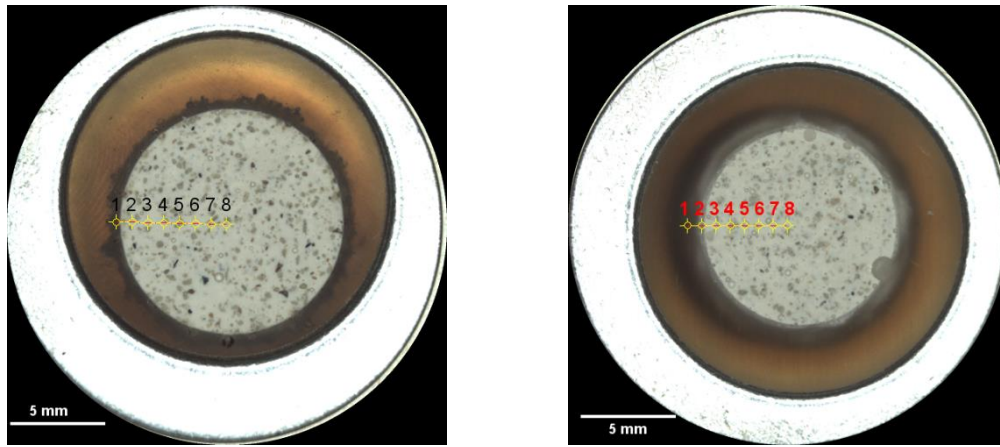


Figure 5. 9. Sampling points in linescan of CGP10 before and after the experiment (top), nitrogen presence in CGP10 before and after nitrogen removal study (bottom)

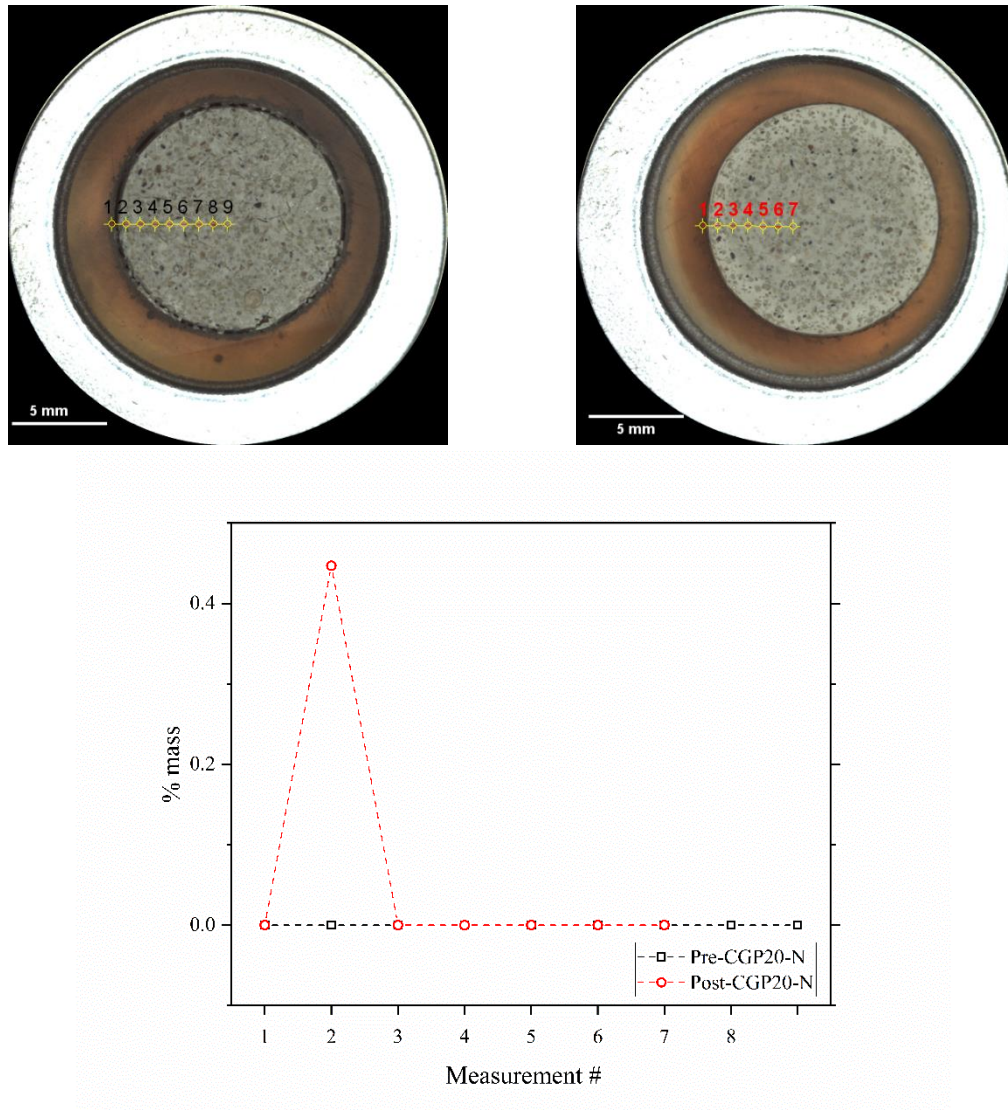


Figure 5. 10. Sampling points in linescan of CGP20 before and after the experiment (top), nitrogen presence in CGP20 before and after nitrogen removal study (bottom)

Line scan is performed starting from epoxy towards to center of the geopolymer. Thus, the first scanned point is not necessarily resulting values to interpret geopolymer structure or any adsorbents. However, points that are followed are in the geopolymer body and according to the figures shown nitrogen is only adsorbed on points that are close to the surface.



## 5.6. Summary

This study is performed to evaluate the use of different geopolymer composites on their ability to remove ammonium from the model solution. Removal studies were performed using PGP and four CGP composites. In addition to removal performances, the effect of geopolymer composite type on solution pH is observed. Results of the pH evolution study are then compared with their impact on pH values of DI water over the same period. Nutrient concentration was not variable throughout the experiments. Thus, the type of geopolymer composite was the key parameter to understand the overall clinoptilolite concentration on removal efficiencies. Comparison of results was a major standpoint to see that effect.

PGP, CGP5, CGP10, CGP15 and CGP20 that are tested for pH evolution tests show that when virgin samples are soaked in DI water in 24 hours pH increases exponentially. After the first hour, the rate of increase in pH becomes lower and final pH readings reached equilibrium quickly. Even though in some cases it starts in the acidic range, pH quickly increases above 9 in all of the tested virgin samples. It is reasonable to conclude that the geopolymer composites have unreacted constituents released into aqueous solutions. On the contrary, when the same geopolymer samples are used in nutrient removal studies they produce lower pH values. Not only staying in acidic range even after 24-hour experimentation model solution, but pH also doesn't reach equilibrium, staying below 7 for all samples. This part of the study takes an important role in understanding the exchangeable ions between the geopolymeric structure and model solutions.

Another key finding of this study was pure geopolymer on ammonium removal efficiency. Removal doesn't take off until the third hour, but eventually reaches up to 100%. This trend can be correlated with pH values reported in the mentioned interval. When pH stabilizes, removal starts taking off and in the pure geopolymer case.

Clinoptilolite, an already well-known cation exchanger, was also effective when it was incorporated into the geopolymeric matrix. With the addition of clinoptilolite in various amounts, removal speed was increased and a large amount of adsorption of above 98% in the first 10 minutes. However, increased clinoptilolite hasn't changed the effectiveness on a larger scale. XRF results have shown that nitrogen adsorption takes place in the first few micrometers of the geopolymer structure. There is no nitrogen occurring on virgin samples while after adsorption studies it was seen on the surface of geopolymers.

## CHAPTER VI

### PHOSPHORUS SEQUESTRATION BY PURE GEOPOLYMER AND CLINOPTILOLITE-GEOPOLYMER COMPOSITES

The performance of geopolymers on anion exchange has not been researched widely due to their net negatively charged structure and their ability on cation exchange. Geopolymers are mentioned as amorphous analogs of zeolites, such as clinoptilolite, therefore they are considered to be cation exchangers as well. Hence, the physical adsorption of phosphates on the surface of geopolymers is not considered as the main path of removal. Instead, precipitation or chemisorption are considered to be the mechanism for the removal of phosphates [65]–[67]. Some phosphorus removal technologies can be listed as chemical precipitation, biological removal, advanced chemical precipitation and crystallization technologies. Additionally, in the early stages of the investigation of phosphorus removal, RIM-NUT, ion exchange and precipitation process (uses a cationic resin followed by an anionic resin) was developed to remove ammonia and phosphate ions by producing crystallites.[68], [69] However, clinoptilolite had investigated for its phosphorus removal efficiencies in the literature and found to be effective on lower levels. Some methods include to make natural zeolites effective on phosphorus removal is to increase the  $\text{Ca}^+$  or  $\text{Mg}^+$  content of the solution or processing adsorbents by modifications to achieve precipitation. [65], [70]. Geopolymers are not extensively tested only for phosphorus

removal and this is one of the major motives of this study. This study focuses on pure geopolymer and clinoptilolite incorporated geopolymers and their phosphorus removal efficiencies. Performance of pure geopolymer (geopolymer without any incorporation) and clinoptilolite added composites (CGP) were compared in terms of their phosphorus removal efficiencies once they are used in batch adsorbent studies. Only three types of composites were selected for this study; PGP, CGP5 and CGP20 to establish a starting point. Comparison to pure geopolymer effectiveness and testing the lowest and highest clinoptilolite composition is aimed to establish the key starting points for future research. Model solutions prepared to have only phosphate ions. The first half of this chapter will focus on pH evolution and the second part will focus on phosphorus removal amounts from model solutions along with XRF and SEM observations.

## **6.1. Model Solutions**

The model solution and replicates are prepared by dissolving  $\text{KH}_2\text{PO}_4$  with water solubility of 168 g/100 g  $\text{H}_2\text{O}$ . [64] Model solutions prepared by dissolving a corresponding amount of potassium dihydrogen phosphate in 500 ml pure water. Method for making model solutions are adapted from EPA Method 365.2, a calibration curve is also created for introducing user defined programs to UV-Vis instrument used in this study. 1 g/L as P.  $\text{KH}_2\text{PO}_4$  was kept in the drying oven for one hour at 105 °C before use, to remove moisture content. This set of solutions is prepared as triplicates for reliable results recording.

## **6.2. Batch Adsorption Study**

Experimental procedure kept the same with nitrogen removal studies. Model solutions of concentration 1g/L-P prepared by dissolving 2.197 g of  $\text{KH}_2\text{PO}_4$  in 500 ml DI water. All solutions were made right before the test and agitated for ten minutes for salts to dissolve completely. The procedure followed by adding adsorbent balls into flasks and kept mixing them at a fixed speed of 60 rpm. Mass of adsorbents was ranging 22-25 grams. As it was in the previous study, the adsorption experiment is considered initialized as soon as adsorbent material is placed in flasks

The duration of the experiment was 24 hours, for the first-hour sampling done at 10, 20, 30 and 45 minutes and every hour after 60 minutes until the end of 8 hours of the experiment. Between the 8th and 24th hours, flasks were kept in mixing conditions and another sampling was done at the end of this period.

Collected samples are tested by using UV-Vis (HACH DR/4000, Loveland, CO) with user defined program which was introduced earlier after creating the calibration curve for phosphorus ions. Results are also checked through programs that are already defined by Hach. For this study Method 8048, PhosVer 3 (Ascorbic Acid) with a detection limit of 0-2.5 mg/L  $\text{PO}_4^{3-}$  was found as suitable for this purpose. Collected samples are diluted into an observable range in order to be able to take measurements through both programs and verified. This procedure is defined as equivalent to USEPA method 365.2 and Standard Method 4500-P-E for wastewater. Water quality measurements done throughout the experiment period to collect information on pH, TDS, conductivity, ionic strength and results are presented in Appendix C.

In this chapter there are three types of geopolymers tested; PGP, CGP5 and CGP20 composites for phosphorus removal. Results are reported in three categories;

- pH evolution during sampling.
- PGP, CGP5 and CGP 20 adsorbents on phosphorus sequestration
- XRF and EDS mapping.

### **6.3. pH Evolution**

No pH adjustment is done before experiments. One reason was to keep track of pH change throughout the study and predict the type of ion being adsorbed on composites. Overnight soaking of adsorbents in DI water is performed and pH values are recorded before the experiments. Results for PGP, CGP5 and CGP20 soaked in DI water is given in Figure 6.

1. From the figure, it can be observed that pH values are almost instantly increasing to

values above 9. PGP was an exception in this case since the release of hydroxide ions were not as fast as it is in CGP composites. However, all three samples have reached an equilibrium in pH values approximately in one hour which shows how quickly the soluble species from parent geopolymer are removed.

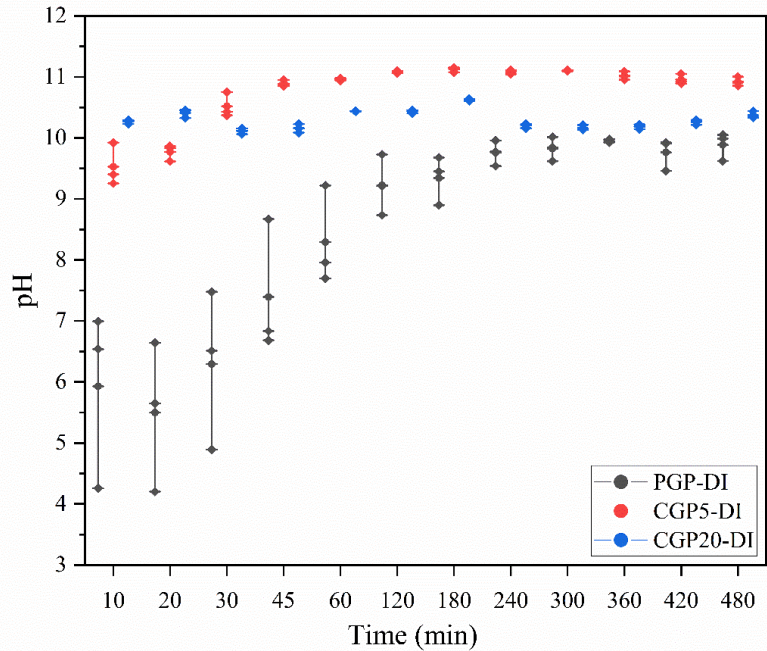


Figure 6. 1. Change in pH over time when test composites are soaked in DI for 8 hours.

The pH is also reported over time as PGP, CGP5 and CGP20 were being tested for their P removal performances in Figure 6. 2. It can be seen that the pH didn't stabilize after 24 hours of adsorption study, yet values are still lower than the ones observed in DI water. The jump in pH values after a day of mixing shows an increase unlike in the case of soaking adsorbents in DI. This is another indicator of pH values haven't come to an equilibrium value. Also, pH values have never reached 7.2 which is an indicator of dominant species in model solutions have  $\text{H}_2\text{PO}_4^-$  as the dominant species after the salt is dissolved.

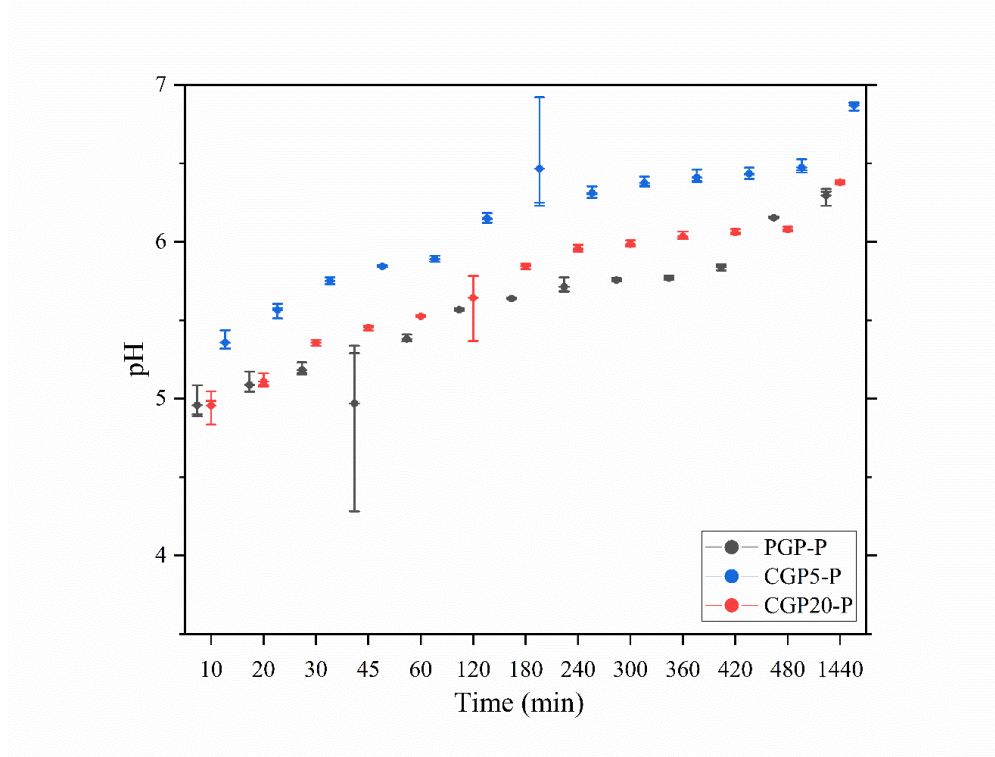


Figure 6. 2. Change in pH over time when PGP, CGP5 and CGP 20 composites are used as an adsorbent in model solutions with phosphorus.

#### 6.4. Phosphorus Removal

Phosphorus removal studies are performed following the same procedure used in nitrogen removal studies. Model solutions are prepared with having nitrogen content as 1 g/L as P at the beginning. Elemental P then converted to  $\text{PO}_4^{3-}$  for better interpretation of results obtained from UV-Vis measurements. Batch adsorption study started once all six adsorbent balls were immersed in homogenously mixed solutions. Mass of adsorbents used is given in Table 6. 1. In addition, volumetric flasks were kept in the stirrer for 24 hours and samples have collected in the interval stated earlier. Figure 6. 3 shows the final phosphorus concentration as P in model solutions after every sampling.



Table 6. 1. Mass of adsorbents used in each replicate of batch adsorption study

	<b>PGP</b>	<b>CGP5</b>	<b>CGP20</b>
<b>Batch Adsorption Study I</b>	23.68	24.16	22.07
<b>Batch Adsorption Study II</b>	23.57	24.62	21.99
<b>Batch Adsorption Study III</b>	23.59	24.27	22.18
<b>Average Mass of Adsorbent (g)</b>	23.61	24.35	22.08

*\*Values for Batch Adsorption Study I-II-III are the total mass of 6 adsorbent balls*

In Figure 6. 3 it is evident that P removal was faster with PGP than it was for N removal. For the first hour, pure geopolymer was showing more satisfactory results on phosphorus removal. However, the concentration of phosphorus didn't stabilize after 3 hours where PGP with nitrogen removal study was showing a steadier removal trend without fluctuations. Also, it should be noted that pH was varying for PGP for the first three hours. The removal efficiency was lower than it was in other studies but increased up to 100% after 24 hours. Clinoptilolite on the other hand was fast on P removal from the model solution, with overall removal of 98.8% CGP5 and %98.9 for CGP20. Figure 6. 4 shows CGP5 and CGP20 on P removal in detail. Both CGP composites are very effective on P removal with no major fluctuations observed. Throughout the study, removal was above 98% and in the first hour, the margin of errors has decreased in all replicate solutions. Calculated removal amounts are presented as percentages in Table 6. 2. Removal calculations are made according to equation (1) given in Chapter 5.

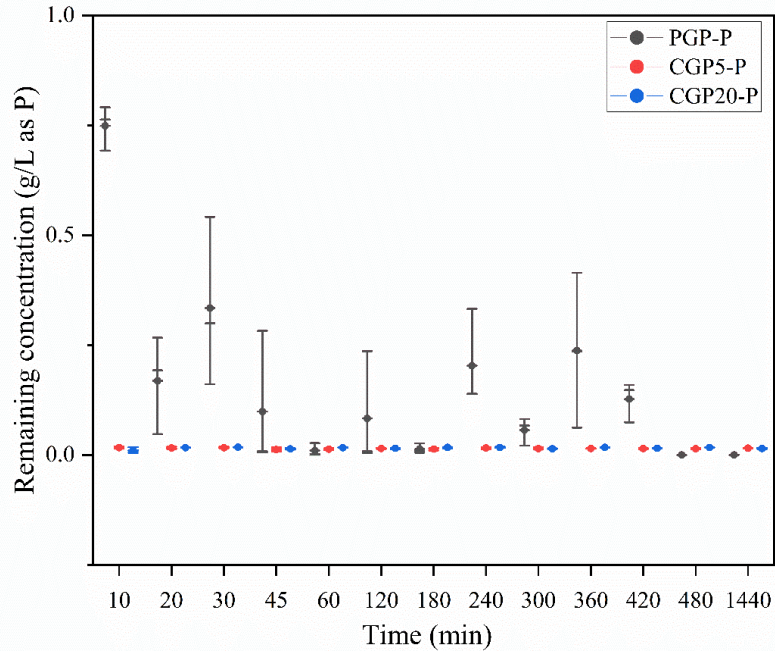


Figure 6. 3. Remaining phosphorus concentration in all studies performed by PGP, CGP5 and CGP20

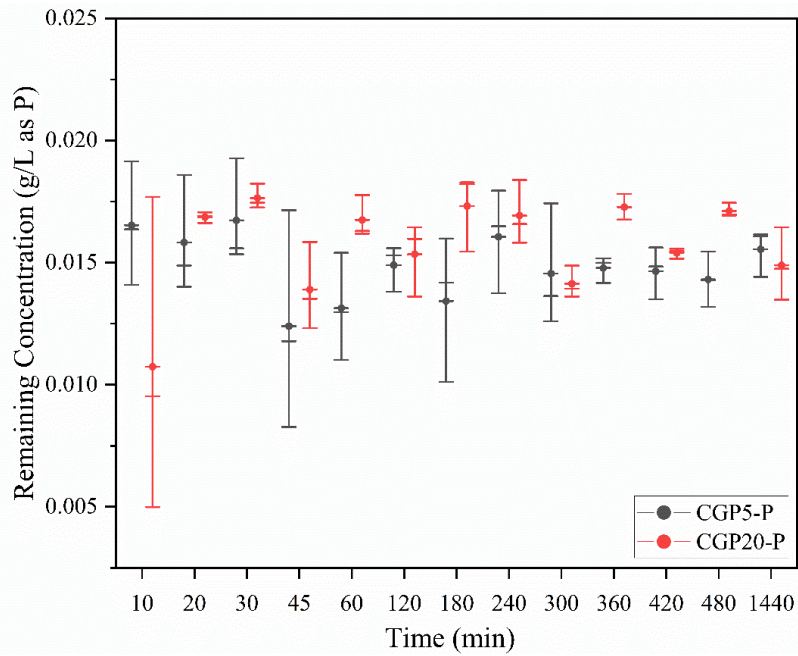


Figure 6. 4. Remaining phosphorus concentration studies performed by CGP5 and CGP20

Table 6. 2. Average phosphorus removal from model solutions by percentage

<b>Time (min)</b>	<b>PGP</b>	<b>CGP5</b>	<b>CGP20</b>
10	25.13	98.35	98.93
20	83.11	98.42	98.31
30	66.58	98.33	98.24
45	90.11	98.76	98.61
60	99.00	98.69	98.33
120	91.69	98.51	98.47
180	98.64	98.66	98.27
240	79.68	98.39	98.31
300	94.33	98.54	98.59
360	76.27	98.52	98.27
420	87.30	98.53	98.46
480	100.00	98.57	98.29
1440	100.00	98.45	98.51

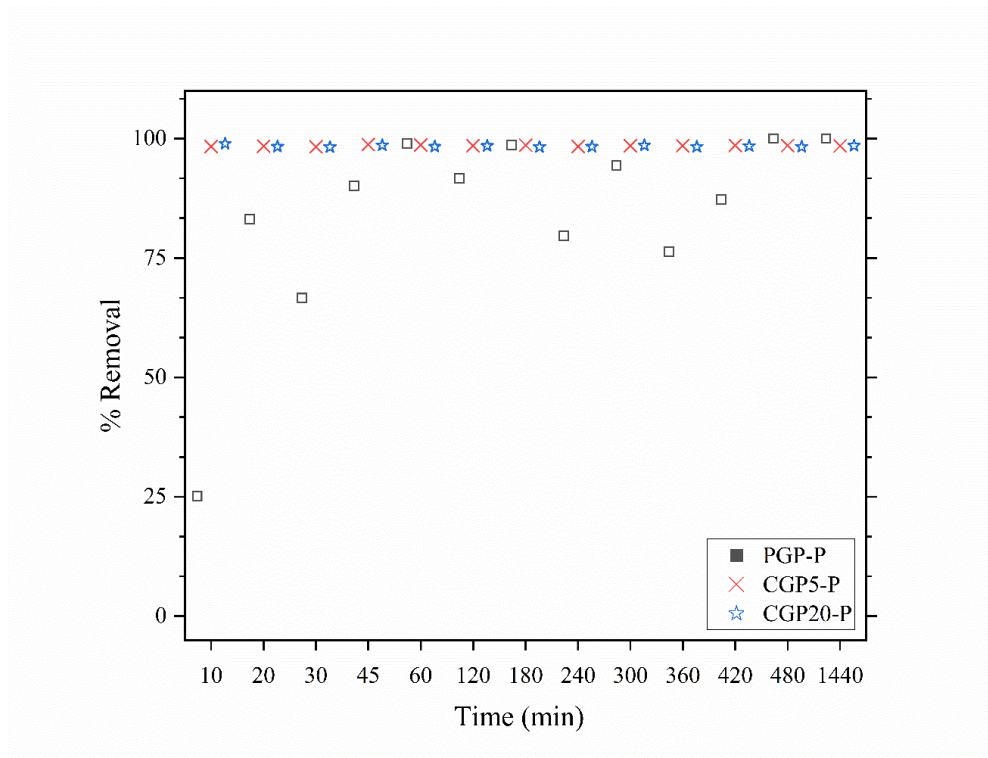


Figure 6. 5. Percent removal of nitrogen in model solutions over time.

XRF was used for investigating phosphorus presence on the geopolymer. It was assumed that adsorbed phosphorus is distributed evenly on all six balls in volumetric flasks.

According to that assumption, mapping is performed using a line scan. Samples are prepared by embedding them in epoxy. After cutting and polishing, samples are dried in vacuum oven prior to testing. Line scan is set to map the cross-section of adsorbent balls. Line scans obtained from virgin and post-evaluation composites are compared according to the measurement points and element concentration from the surface to the core of adsorbent balls.

Virgin pure geopolymers samples have not shown elemental P or  $P_2O_5$ . On the other hand, virgin geopolymers with clinoptilolite show a certain amount of phosphorus as it originates

from clinoptilolite itself. Results are presented from Figure 6. 6 and Figure 6. 8, the image on top showing virgin samples and bottom showing post-evaluation of that composite.

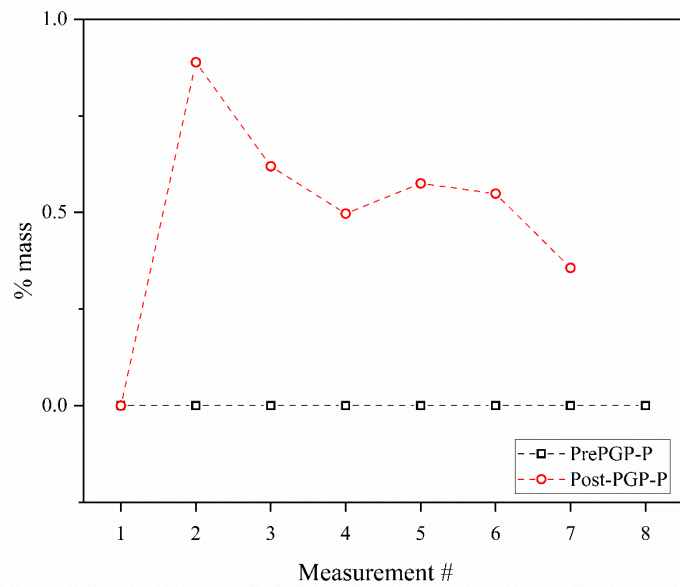
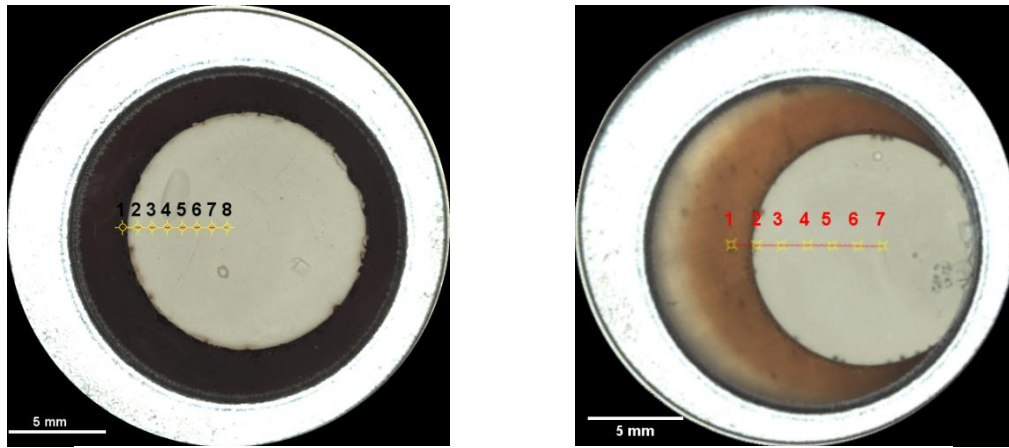


Figure 6. 6. Sampling points in linescan of PGP before and after the experiment (top), phosphorus presence in PGP before and after phosphorus removal study (bottom)



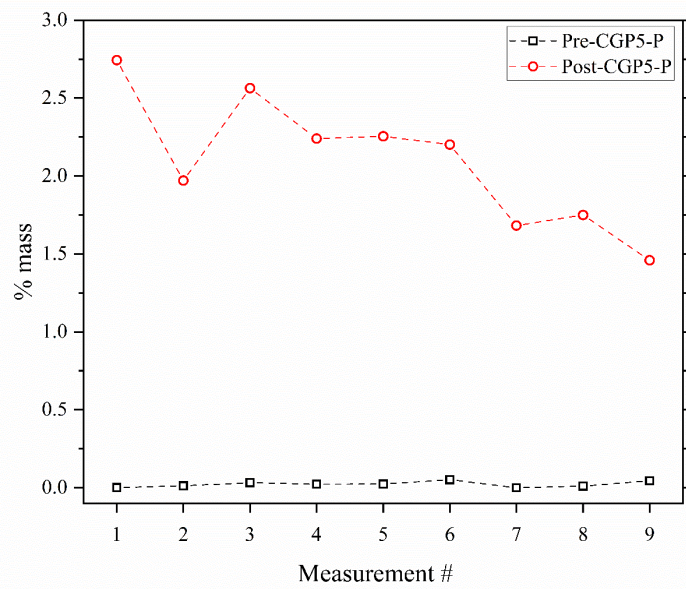
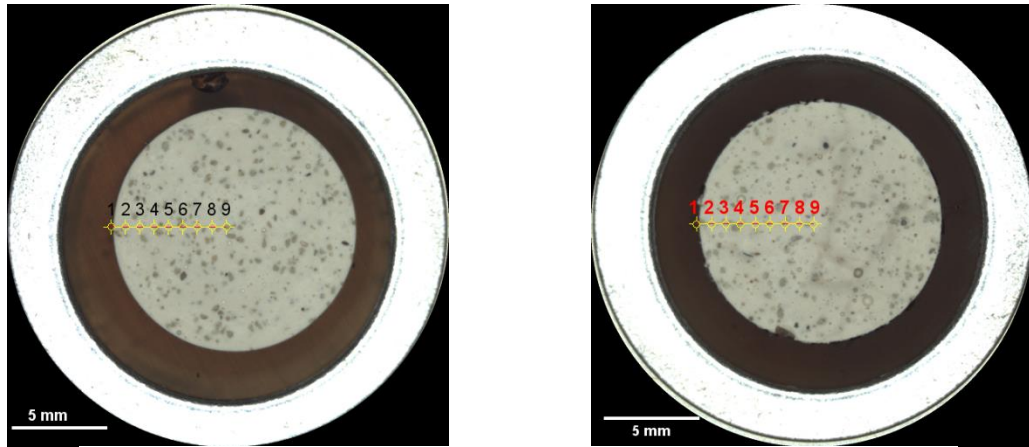


Figure 6. 7. Sampling points in linescan of CGP5 before and after the experiment (top), phosphorus presence in CGP5 before and after phosphorus removal study (bottom)

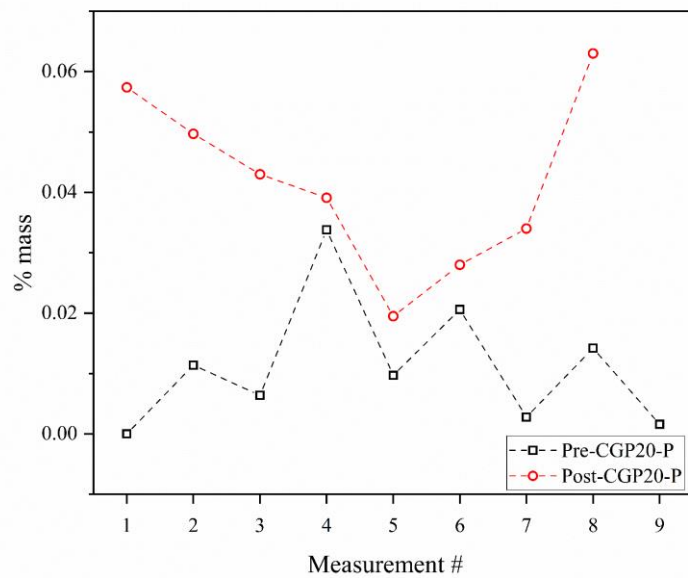
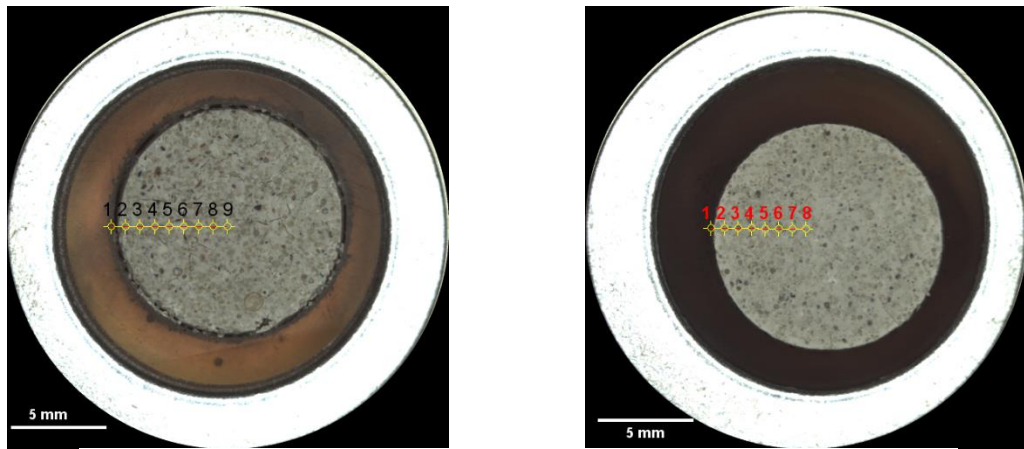


Figure 6. 8. Sampling points in linescan of CGP20 before and after the experiment (top), phosphorus presence in CGP20 before and after phosphorus removal study (bottom)

The general trend shows adsorption takes place on the adsorbent surface and decreases through the core and unlike nitrogen, phosphorus is kept in structure in inner locations as well. Another proof for phosphorus existence is that phosphorus content in post-evaluation samples showing more phosphorus comparing to virgin samples.

EDS mapping was done on pure geopolymer samples used for adsorption studies. The following figures show the area that is mapped, key elements that exist, phosphorus localization on samples and normalized elemental distribution throughout the mapped area.

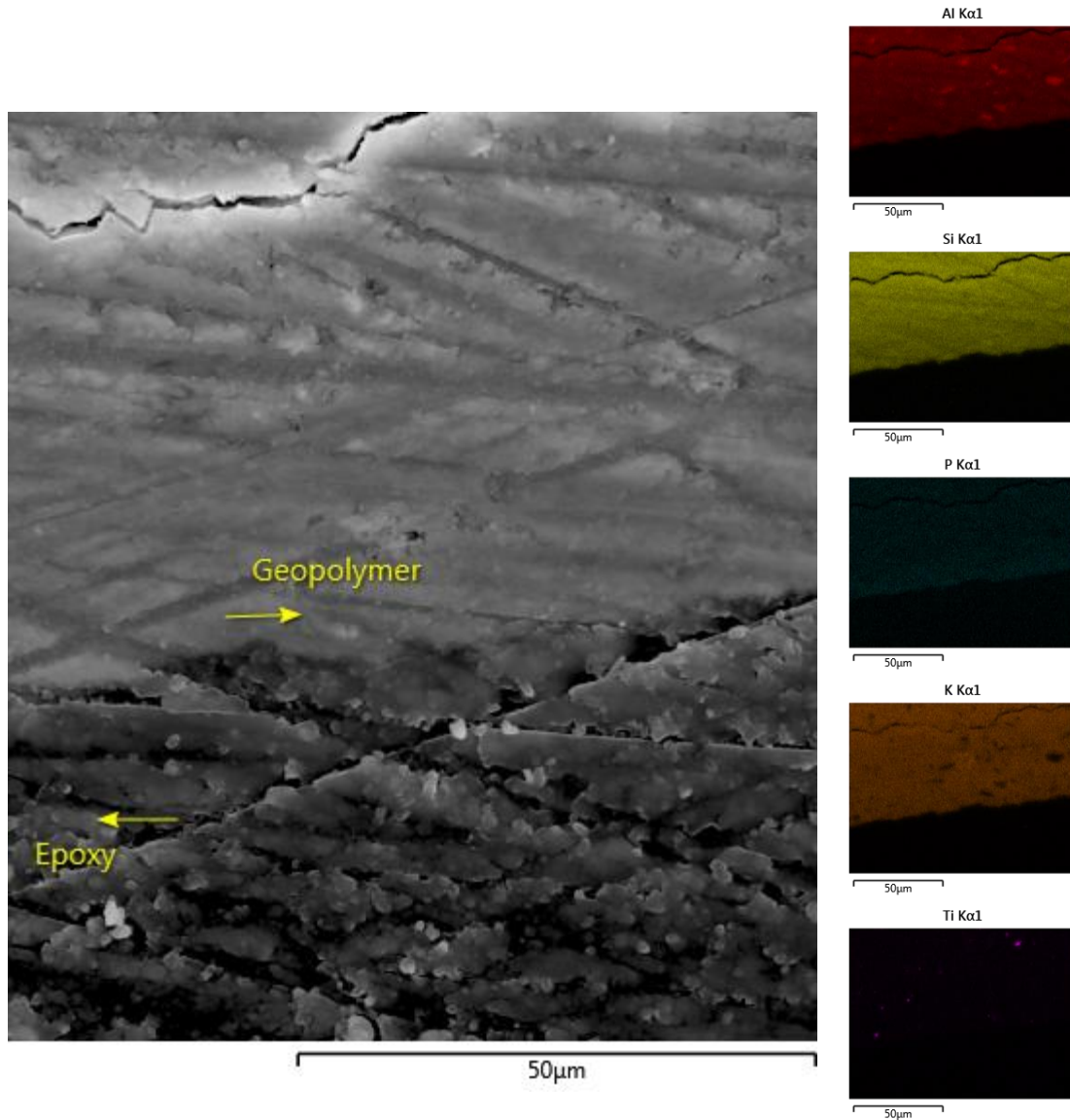


Figure 6. 9. Pure geopolymer image captured at x1.0k magnification (right) and major elements reported by EDS mapping auto identification.



Table 6. 3. Normalized elemental composition obtained from EDS mapping of the selected area.

<b>Element</b>	<b>Line Type</b>	<b>Apparent Concentration</b>	<b>k Ratio</b>	<b>Wt%</b>	<b>Wt% Sigma</b>	<b>Atomic %</b>	<b>Standard Label</b>
<b>Al</b>	K series	27.48	0.197	19.35	0.03	22.06	Al <sub>2</sub> O <sub>3</sub>
<b>Si</b>	K series	49.98	0.396	45.58	0.04	49.92	SiO <sub>2</sub>
<b>P</b>	K series	1.76	0.001	1.68	0.02	1.66	GaP
<b>Cl</b>	K series	3.39	0.030	3.60	0.02	3.12	NaCl
<b>K</b>	K series	33.04	0.280	28.52	0.03	22.44	KBr
<b>Ti</b>	K series	0.97	0.010	1.01	0.02	0.65	Ti
<b>Fe</b>	K series	0.29	0.003	0.27	0.02	0.15	Fe
<b>Total:</b>				100.00		100.00	

In Figure 6. 9, PGP was investigated in terms of mapping the adsorption of phosphorus. Quantification of elemental distribution through EDS was helpful on phosphorus identification on geopolymer surface. Mapping is performed using lower magnification due to the necessity of identification of nutrients on the geopolymer-epoxy interface. Table 6. 3 is showing the approximate weight % of phosphorus in the mapped area.

## 6.5. Summary

This study is done to evaluate geopolymers and geopolymer composites on their phosphorus removal efficiencies. Batch adsorption studies were performed by using three forms of geopolymeric adsorbents; PGP, CGP5 and CGP20. As in nitrogen removal studies, pH evolution is observed in phosphorus removal studies as well. Initial nutrient concentration was kept constant for each experiment and once again type of composite was the key parameter on the comparison of the results.

PGP on phosphorus removal was an encouraging finding considering geopolymeric structure known to have a negatively charged structure. Despite having some unstable removal trend at the beginning test period, model solutions had reached 25% removal in the first 10 minutes. Meaning removal was taking place effectively on pure geopolymers even though it was slow.

In terms of phosphorus removal, clinoptilolite incorporated geopolymer composites (CGP5 and CGP20) gave promising results as PGP samples. Despite differences in the rate of removal of phosphorus ions at the beginning, both CGPs has shown similar performances after some time. An interesting finding was that CGP samples were faster in phosphorus removal than PGP samples, indicating the clinoptilolite incorporation was effective on phosphorus removal from aqueous solutions. It shows that despite clinoptilolite and geopolymers having a negatively charged framework, anions were able to be displaced from aqueous solutions rapidly. XRF mapping results are giving a basis for this mechanism by looking at the quantification of present data.

## CHAPTER VII

### SIMULTANEOUS SEQUESTRATION OF NUTRIENTS BY PURE GEOPOLYMER AND GEOPOLYMER COMPOSITES

Accumulation of nitrogen and phosphorus are major causes of eutrophication. Excessive release of these nutrients caused by false management of poultry litter and its release to surface and groundwater by runoff is the major threat to the poultry industry. Up to this point, nitrogen and phosphorus removal by geopolymer and geopolymer composites have been investigated. However, different pollutants accompany natural systems, therefore their impact of one to the other creates some advantages and challenges at the same time in treatment processes.

Simultaneous removal of ammonium and phosphates are studied in some publications with various removal practices using solid materials such as zeolites, acid-treated natural rocks, metal-enriched natural materials (e.g.  $\text{Al}^{3+}$ ,  $\text{Mg}^{2+}$ ), biochar based nanocomposites, zeolite modified fly ash, etc. [69]–[73]. Although some covered simultaneous removal, mostly they were limited on focusing one nutrient at a time.

It was mentioned in earlier chapters that natural clays in general are well-known and well-studied adsorbents on ammonium removal. [25], [28], [74], [75][27], [66]. Since the geopolymer surface has a net negative surface charge, similar to zeolite structure, they reportedly had considerable removal efficiencies [32], [35], [75], [76]

Phosphorus removal similarly has been studied in a wide range of treatment technologies including adsorption. Due to physical restrictions of geopolymers and natural clays, they either need to be tailored to increase anion adsorption capacity or have to be precipitated by metal inorganic salts to elevate the crystallization and precipitation process of phosphorus in the waste [25], [31], [40], [77], [78]

In this study, simultaneous removal is the major focus and fabricating suitable geopolymer composites for this purpose is the starting point. Processing the geopolymers using affordable materials and keeping the preparation steps simple as possible is another aim of this study in a broader aspect. Since magnesium oxide (MgO) is an ionic material found in nature, it is selected to be the additional incorporation to composites researched in this thesis.

Magnesium incorporated geopolymer composite prepared by adding 5% of MgO powder by volume into geopolymer slurry. MGP5 is added to the research solely to investigate the effect of a metal oxide powder on the removal of phosphorus and nitrogen. In previous chapters, individual performances of pure geopolymer and clinoptilolite were investigated and reported. However, the fluctuations in phosphorus removal, especially in the early stages of adsorption studies lead this research to go forward and investigate further parameters affecting the adsorption process. For this chapter key objectives were defined as;

- Observing the geopolymer and geopolymer composite efficiency on removal in the presence of both ammonium and phosphate ions
- Observing metal oxide incorporation effect on geopolymer removal efficiency
- Quantifying the matrix effect caused by model solutions on removal

## **7.1. Model Solutions**

The model solution and replicates are prepared by dissolving  $\text{KH}_2\text{PO}_4$  with water solubility of 168 g/100 g  $\text{H}_2\text{O}$  and  $\text{NH}_4\text{Cl}$  salt with water solubility of 39.5 g/100 g  $\text{H}_2\text{O}$  [64] Model solutions prepared as triplicates having 1 g/L as P.  $\text{KH}_2\text{PO}_4$  and 1 g/L as  $\text{NH}_3\text{-N}$ .  $\text{NH}_4\text{Cl}$  and  $\text{KH}_2\text{PO}_4$  were kept in a drying oven for one hour at 105 °C before use to remove moisture content. Solutions are stirred thoroughly to dissolve the salt completely.

## **7.2. Batch Adsorption Study**

To test the adsorbent efficiencies on the removal of nutrients simultaneously, model solutions are prepared by mixing two salts in the same beaker with corresponding amounts. After desired amounts are weighed they are mixed for ten minutes before adsorbent balls are released into the solution. Right after adsorbent balls are added beakers kept mixing at a fixed speed of 60rpm. Mass of adsorbents was ranging between 22-24.5 grams. Adsorption study considered to start right after adsorbent balls are added.

The duration of the experiment was the same with nitrogen and phosphate removal studies. The first hour was crucial in order to observe how fast the adsorption was. After the first-hour sampling is done at the end of every hour. After the 8th hour flasks kept mixing overnight and final sampling is done at the end of 24 hours.

Collected samples are tested immediately by using UV-Vis. Methods 8048 and 8038 are used for measuring  $\text{PO}_4^{3-}$  and  $\text{NH}_3\text{-N}$  concentrations. All samples have run with user defined programs which had been introduced beforehand by using stock solutions and creating a calibration curve for those nutrients.

In this chapter there are four types of geopolymers tested; PGP, CGP5, CGP20 and MGP5 for nitrogen and phosphate removal simultaneously. Meaning that both nutrients existing in the same solution. The results are reported in two categories,

- pH evolution in model solutions during the experiment
- PGP, CGP5, CGP20 and MGP5 adsorbents on sequestration of nutrients.
- EDS and XRF mapping for phosphorus tracing.

Water quality measurements done throughout the experiment period to collect information on pH, TDS, conductivity, ionic strength and results are presented in Appendix C.

### **7.3. pH Evolution**

Test solutions are not pH adjusted before experiments. Overnight soaking of adsorbents in DI water results can be looked at in Chapter 5. Impact of composite type on pH when composites used for simultaneous removal studies can be looked at in Figure 7. 1. The increasing trend of pH is very similar to previous studies, there is a positive rate of increase in values and equilibrium hasn't reached after a day of the experiment. As in Chapter 6, Figure 6.2., pH values show significant raise due to the model ion exchange process hasn't come to an end. Another finding was, composites are used for phosphate removal studies only, initial and final pH values are higher than ammonium removal or simultaneous removal studies. This applies to most composite types tested.

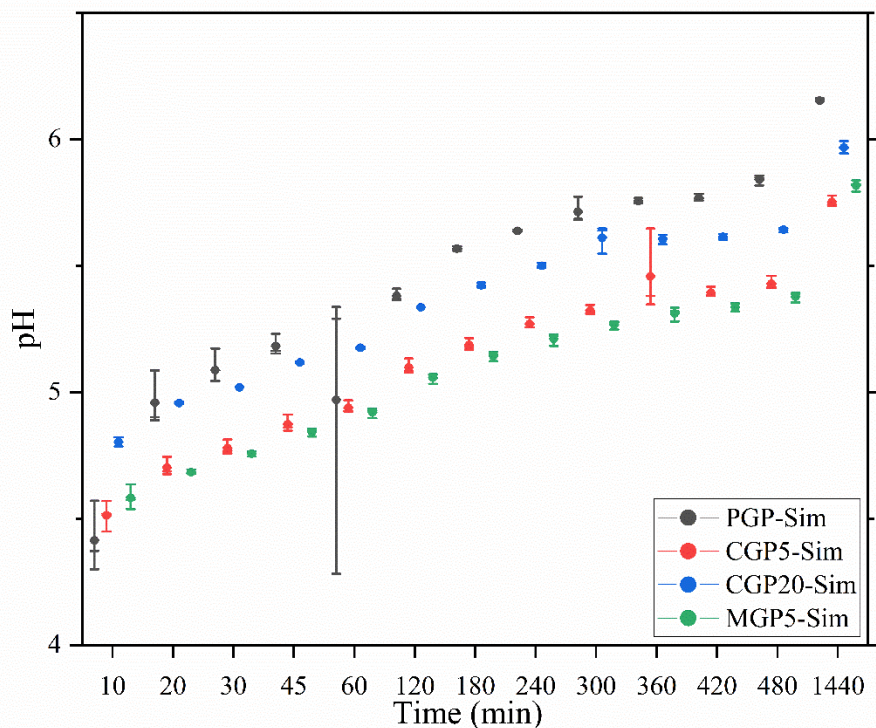


Figure 7. 1. pH evolution over time with geopolymer composites used in simultaneous nutrient removal studies

#### 7.4. Nitrogen and Phosphate removal

Phosphorus and ammonium removal studies are performed following the same procedure used in previous studies. The difference is, model solutions are prepared with having both ammonium and phosphate content. Initial concentrations for simultaneous nutrient adsorption is 1 g/L as  $\text{NH}_3\text{-N}$  and 1 g/L as P. For consistency purposes,  $\text{PO}_4^{3-}$  is converted into elemental P. Similarly, ammonium numbers can be observed after results are converted into  $\text{NH}_4\text{-N}$ . Batch adsorption study started once all 6 adsorbent balls were immersed in homogeneously mixed solutions. Mass of adsorbents used is given in Table 7. 1. In addition, beakers were kept in stirrer for 24 hours and samples have collected in the interval stated earlier.

Table 7. 1. Mass of adsorbent used in batch adsorption studies on phosphate removal.

	<b>PGP</b>	<b>CGP5</b>	<b>CGP20</b>	<b>MGP5</b>
<b>Batch Adsorption Study I</b>	23.45	24.41	21.83	24.77
<b>Batch Adsorption Study II</b>	23.49	24.57	21.98	24.59
<b>Batch Adsorption Study III</b>	23.3	24.76	22.03	24.31
<b>Average Mass of Adsorbent (g)</b>	23.45	24.41	21.83	24.77
<b>Batch Adsorption Study I</b>	23.41	24.58	21.95	24.56

*\*Values for Batch Adsorption Study I-II-III are the total mass of 6 adsorbent balls*

In Figure 7. 2, both figures show that composites are showing a considerable amount of removal of ammonium and phosphate. Comparing to individual removal studies, sequestration of both nutrients at the same time showed a similar trend with different initial reactions.

The first difference is the pH effect on the PGP uptake trend. In model solutions having only phosphorus ions, as pH kept increasing phosphorus uptake by the adsorbent increased too. When both nutrients present, phosphorus uptake is observed to be faster. In this sense, the co-existence of nutrients looks more promising on phosphate removal efficiency of pure geopolymer. This outcome can be addressed by looking at percent removal rates (Table 6. 2. and Table 7. 2). Data shows a steadier trend when both nutrients exist in model solutions. For ammonium removal, on the other hand, pure geopolymers show a considerable increase in ammonium removal when both nutrients exist. Comparing to data from previous chapters, pure geopolymer in simultaneous removal is more effective than it was in individual removal tests.



In terms of CGP composite performance, phosphorus uptake by CGP5 and CGP20 composites can be evaluated as being as efficient as it is in individual nutrient removal studies. Ammonium removal in simultaneous studies, on the other hand, showed only a slight difference from individual nitrogen removal tests where removal numbers are recorded to be better in ammonium removal. (decreased ~98% to ~94%) However, the change in the removal in certain time intervals decreases down to 73% in the simultaneous study, indicating a competitive adsorption trend.

MGP5 composite showed immediate removal of both ammonium and phosphates. It can be seen that from the beginning of batch adsorption tests no ammonium is detected in model solutions. This indicates immediate uptake of nitrogen content. Regarding phosphate concentration, model solutions showed a little phosphate content left in them. 98% of phosphate removal was observed in the first 10 minutes and removal efficiency stayed steady throughout the test period. For simultaneous studies, it can be stated that MGP5 showed a better performance than CGP composites on the removal of ammonium content.

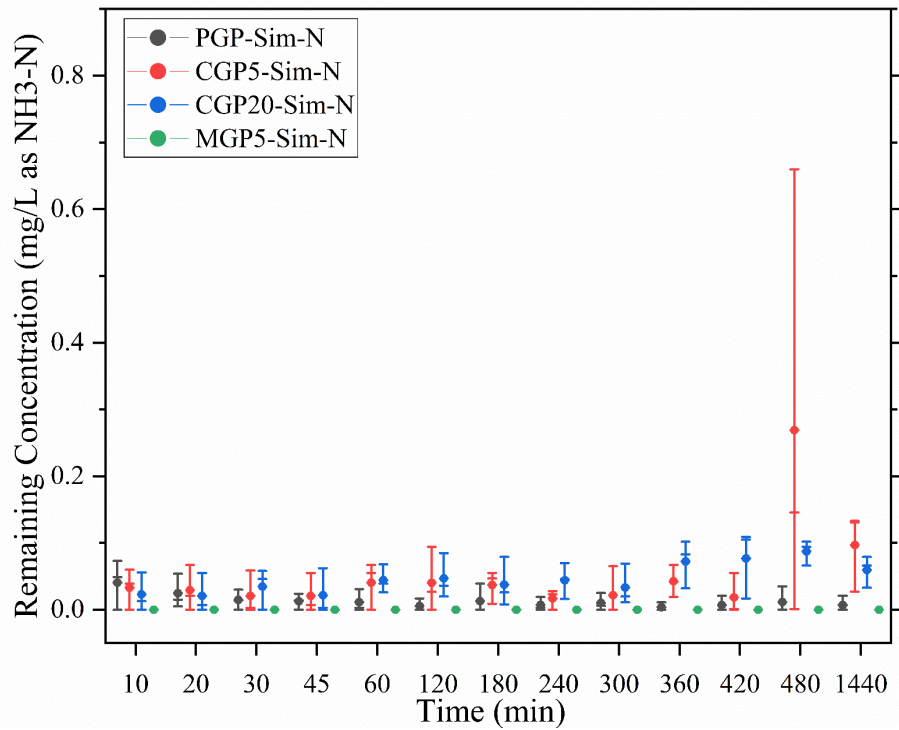
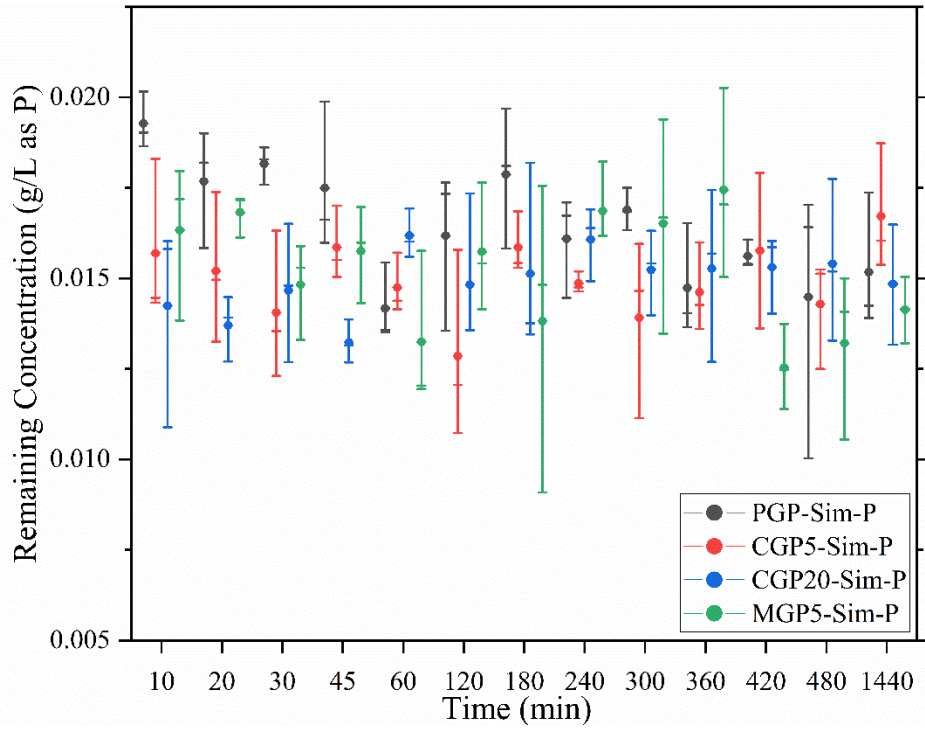


Figure 7. 2. Phosphorus (top) and nitrogen (bottom) concentrations remaining in model solutions over time

Table 7. 2. Average ammonium nitrogen and phosphate removal from model solutions by percentage.

Time (min)	PGP (%)		CGP5N (%)		CGP20 (%)		MGP5 (%)	
	P	N	P	N	P	N	P	N
10	98.07	96.37	98.43	97.07	98.58	97.90	98.37	100.00
20	98.23	97.53	98.48	97.37	98.63	98.00	98.32	100.00
30	98.18	99.30	98.59	98.20	98.53	96.60	98.52	100.00
45	98.25	99.67	98.41	98.30	98.68	97.90	98.42	100.00
60	98.58	99.93	98.53	96.10	98.38	95.57	98.68	100.00
120	98.38	100.00	98.71	96.23	98.52	95.30	98.43	100.00
180	98.21	100.00	98.41	96.30	98.49	96.23	98.62	100.00
240	98.39	100.00	98.51	98.40	98.39	95.60	98.31	100.00
300	98.31	99.97	98.61	97.90	98.48	96.67	98.35	100.00
360	98.53	100.00	98.54	95.73	98.47	92.77	98.26	100.00
420	98.44	100.00	98.42	98.33	98.47	92.30	98.75	100.00
480	98.55	100.00	98.57	73.10	98.46	91.27	98.68	100.00
1440	98.48	100.00	98.33	90.73	98.52	94.07	98.59	100.00

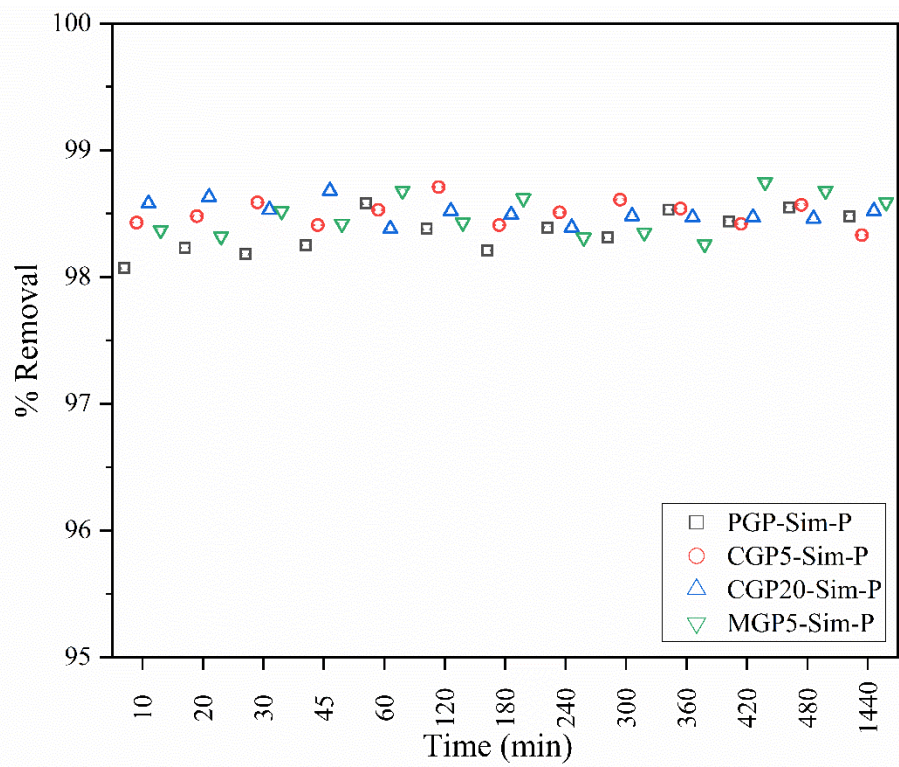
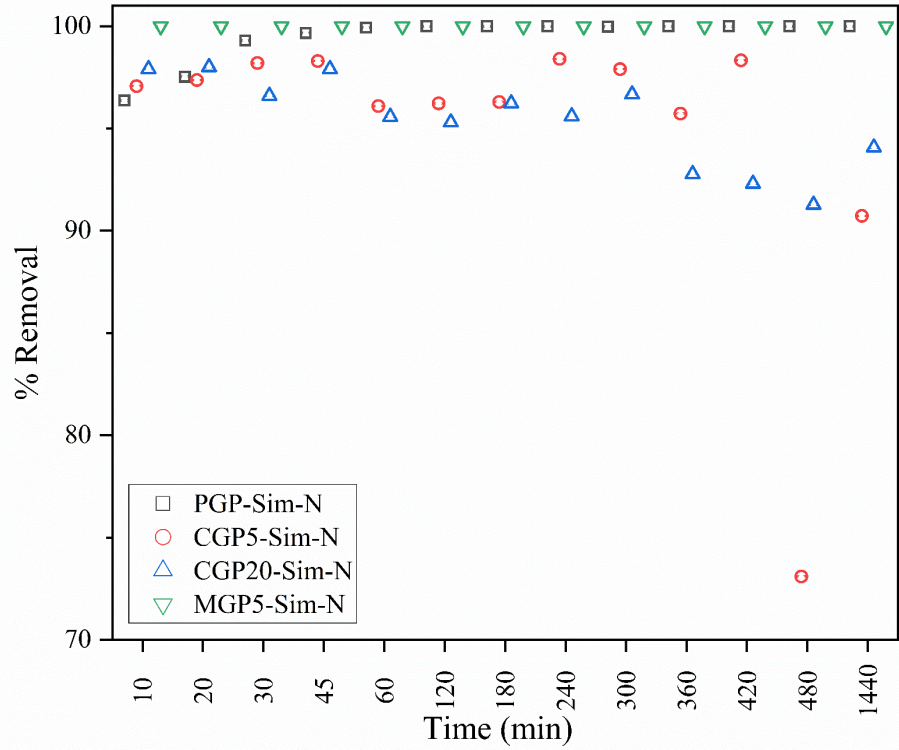


Figure 7. 3. Ammonium and phosphate removal amounts from model solutions.



XRF was used once again to investigate ammonium and phosphate presence on geopolymer composites after batch adsorption studies. It was assumed that adsorbed nutrients were distributed evenly on all six balls in volumetric flasks. Samples are prepared by embedding them in epoxy as it was in previous studies performed in Chapter 5 and Chapter 6. Line scan was the key to compare elemental nitrogen and phosphorus throughout the sample body. The following graphs show the trend of nutrients on geopolymers from the surface to the core of composite balls.

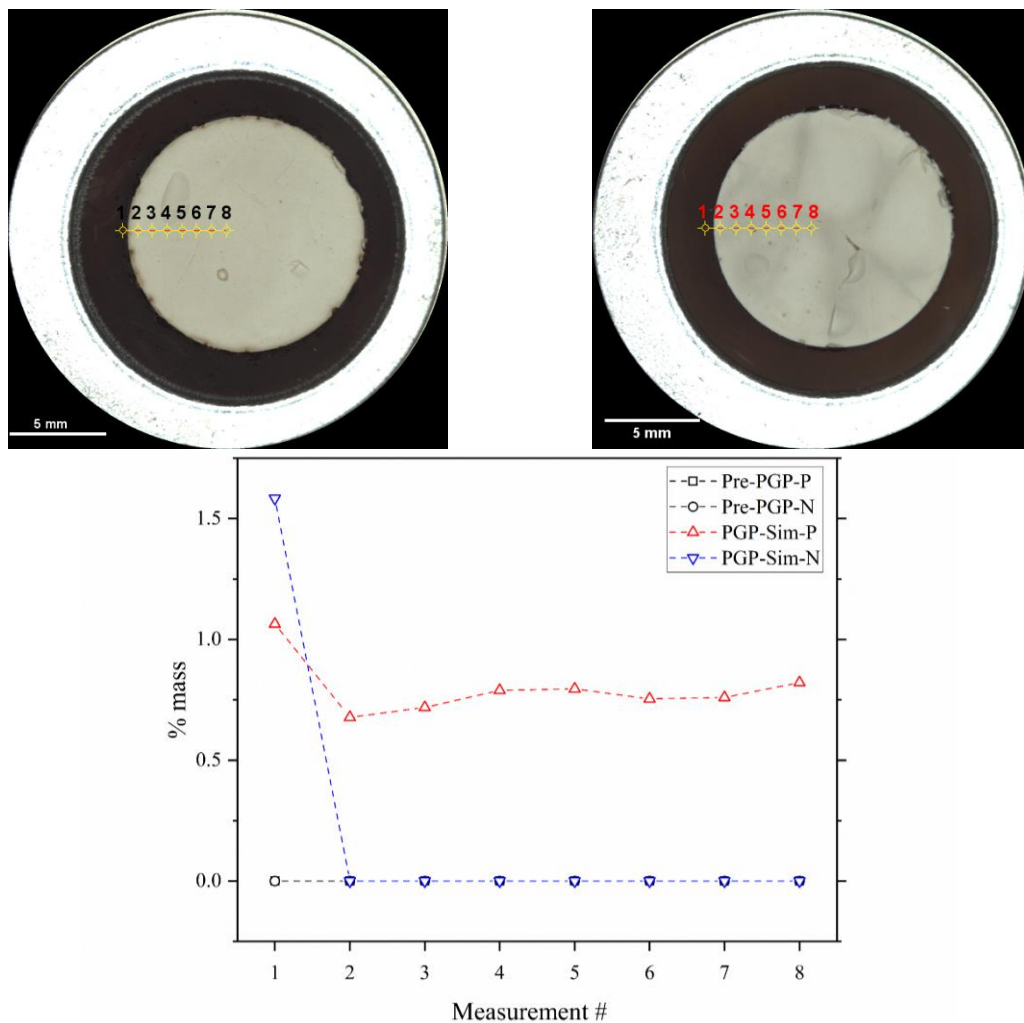


Figure 7. 4. Sampling points in linescan of PGP before and after the experiment (top), nitrogen and phosphorus presence in PGP before and after phosphorus removal study (bottom)

Virgin pure geopolymers don't show elemental nitrogen and phosphorus content. However, it was possible to detect nutrients after batch adsorption tests through XRF mapping. For simultaneous removal nitrogen and phosphorus once again present only on the surface. Inner locations were still able to show phosphorus, but lower than it is on the surface. (Figure 7. 4)

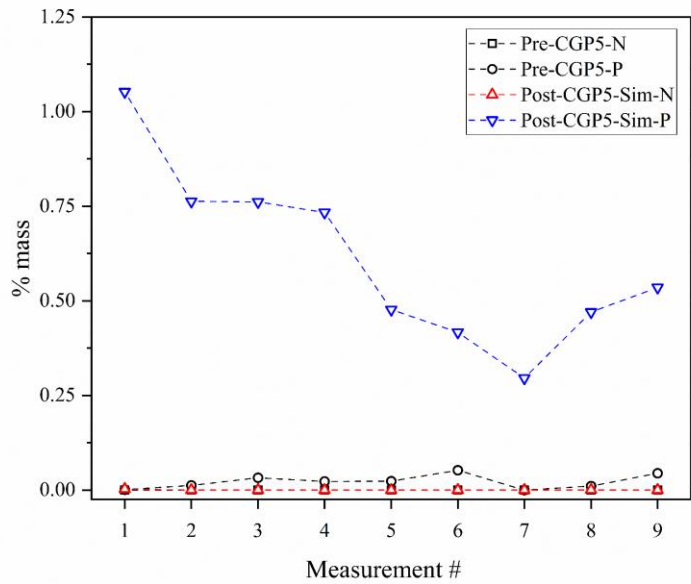
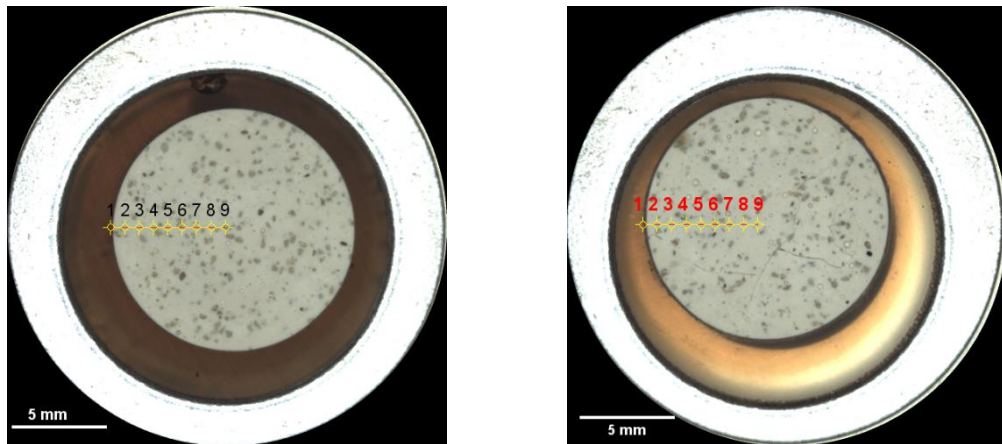


Figure 7. 5. Sampling points in linescan of CGP5 before and after the experiment (top), nitrogen and phosphorus presence in CGP5 before and after phosphorus removal study (bottom)

In Figure 7. 5, phosphorus can be observed on the surface and decreases towards the center. There is an increase can be observed in the center as well. Nitrogen on the other hand is showing a minor appearance throughout the scanned line. For CGP20, phosphorus is adsorbed majorly on the surface where nitrogen doesn't have a strong presence in the composite. (Figure 7. 6)

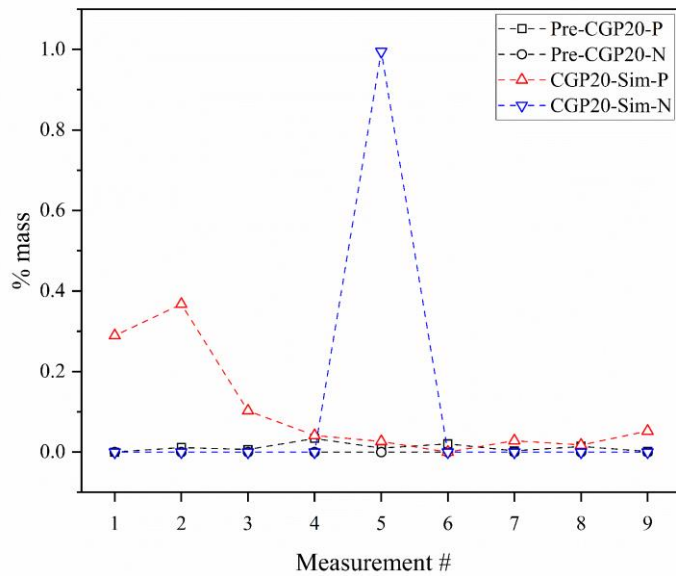
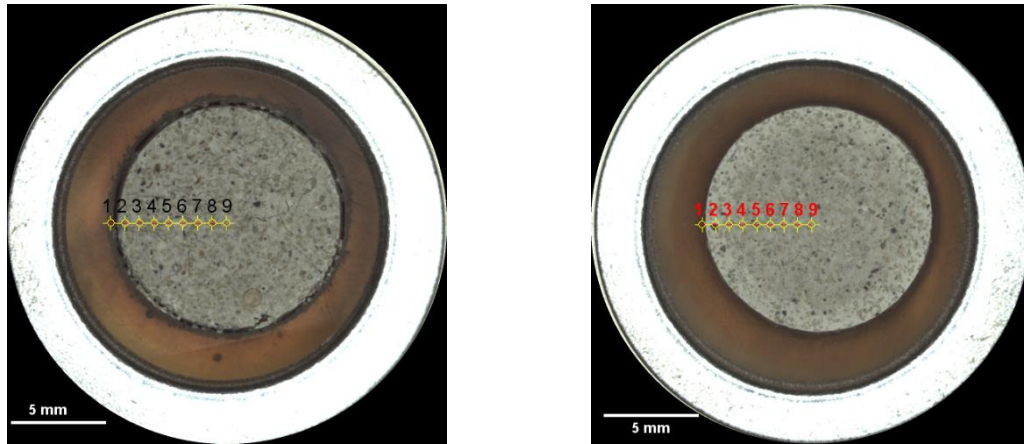


Figure 7. 6. Sampling points in linescan of CGP20 before and after the experiment (top), nitrogen and phosphorus presence in CGP20 before and after phosphorus removal study (bottom)

Figure 7. 7 shows XRF mapping of MGP5 composite where both phosphorus and nitrogen showed a significant presence. Contrasting earlier findings nitrogen was found towards the center of the structure.

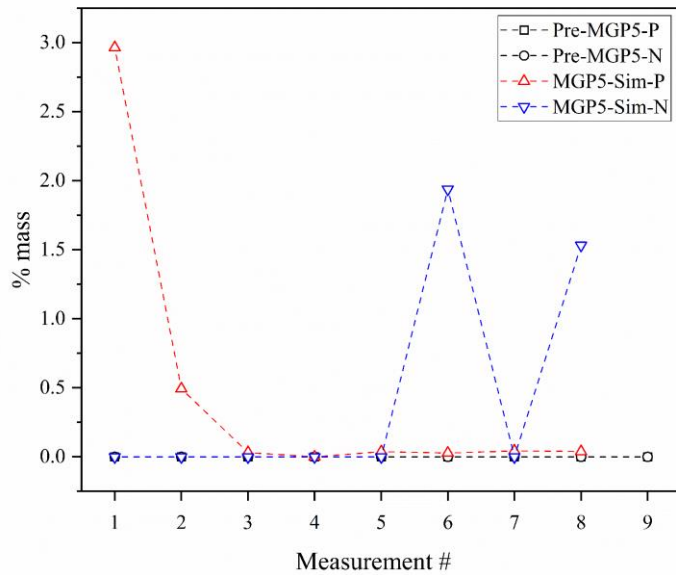
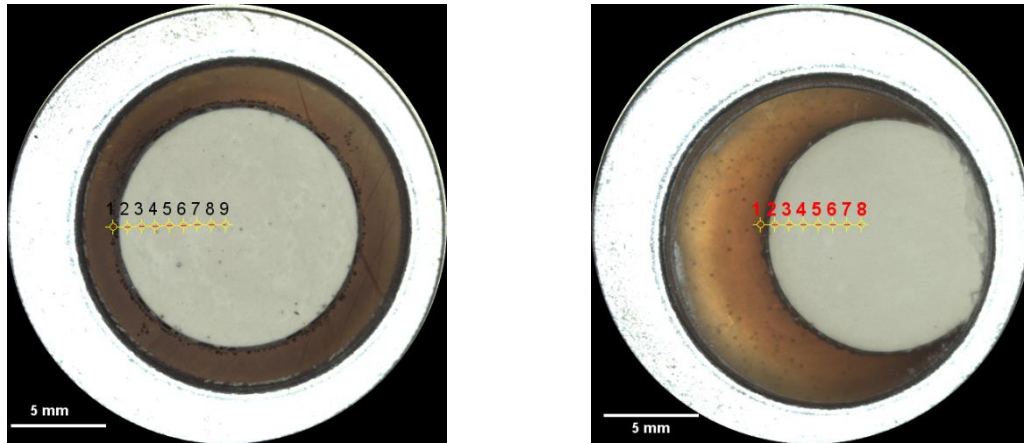


Figure 7. 7. Sampling points in linescan of MGP5 before and after the experiment (top), nitrogen and phosphorus presence in MGP5 before and after phosphorus removal study (bottom)

EDS mapping done to identify the phosphorus and nitrogen that is in the structure.

Quantifying the nitrogen was the challenge due to its low atomic number. FE-SEM used in



this study was not suitable to work with lower accelerating voltages, therefore with working protocol used for this study made it very difficult to detect it in some cases. First obstacle is that most EDS detectors use entrance windows made of Be (as it was in this case) where it doesn't transmit X-rays for light elements. Even it was possible to ionize the nitrogen in geopolymer composites another case to consider is that they generate X-rays result in weaker signals. Generated X-rays are easily absorbed by the specimen itself or stay in the sample.

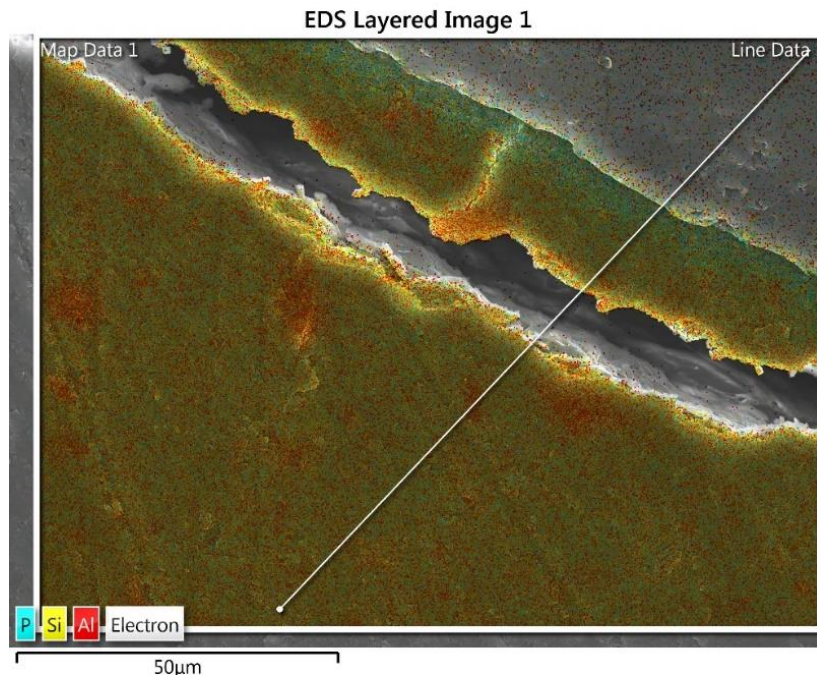


Figure 7. 8. Layered EDS image showing P, Al and Si distribution in PGP after simultaneous removal

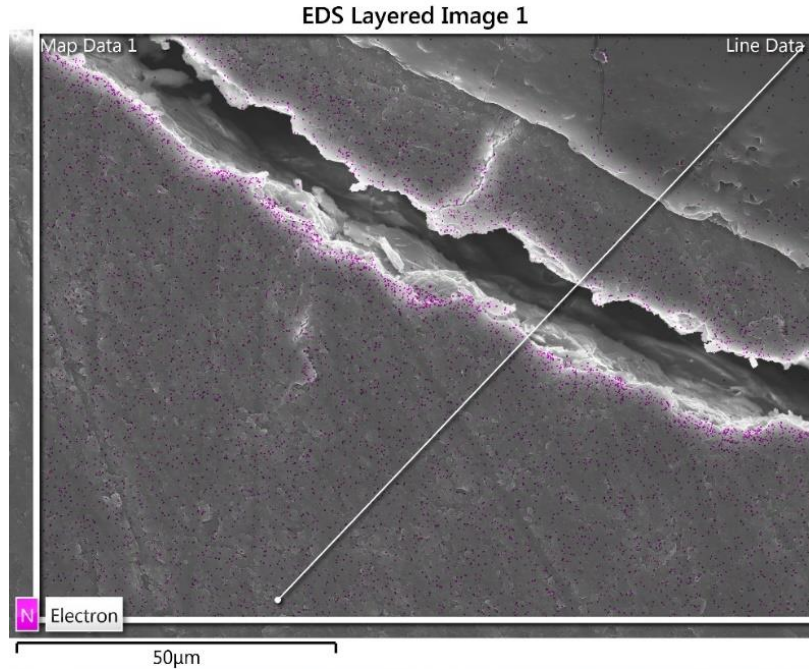
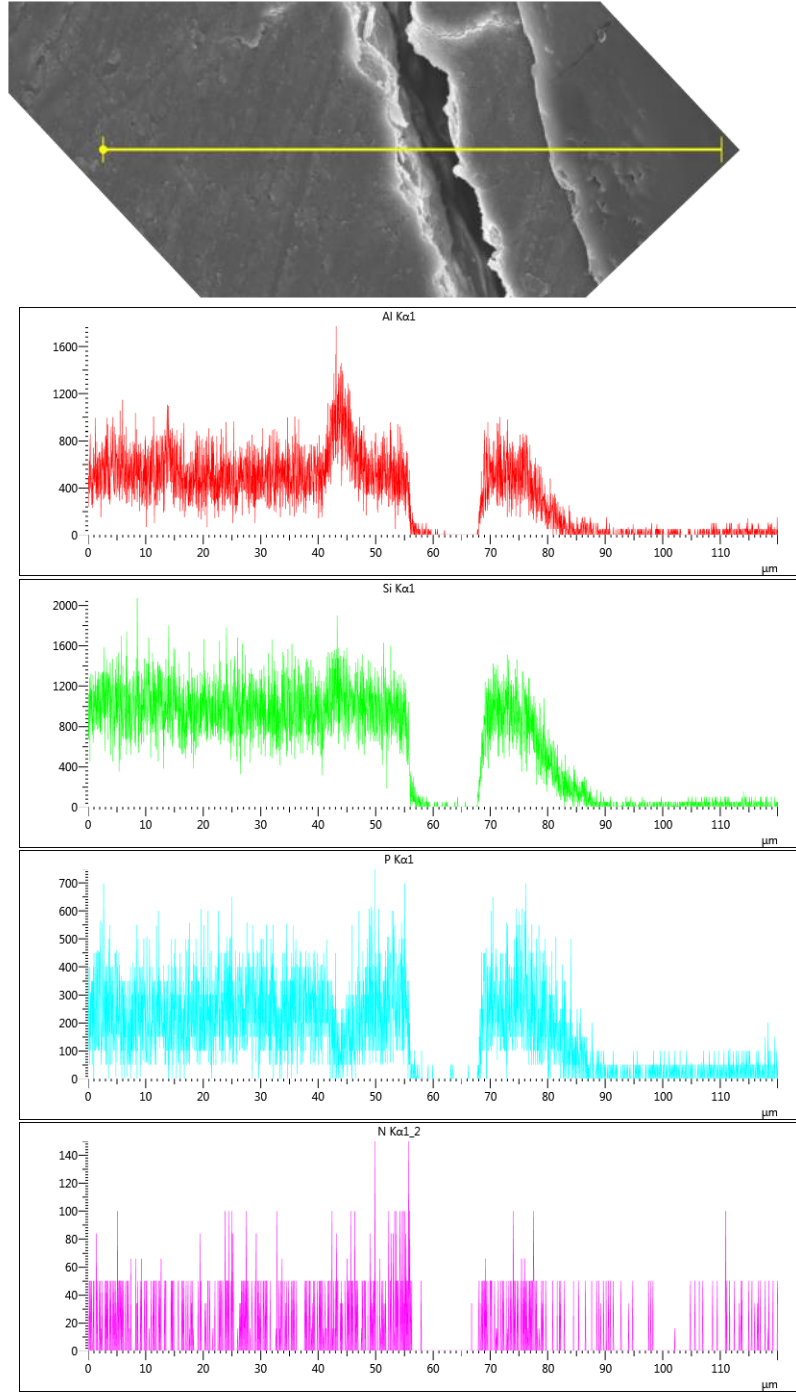


Figure 7. 9. Layered EDS image showing nitrogen distribution in PGP after simultaneous removal

Figure 7. 8 and Figure 7. 9 is showing pure geopolymer after simultaneous removal study. Line passing through from epoxy to geopolymer body is about 120 $\mu\text{m}$  where it was analyzed for key elements later on. It is possible to observe nitrogen and phosphorus on the edge of the geopolymer and at the edge of the cracks, approximately 20 $\mu\text{m}$  deep from the surface. (Figure 7. 10)



*\*Graphs show cps (Y-axis) vs μm (X-axis)*

Figure 7. 10. Line Scan performed on PGP after simultaneous study, Al, Si, P and N from the surface (right) to inner structure (left)

AutoID method is used to identify major contributors at first. As can be seen in Table 7. 3, nitrogen wasn't identified automatically. Results that show nitrogen presence is generated after nitrogen was introduced by the user. The atomic ratio of Si/Al was identified as 1.8 which was very close to the theoretical ratio for geopolymers formulated for this study.

Table 7. 3. AutoID results of overall EDS map analysis and normalized values for elemental distribution.

<b>Element</b>	<b>Line Type</b>	<b>Apparent Concentration</b>	<b>k Ratio</b>	<b>Wt%</b>	<b>Wt% Sigma</b>	<b>Atomic %</b>	<b>Standard Label</b>
<b>O</b>	K series	23.53	0.079	46.46	0.10	62.81	SiO <sub>2</sub>
<b>Al</b>	K series	12.20	0.088	10.38	0.03	8.32	Al <sub>2</sub> O <sub>3</sub>
<b>Si</b>	K series	21.80	0.173	19.56	0.04	15.06	SiO <sub>2</sub>
<b>P</b>	K series	8.28	0.046	5.94	0.03	4.15	GaP
<b>Cl</b>	K series	0.46	0.004	0.42	0.01	0.26	NaCl
<b>K</b>	K series	21.29	0.180	16.39	0.04	9.06	KBr
<b>Ti</b>	K series	0.45	0.005	0.43	0.01	0.19	Ti
<b>Fe</b>	K series	0.14	0.001	0.13	0.02	0.05	Fe
<b>Cu</b>	K series	0.34	0.003	0.31	0.03	0.10	Cu
<b>Total</b>				100.00		100.00	

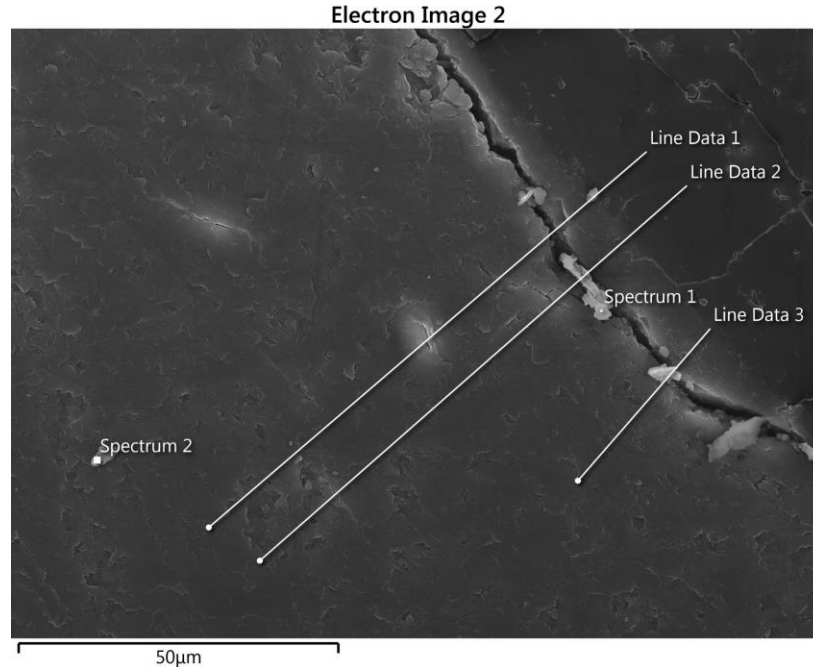
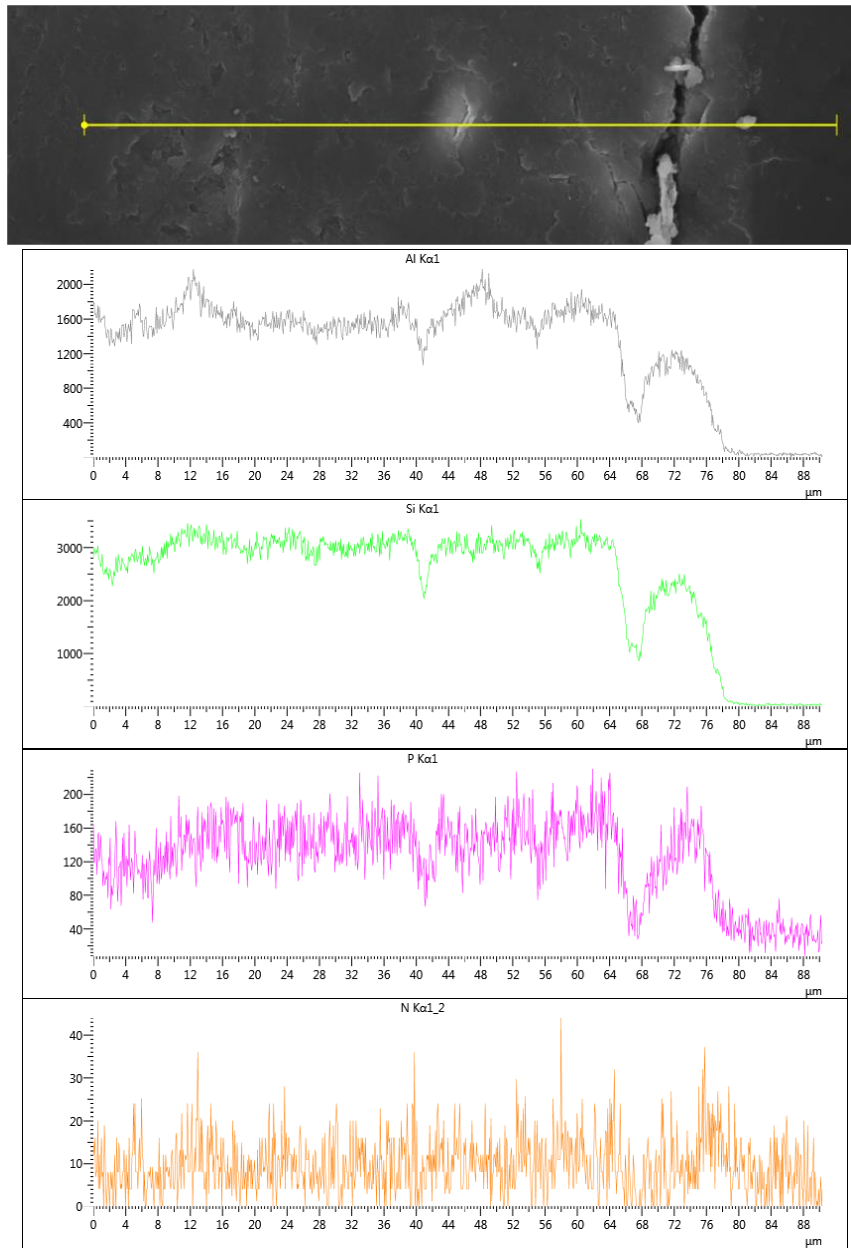


Figure 7. 11. EDS image of CGP5 and scanned the area with selected line scans in CGP5 after simultaneous removal

Figure 7. 11 is showing a captured image of CGP5 after a simultaneous removal study. Line passing through from epoxy to geopolymer body is about 90µm where it was analyzed for key elements later on. It is possible to observe phosphorus on the composite, which is mostly distributed evenly. First 10µm, phosphorus is present but not more than the overall distribution throughout the sample. From the line scan of Line1 Figure 7. 12, it can be observed that key elements were distributed evenly. Although Al, Si and P showed trends where they decrease on the surface of the crack, nitrogen is relatively even through the sample.

As can be seen in Table 7. 4, nitrogen doesn't have any effect on the results. The atomic ratio of Si/al is closer to what is formulated for geopolymer. However, nitrogen was then added to calculations and for Spectrum 1 (can be seen in Figure 7. 11), point identification

showed reportable amounts of nitrogen. In this case, Si/Al ratio was around 6, which is closer to clinoptilolite structure. Results for Spectrum 1 can be observed in



*\*Graphs show cps (Y-axis) vs μm (X-axis)*

Figure 7. 12. Line Scan performed on CGP5 after simultaneous study, Al, Si, P and N from the surface (right) to inner structure (left)

Table 7. 4. AutoID results of overall EDS map analysis of CGP5, normalized values for elemental distribution

<b>Element</b>	<b>Line Type</b>	<b>Apparent Concentration</b>	<b>k Ratio</b>	<b>Wt%</b>	<b>Wt% Sigma</b>	<b>Atomic %</b>	<b>Standard Label</b>
<b>O</b>	K series	69.96	0.23543	42.73	0.07	58.71	SiO <sub>2</sub>
<b>Na</b>	K series	0.89	0.00374	0.25	0.01	0.23	Albite
<b>Al</b>	K series	50.24	0.36082	12.54	0.02	10.21	Al <sub>2</sub> O <sub>3</sub>
<b>Si</b>	K series	93.91	0.74413	25.79	0.04	20.18	SiO <sub>2</sub>
<b>P</b>	K series	4.58	0.02563	1.07	0.01	0.76	GaP
<b>Cl</b>	K series	5.46	0.04769	1.52	0.01	0.94	NaCl
<b>K</b>	K series	65.41	0.55408	15.37	0.03	8.64	KBr
<b>Ti</b>	K series	1.83	0.01830	0.52	0.01	0.24	Ti
<b>Fe</b>	K series	0.47	0.00471	0.13	0.01	0.05	Fe
<b>Cu</b>	K series	0.33	0.00332	0.09	0.02	0.03	Cu
<b>Total:</b>				100.00		100.00	

Table 7. 5. Normalized elemental distribution for Spectrum 1 point on CGP5

<b>Element</b>	<b>Line Type</b>	<b>Apparent Concentration</b>	<b>k Ratio</b>	<b>Wt%</b>	<b>Wt% Sigma</b>	<b>Atomic %</b>	<b>Standard Label</b>
<b>N</b>	K series	3.77	0.0067	3.35	1.08	5.05	BN
<b>O</b>	K series	72.79	0.2449	43.58	0.61	57.52	SiO <sub>2</sub>
<b>Al</b>	K series	44.41	0.319	11.04	0.18	8.64	Al <sub>2</sub> O <sub>3</sub>
<b>Si</b>	K series	103.39	0.8193	27.79	0.38	20.9	SiO <sub>2</sub>
<b>P</b>	K series	4.17	0.0233	0.99	0.06	0.67	GaP
<b>Cl</b>	K series	3.83	0.0335	1.08	0.06	0.64	NaCl
<b>K</b>	K series	51.52	0.4364	12.18	0.19	6.58	KBr
<b>Total:</b>				100		100	

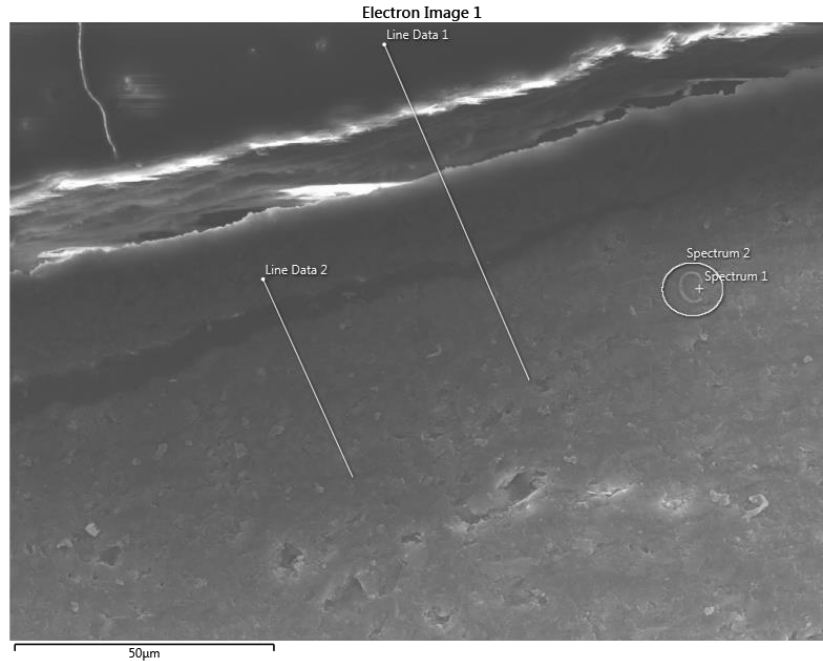


Figure 7. 13. EDS image of CGP20 and scanned area with selected line scans in CGP5 after simultaneous removal

Figure 7. 13 is showing the image of CGP20 after the simultaneous removal study. Line 1 passing through from epoxy to geopolymer body is about 60µm where it was analyzed for key elements. The apparent crack on the surface is the separation of epoxy from geopolymer, possibly caused by irregularities from curing of epoxy. From the line scan of Line 1 Figure 7. 14, it can be observed that key elements were distributed evenly. Al, Si, P and N showed trends where they decrease on the surface on another crack located between 45-50µm. Nutrients are distributed evenly through geopolymer structure by looking at the same image. Considering that the line scan is done on the first 60µm, it can be interpreted as nutrients are adsorbed on the surface of CGP20.



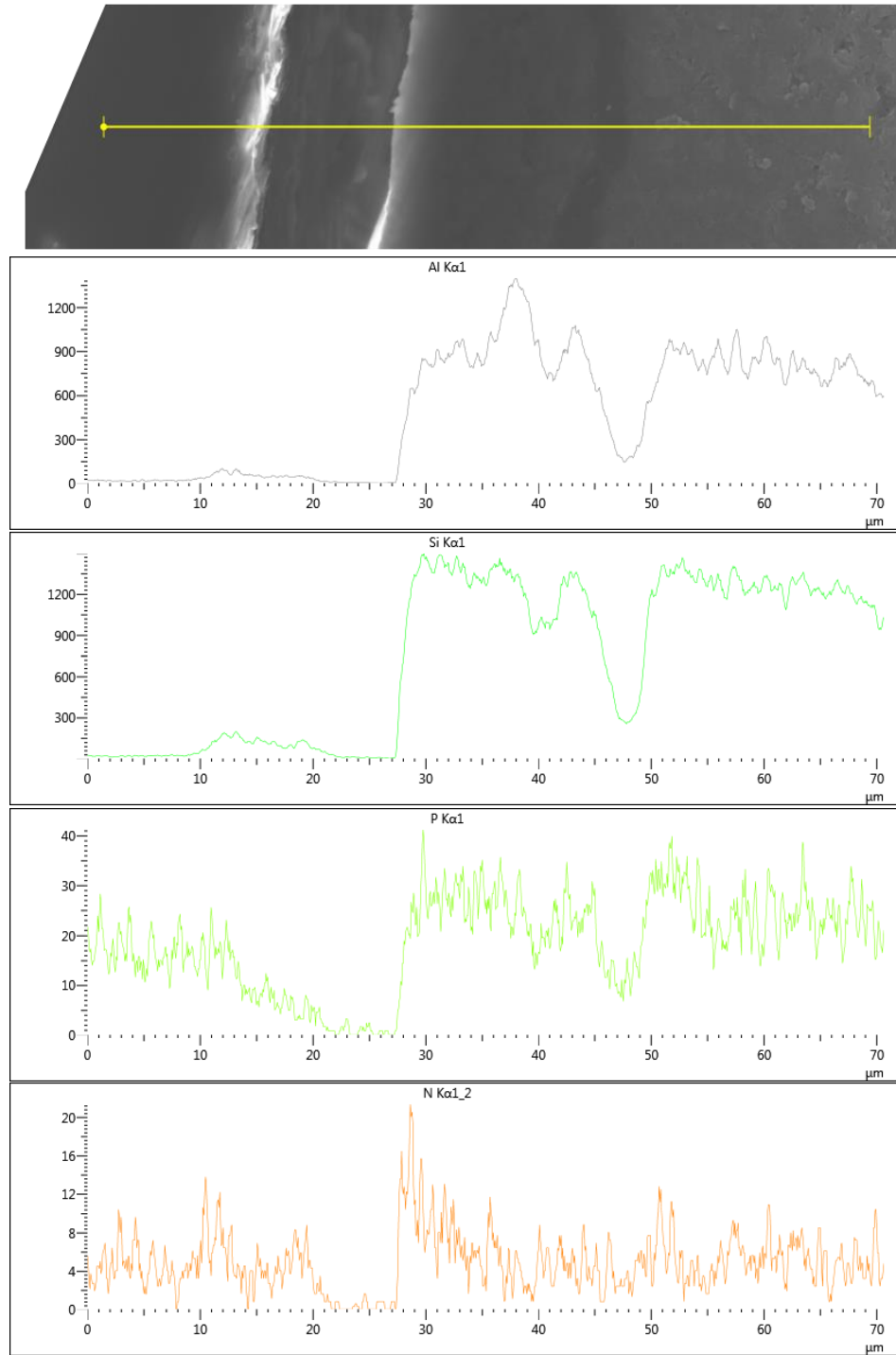


Figure 7. 14. Line Scan performed on CGP20 after simultaneous study, Al, Si, P and N from the surface (left) to inner structure (right)

Table 7. 6. Map spectrum results of CGP20, normalized values for elemental distribution

<b>Element</b>	<b>Line Type</b>	<b>Apparent Concentration</b>	<b>k Ratio</b>	<b>Wt%</b>	<b>Wt% Sigma</b>	<b>Atomic %</b>	<b>Standard Label</b>
<b>N</b>	K series	3.85	0.007	3.88	0.20	5.64	BN
<b>O</b>	K series	65.90	0.222	46.83	0.12	59.62	SiO <sub>2</sub>
<b>Al</b>	K series	44.63	0.321	15.33	0.04	11.57	Al <sub>2</sub> O <sub>3</sub>
<b>Si</b>	K series	67.59	0.536	26.78	0.07	19.42	SiO <sub>2</sub>
<b>P</b>	K series	0.19	0.001	0.07	0.01	0.04	GaP
<b>K</b>	K series	21.66	0.183	7.11	0.02	3.71	KBr
<b>Total:</b>				100.00		100.00	

Figure 7. 15 and Figure 7. 16 are showing the image of MGP5 after simultaneous removal study and elements identified from EDS mapping. Line 1 passing through from epoxy to geopolymer body is about 50µm where it was analyzed for key elements. From the line scan of Line1Figure 7. 17, it can be observed that key elements were distributed evenly. Al, Si, Mg, P and N showed low or no presence where they increased over the distance towards inner locations. Nutrients are distributed evenly through geopolymer structure by looking at the same image. Considering that the line scan is done on the first 50µm, it can be interpreted as nutrients are adsorbed on the surface of MGP5.

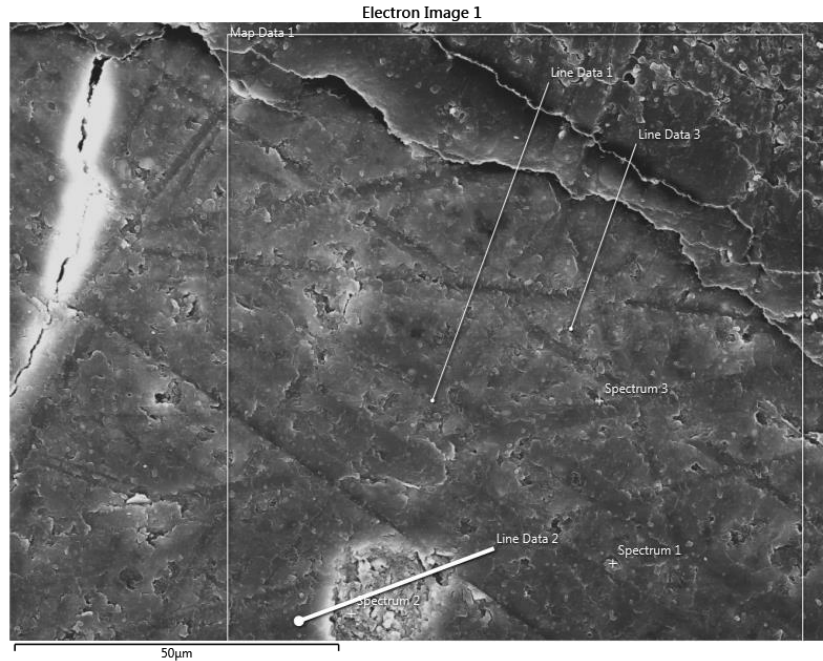
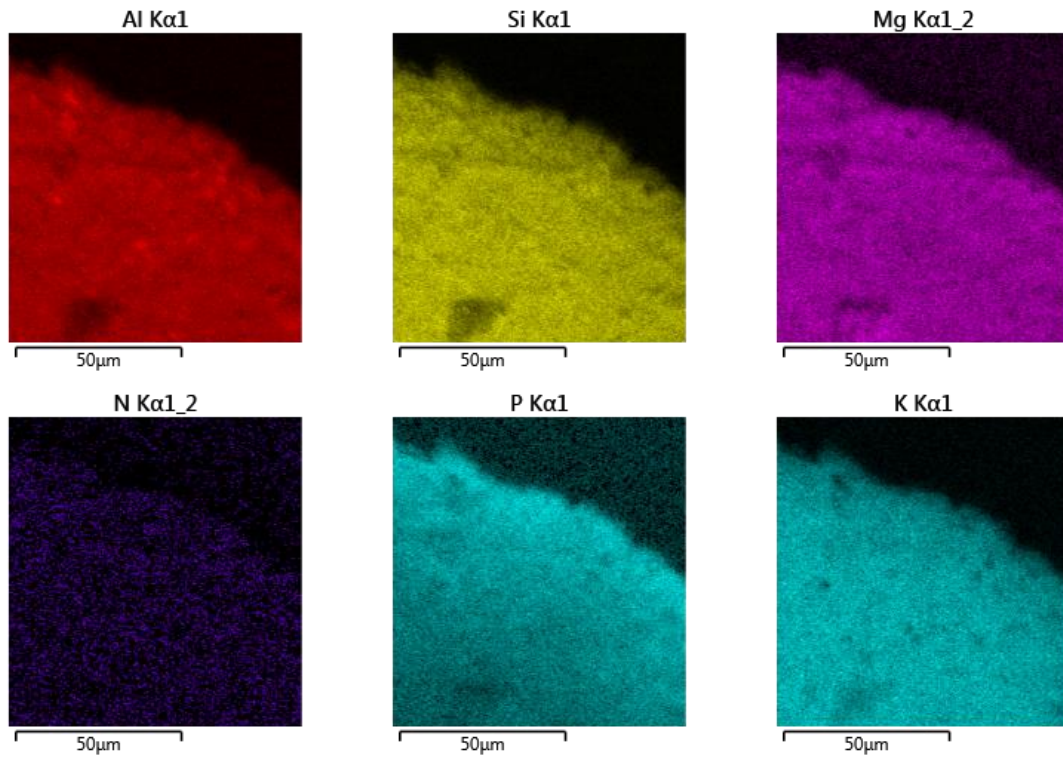
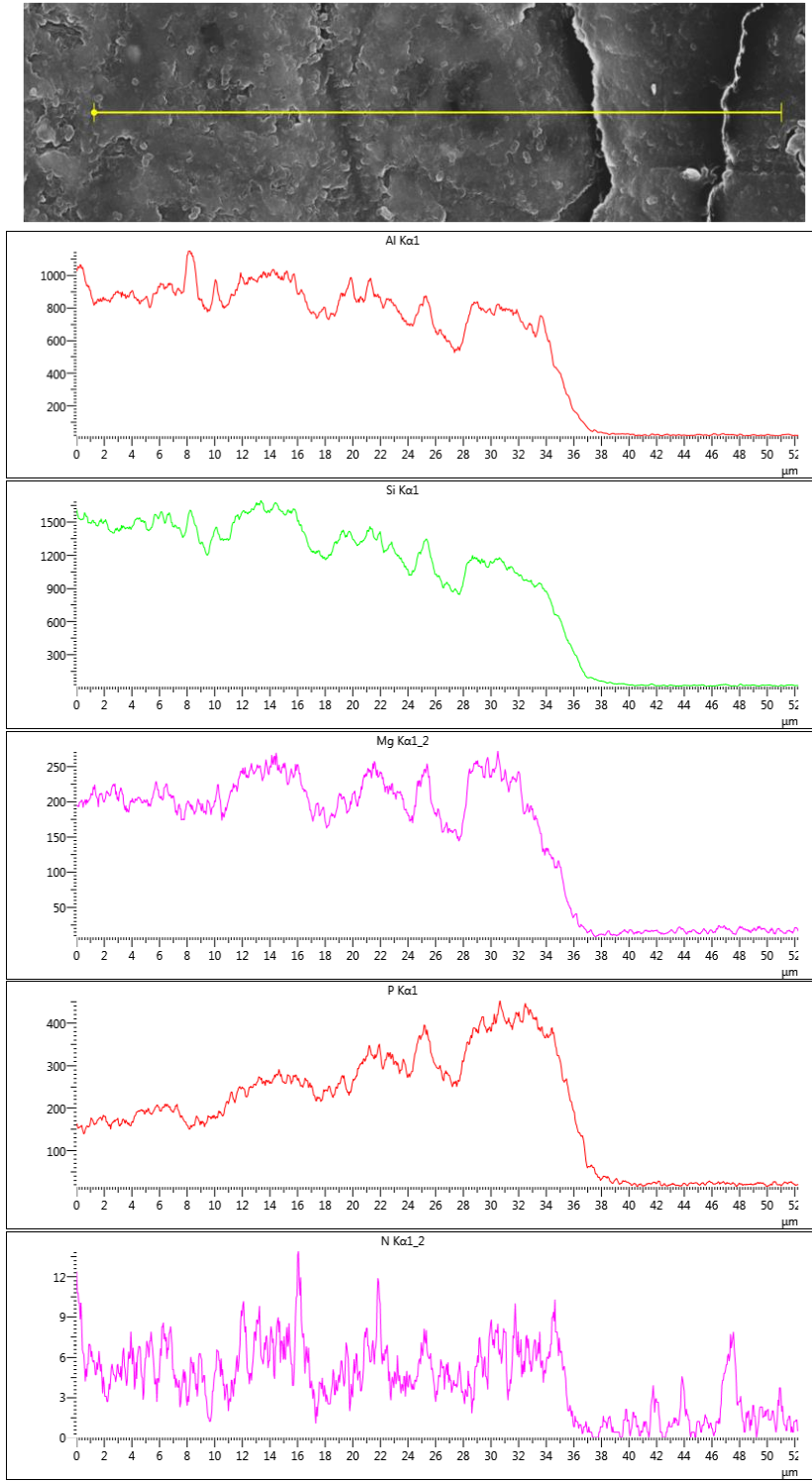


Figure 7. 15. EDS image of MGP5 and scanned area with selected line scans in CGP5 after simultaneous removal



*\*Binning increased to enhance visualization of element identification*

Figure 7. 16. EDS image layers showing Al, Si, Mg, N, P and K distribution in MGP5 after simultaneous removal.



\*Graphs show cps (Y-axis) vs μm (X-axis)

Figure 7. 17. Line Scan performed on MGP5 after simultaneous study, Al, Si, Mg, P and N from the surface (right) to inner structure (left)

## 7.5. Summary

This study is performed to evaluate geopolymers and geopolymer composites on their simultaneous nutrient removal efficiencies. Batch adsorption studies were performed by using four forms of geopolymeric adsorbents; PGP, CGP5, CGP20 and MGP5. As in individual studies performed in Chapter 5 and Chapter 6, pH evolution is observed in phosphorus removal studies as well. Initial nutrient concentration was kept constant for each experiment and once again type of composite was the key parameter on the comparison of the results.

PGP on simultaneous removal showed increased efficiency (>95%) and speed of uptake on both nutrients' removal. Co-existing nutrients in model solutions increased the removal rate and speed in this case.

In terms of simultaneous removal, clinoptilolite incorporated geopolymer composites (CGP5 and CGP20) showed promising results, however, their nitrogen removal efficiencies have decreased from ~98% to ~94%. Decrease in the efficiency was not drastic, but it was an indicator of the matrix effect caused by phosphorus ions.

A new composite, MGP5 was introduced in this study to observe simultaneous removal with the addition of metal cation source,  $Mg^{+}$ . Removal efficiency by MGP was better on phosphorus removal comparing to PGP and faster removal of nitrogen was observed comparing to CGP composites.

XRF mapping results are giving a basis for this mechanism by looking at the quantification of present data. The possibility of precipitation reaction shows itself of MGP5 composite,

where both phosphorus and nitrogen were detected through mapping studies as well as increased removal efficiency. Other composites were also presenting both nutrients, but especially for nitrogen results were very low to observe.

## **CHAPTER VIII**

### **CONCLUSIONS AND FUTURE WORK**

This research was focused on evaluating inexpensive novel clay-based materials, geopolymers, on their nitrogen and phosphorus removal efficiencies from aqueous solutions. The work was categorized into three primary objectives. First, geopolymer based composite adsorbents were processed and their surface properties, microstructure, and mechanical strength were characterized. Second, their individual nutrient removal capabilities were assessed. This focus was specifically on ammonium and phosphorus removal separately. Third, simultaneous removal of ammonium and phosphorus by select geopolymer composites adsorbents were evaluated to understand if the presence of a competing ion would influence the removal efficiencies.

This chapter summarizes the findings of this research. Suggestions are also provided to guide future work on this subject.

## **8.1. Conclusions**

Key findings from this research are presented under three subheadings below:

### **Geopolymer based adsorbents:**

Although geopolymers can have a range of compositions, stoichiometric addition of the components and curing conditions can impact the integrity of the processed geopolymer composite. Optimal curing conditions identified and used in this study were 40°C and 80 relative humidity for at least 72 hours.

Inclusion of clinoptilolite in pure geopolymer increased the compressive strength of the composite up to 10 volume percent addition of clinoptilolite; further increase in the clinoptilolite content resulted in a sharp decline in the mechanical properties.

Based on gas adsorption studies conducted on powder samples prepared from the processed composites, it was observed that increasing the amount of clinoptilolite in geopolymer composites decreased the surface area as well as the average pore diameter size. Approximately 77% reduction in surface area and a 29% decrease in average pore diameter was observed when the clinoptilolite content was increased from 5 to 20 volume % in the geopolymer matrix.

Mercury intrusion studies on solid samples confirmed that the inclusion of clinoptilolite in pure geopolymer decreased the overall porosity of the composite, however, the permeability and tortuosity of the adsorbent microstructure showed a notable increase. The above observations suggest an interesting opportunity in tailoring the adsorption properties of the geopolymer composites by varying the clinoptilolite content.



### **Individual nitrogen and phosphorus removal:**

Ammonium removal from aqueous solutions - Inclusion of clinoptilolite in pure geopolymer matrix accelerated the removal of ammonium from aqueous solutions in the first 3 hours by 10 to 50 folds. In the case of pure geopolymer, ammonium removal slowly increased to 96% in 3 hours, however, the removal efficiency fluctuated and 100% removal was observed only after 8 hours. In contrast, the efficiency of removal of ammonium by clinoptilolite geopolymer composites was steady throughout the 24-hour duration of the experiment and was approximately 98%.

Phosphorus removal from aqueous solutions – For these investigations pure geopolymer and two composites having 5 and 20 % clinoptilolite were selected. Pure geopolymer demonstrates a fluctuating pattern of adsorption for the first 8 hours of the experiment, ranging between 25 %-100% for the first three hours and 76 – 100% for the rest of the experiment. The efficiency of phosphorus removal reached and stayed at 100% after 8 hours. The efficiency of phosphorus removal from aqueous solutions by clinoptilolite incorporated composites was approximately 98% and steady throughout the experiment duration.

### **Simultaneous nitrogen and phosphorus removal:**

Pure geopolymer, clinoptilolite incorporated composites and MgO incorporated composites were used in simultaneous nitrogen and phosphorus removal from aqueous solutions. Pure geopolymer demonstrated removal efficiency of 98% on phosphorus removal and approximately 99% on nitrogen. The removal process was steady through the

experiment period. The removal efficiency of phosphorus by geopolymer composites were approximately 98% for both 5 and 20 volume % clinoptilolite incorporation. However, nitrogen removal efficiency decreased down to 94.9% and 95.4%. Composites with 5 volume % MgO incorporation exhibited outstanding removal efficiency for nitrogen and phosphorus of 100% and 98.5%. Every adsorbent used in this experiment reached high removal in the first 10 minutes and remained steady through the test period. Based on these observations it was concluded that the concurrent presence of ammonium and phosphate ions in the aqueous solutions did not limit the removal efficiencies of nitrogen and phosphorus by the geopolymer based adsorbents.

## **8.2. Future Work**

This research has conclusively established the use of geopolymer and geopolymer based composites for the removal of ammonium and phosphate ions from aqueous solutions, both in isolation and in concurrence. It has paved the way for future studies that should address both fundamental questions as well as application specific developments. It will be of immense interest to confirm that ion-exchange is the primary mechanism for ammonium ion removal from aqueous solutions. More importantly, a deeper understanding of the dominant mechanism for phosphate ion removal is warranted, for example, whether it is surface mediated ligand exchange reaction or merely physisorption. Such investigations should guide microstructure tailoring, primarily porosity, permeability and surface modification, for maximal removal of these ions from solutions using geopolymer composites.

This study was primarily motivated by its potential for impact in the poultry farming industry. Its promise sits at the cusp of the food-energy-water nexus, with the potential for positively addressing food scarcity, conserve energy and minimizing the adverse effects of poultry farming on water resources. Accordingly, future studies for the application of these adsorbents in the poultry industry should focus on the efficacy of the use of these adsorbents as fertilizer. For this purpose, leaching of N, P and K nutrients to the soil from geopolymer composite subsequent to their use as adsorbents for N and P should be evaluated. Another direction of research should focus on the ability of the adsorbents to arrest the ammonium ion and prevent its release to air as ammonia gas under conditions prevalent in the poultry farms. This will have an immediate impact in minimizing the energy consumption in poultry farms by decreasing heat losses associated with the current practices of frequent ventilation to maintain ammonia below toxic levels in the air in the poultry sheds. Lastly, but most importantly for the application of these adsorbents in the poultry farms, a comprehensive understanding of the matrix effect on the efficiency of nitrogen and phosphorus removal should be established.

## REFERENCES

- [1] National Science Foundation, “Innovations at the Nexus of Food, Energy and Water Systems(INFEWS),”2018.[Online].Available:  
[https://www.nsf.gov/publications/pub\\_summ.jsp?WT.z\\_pims\\_id=505241&ods\\_key=nsf18545](https://www.nsf.gov/publications/pub_summ.jsp?WT.z_pims_id=505241&ods_key=nsf18545).
- [2] North American Meat Institute, “The United States Meat Industry at a Glance,” 2019. <https://www.meatinstitute.org/index.php?ht=d/sp/i/47465/pid/47465>.
- [3] The Poultry Federation, “Poultry in Oklahoma: Facts & Figures,” 2020.
- [4] S. Ramos, K. Ha, and A. Melton, “Livestock, dairy, and poultry outlook,” 2018. [Online]. Available: <https://www.ers.usda.gov/webdocs/publications/89008/ldp-m-287.pdf?v=0>.
- [5] National Agricultural Statistics Service (NASS) and U.S. Department of Agriculture (USDA), “Overview of U.S. Livestock, Poultry, and Aquaculture Production in 2017,” 2018.
- [6] USDA National Agricultural Statistics Service Oklahoma Field Office, “Oklahoma Poultry Review,” 2019.
- [7] K. F. Davis, J. A. Gephart, K. A. Emery, A. M. Leach, J. N. Galloway, and P. D’Odorico, “Meeting future food demand with current agricultural resources,” *Glob. Environ. Chang.*, vol. 39, pp. 125–132, 2016, doi: 10.1016/j.gloenvcha.2016.05.004.

- [8] G. E. Bradford, "Contributions of animal agriculture to meeting global human food demand," *Livest. Prod. Sci.*, vol. 59, no. 2–3, pp. 95–112, 1999, doi: 10.1016/S0301-6226(99)00019-6.
- [9] D. R. Edwards and T. C. Daniel, "Environmental impacts of on-farm poultry waste disposal - A review," *Bioresour. Technol.*, vol. 41, no. 1, pp. 9–33, 1992, doi: 10.1016/0960-8524(92)90094-E.
- [10] S. Mukhtar, "Poultry Production: Manure and Wastewater Management," *Encyclopedia of Animal Science*, no. December. Marcel Dekker, Inc, pp. 1–5, 2005, doi: 0.1081/E-EAS 120023828.
- [11] R. K. Singh, "Latest Approach to Poultry Waste Management," 2019. <https://www.pashudhanpraharee.com/poultry-waste-management/>.
- [12] U.S. Department of Agriculture (USDA), "Agricultural Waste Management Systems," in *Agricultural Waste Management Field Handbook*, pp. 1–28.
- [13] J. Collins, E.R., J. C. Barker, L. E. Carr, H. L. Brodie, and J. Martin, J.H., "Poultry Waste Management Handbook," Ithaca, NY, 1999, pp. 1–64.
- [14] U.S. Department of Agriculture, "Agricultural Wastes and Water , Air , and Animal Contents :," in *Agricultural Waste Management Field Handbook*, USDA, pp. 3–27.
- [15] J. P. Chastain, J. J. Camberato, and P. Skewes, "Poultry Manure Production and Nutrient Content," 2010. [Online]. Available: <https://www.clemson.edu/extension/camm/manuals/>.
- [16] A. Sharpley *et al.*, "Nutrient Analysis of Poultry Litter," *Environmental Sciences*, Fayetteville, pp. 1–6, 2007.

- [17] A. N. Sharpley and B. Moyer, “Forms of phosphorus in manures and composts and their dissolution during rainfall.,” *J. Environ. Qual.*, vol. 29, pp. 1462–1469, 2000.
- [18] M. Allison, “New regulations proposed as Oklahoma chicken industry grows,” *KJRH*, 2019.
- [19] P. A. Office, W. Regulations, and S. Washington, “EPA Gold Book,” 1986.
- [20] U. S. Environmental Protection Agency, “Quality Criteria for Water. Office of Water Planning and Standards,” 1976.
- [21] M. M. Amanullah, S. Sekar, and P. Muthukrishnan, “Prospects and potential of poultry manure,” *Asian J. Plant Sci.*, vol. 9, no. 4, pp. 172–182, 2010, doi: 10.3923/ajps.2010.172.182.
- [22] J. Lorimor, W. Powers, and A. Sutton, “Manure Characteristics,” 2004.
- [23] C. Liu, “A study on the utilization of zeolite for ammonia removal from composting leachate,” The University of British Columbia, 2000.
- [24] F. Mazloomi and M. Jalali, “Ammonium removal from aqueous solutions by natural Iranian zeolite in the presence of organic acids , cations and anions,” *Biochem. Pharmacol.*, vol. 4, no. 1, pp. 240–249, 2016, doi: 10.1016/j.jece.2015.11.001.
- [25] S. Başakçılardan-Kabakci, A. N. Ipekoğlu, and L. Talinli, “Recovery of ammonia from human urine by stripping and absorption,” *Environ. Eng. Sci.*, vol. 24, no. 5, pp. 615–624, 2007, doi: 10.1089/ees.2006.0412.
- [26] A. Mohammed-Nour, M. Al-Sewailem, and A. H. El-Naggar, “The influence of alkalization and temperature on Ammonia recovery from cow manure and the chemical properties of the effluents,” *Sustain.*, vol. 11, no. 8, 2019, doi: 10.3390/su11082441.

- [27] S. E. Jorgensen, O. Libor, K. Lea Graber, and K. Barkacs, “Ammonia removal by use of clinoptilolite,” *Water Res.*, vol. 10, no. 3, pp. 213–224, 1976, doi: 10.1016/0043-1354(76)90130-5.
- [28] J. Huang, N. R. Kankanamge, C. Chow, D. T. Welsh, T. Li, and P. R. Teasdale, “Removing ammonium from water and wastewater using cost-effective adsorbents: A review,” *J. Environ. Sci. (China)*, vol. 63, pp. 174–197, 2018, doi: 10.1016/j.jes.2017.09.009.
- [29] T. Luukkonen, E. Nurmesniemi, H. Runtti, and K. Kemppainen, “Application of geopolymers as adsorbents in wastewater treatment – project GeoSorbents,” no. November, pp. 2–3, 2015, doi: 10.13140/RG.2.1.4682.6326.
- [30] J. T. Bunce, E. Ndam, I. D. Ofiteru, A. Moore, and D. W. Graham, “A Review of Phosphorus Removal Technologies and Their Applicability to Small-Scale Domestic Wastewater Treatment Systems,” *Frontiers in Environmental Science*, vol. 6, p. 8, 2018, [Online]. Available: <https://www.frontiersin.org/article/10.3389/fenvs.2018.00008>.
- [31] H. Yin and M. Kong, “Simultaneous removal of ammonium and phosphate from eutrophic waters using natural calcium-rich attapulgite-based versatile adsorbent,” *Desalination*, vol. 351, pp. 128–137, 2014, doi: 10.1016/j.desal.2014.07.029.
- [32] J. Davidovits, “Geopolymers - Inorganic polymeric new materials,” *J. Therm. Anal.*, vol. 37, no. 8, pp. 1633–1656, Aug. 1991, doi: 10.1007/BF01912193.
- [33] E. Arioz, Ö. Arioz, and Ö. M. Koçkar, “The Effect of Curing Conditions on the Properties of Geopolymer Samples,” *Int. J. Chem. Eng. Appl.*, vol. 4, no. 6, pp. 423–426, 2013, doi: 10.7763/ijcea.2013.v4.339.

- [34] M. Naghsh and K. Shams, "Synthesis of a kaolin-based geopolymer using a novel fusion method and its application in effective water softening," *Appl. Clay Sci.*, vol. 146, no. March, pp. 238–245, 2017, doi: 10.1016/j.clay.2017.06.008.
- [35] T. Skorina, "Ion exchange in amorphous alkali-activated aluminosilicates: Potassium based geopolymers," *Appl. Clay Sci.*, vol. 87, pp. 205–211, 2014, doi: 10.1016/j.clay.2013.11.003.
- [36] C. Bai *et al.*, "High-porosity geopolymer foams with tailored porosity for thermal insulation and wastewater treatment," *J. Mater. Res.*, vol. 32, no. 17, pp. 3251–3259, 2017, doi: 10.1557/jmr.2017.127.
- [37] C. Bai and P. Colombo, "Processing, properties and applications of highly porous geopolymers: A review," *Ceramics International*, vol. 44, no. 14. Elsevier Ltd, pp. 16103–16118, Oct. 01, 2018, doi: 10.1016/j.ceramint.2018.05.219.
- [38] H. M. Mbuvi, F. M. Maingi, H. M. Mbuvi, M. M. Ng'ang', and H. Mwangi, "Adsorption Kinetics and Isotherms of Methylene blue by Geopolymers Derived from Common Clay and Rice Husk Ash," *Phys. Chem.*, vol. 7, no. 4, pp. 87–97, 2017, doi: 10.5923/j.pc.20170704.02.
- [39] T. H. Tan, K. H. Mo, T. C. Ling, and S. H. Lai, "Current development of geopolymer as alternative adsorbent for heavy metal removal," *Environ. Technol. Innov.*, vol. 18, p. 100684, 2020, doi: 10.1016/j.eti.2020.100684.
- [40] B. Ventosa i Capell, "Simultaneous ammonium and phosphate removal by metal inorganic salt modification of natural zeolite," Escola Tècnica Superior d'Enginyeria Industrial de Barcelona, 2015.



- [41] L. Ricciotti, A. J. Molino, V. Roviello, E. Chianese, P. Cennamo, and G. Roviello, “Geopolymer composites for potential applications in cultural heritage,” *Environ. - MDPI*, vol. 4, no. 4, pp. 1–15, 2017, doi: 10.3390/environments4040091.
- [42] D. D. B. Nergis, M. M. A. B. Abdullah, P. Vizureanu, and M. F. M. Tahir, “Geopolymers and Their Uses : Review,” in *IOP Conf. Series: Materials Science and Engineering*, 2018, pp. 0–10, doi: 10.1088/1757-899X/374/1/012019.
- [43] M. Strozi Cilla, P. Colombo, and M. Raymundo Morelli, “Geopolymer foams by gelcasting,” *Ceram. Int.*, vol. 40, no. 4, pp. 5723–5730, 2014, doi: 10.1016/j.ceramint.2013.11.011.
- [44] P. Duxson, A. Fernández-Jiménez, J. L. Provis, G. C. Lukey, A. Palomo, and J. S. J. Van Deventer, “Geopolymer technology: The current state of the art,” *J. Mater. Sci.*, vol. 42, no. 9, pp. 2917–2933, 2007, doi: 10.1007/s10853-006-0637-z.
- [45] J. Davidovits, “Geopolymers and geopolymeric materials,” *J. Therm. Analysis*, vol. 35, pp. 429–441, 1989.
- [46] G. Sung, Y. Bok, K. Taek, and Y. Soo, “The mechanical properties of fly ash-based geopolymer concrete with alkaline activators,” *Constr. Build. Mater.*, vol. 47, no. 2013, pp. 409–418, 2013, doi: 10.1016/j.conbuildmat.2013.05.069.
- [47] Geopolymer Institute, “What is a Geopolymer? Introduction,” 2006. <https://www.geopolymer.org/science/introduction/>.
- [48] P. J. Davidovits, “30 Years of Successes and Failures in Geopolymer Applications . Market Trends and Potential Breakthroughs .,” pp. 1–16, 2002.
- [49] J. R. Gasca-Tirado *et al.*, “Ion Exchange in Geopolymers,” *IntechOpen*, vol. i, p. 13, 2018, doi: <http://dx.doi.org/10.5772/intechopen.80970>.

- [50] A. Fernandez-Jimenez, A. Palomo, I. Sobrados, and J. Sanz, “The role played by the reactive alumina content in the alkaline activation of fly ashes,” *Microporous Mesoporous Mater.*, vol. 91, pp. 111–119, 2006, doi: 10.1016/j.micromeso.2005.11.015.
- [51] F. Škvára, L. Kopecký, L. Myšková, V. Í. T. Šmilauer, L. Alberovská, and L. Vinšová, “Aluminosilicate Polymers - Influence Of Elevated Temperatures , Efflorescence,” *Ceram. – Silikáty*, vol. 53, no. 4, pp. 276–282, 2009.
- [52] M. Vocciante *et al.*, “Adsorption of ammonium on clinoptilolite in presence of competing cations: Investigation on groundwater remediation,” *J. Clean. Prod.*, vol. 198, pp. 480–487, 2018, doi: 10.1016/j.jclepro.2018.07.025.
- [53] J. Weitkamp, “Zeolites and catalysis,” *Solid State Ionics*, vol. 131, pp. 175–188, 2000.
- [54] A. Gibson and M. Maniocha, “The Use Of Magnesium Hydroxide Slurry For Biological Treatment Of Municipal And Industrial Wastewater.”
- [55] J. G. Jang, S. M. Park, G. M. Kim, and H. K. Lee, “Stability of MgO-modified geopolymeric gel structure exposed to a CO<sub>2</sub>-rich environment,” *Constr. Build. Mater.*, vol. 151, pp. 178–185, 2017, doi: 10.1016/j.conbuildmat.2017.06.088.
- [56] Lucideon Materials Development and Commercialization, “Brunauer-Emmett-Teller (BET) Surface Area Analysis and Barrett-Joyner-Halenda (BJH) Pore Size and Volume Analysis,” 2020. <https://www.lucideon.com/testing-characterization/techniques/bet-surface-area-analysis-bjh-pore-size-volume-analysis>.

- [57] J. Davidovits, *Geopolymer Chemistry and Applications*, 4th ed. Saint-Quentin: Institut Géopolmére, 2008.
- [58] A. Van Riessen, W. D. A. Rickard, R. P. Williams, and G. A. Van Riessen, “Methods for geopolymer formulation development and microstructural analysis,” *J. Ceram. Sci. Technol.*, vol. 8, no. 3, pp. 421–432, 2017, doi: 10.4416/JCST2017-00065.
- [59] S. Alehyen, M. E. L. Achouri, and M. Taibi, “Characterization, microstructure and properties of fly ash-based geopolymer,” vol. 8, no. 5, pp. 1783–1796, 2017.
- [60] C. Suryanarayana, “Microstructure : An Introduction,” in *Aerospace Materials and Material Technologies*, no. January, Springer Science+Business Media, 2017, pp. 105–123.
- [61] H. Clemens, S. Mayer, and C. Scheu, “Microstructure and Properties of Engineering Materials,” in *Neutrons and Synchrotron Radiation in Engineering Materials Science: From Fundamentals to Applications*, 2nd ed., Wiley-VCH Verlag GmbH & Co. KGaA, 2017, pp. 1–20.
- [62] ASTM International, “C39/C39M-18 Standard Test Method for Compressive Strength of Cylindrical Concrete Specimens 1,” West Conshohocken, PA, 2018. doi: 10.1520/C0039\_C0039M-18.
- [63] ASTM International, “D5550-14 Standard Test Method for Specific Gravity of Soil Solids by Gas Pycnometer.” ASTM International, West Conshohocken, 2014, doi: 10.1520/D5550-14.
- [64] D. R. Lide, *CRC Handbook of Chemistry and Physics*. CRC Press LLC, 2005.

- [65] A. Hedström and L. R. Amofah, “Adsorption and desorption of ammonium by clinoptilolite adsorbent in municipal wastewater treatment systems,” *J. Environ. Eng. Sci.*, vol. 7, no. 1, pp. 53–61, 2008, doi: 10.1139/S07-029.
- [66] D. E. . Vaughan, *Properties of Natural Zeolites*. Oxford: Pergamon Press, 1978.
- [67] V.P. Evangelou, *Environmental Soil and Water Chemistry: Principles and Applications*. A Wiley-Interscience Publication JOHN WILEY & SONS, INC., 1998.
- [68] G. K. Morse, S. W. Brett, J. A. Guy, and J. N. Lester, “Review: Phosphorus removal and recovery technologies,” *Sci. Total Environ.*, vol. 212, no. 1, pp. 69–81, 1998, doi: 10.1016/S0048-9697(97)00332-X.
- [69] L. Liberti, A. Laricchiuta, A. Lopez, R. Passino, and G. Boari, “The RIM-NUT process at west bari for removal of nutrients from wastewater: second demonstration,” *Resour. Conserv.*, vol. 15, no. 1–2, pp. 95–111, 1987, doi: 10.1016/0166-3097(87)90040-X.
- [70] N. Karapinar, “Application of natural zeolite for phosphorus and ammonium removal from aqueous solutions,” *J. Hazard. Mater.*, vol. 170, no. 2–3, pp. 1186–1191, 2009, doi: 10.1016/j.jhazmat.2009.05.094.
- [71] B. hua ZHANG, D. yi WU, C. WANG, S. bing HE, Z. jia ZHANG, and H. nan KONG, “Simultaneous removal of ammonium and phosphate by zeolite synthesized from coal fly ash as influenced by acid treatment,” *J. Environ. Sci.*, vol. 19, no. 5, pp. 540–545, 2007, doi: 10.1016/S1001-0742(07)60090-4.

- [72] B. B. Lind, Z. Ban, and S. Bydén, “Nutrient recovery from human urine by struvite crystallization with ammonia adsorption on zeolite and wollastonite,” *Bioresour. Technol.*, vol. 73, no. 2, pp. 169–174, 2000, doi: 10.1016/S0960-8524(99)90157-8.
- [73] R. Li *et al.*, “Simultaneous capture removal of phosphate, ammonium and organic substances by MgO impregnated biochar and its potential use in swine wastewater treatment,” *J. Clean. Prod.*, vol. 147, pp. 96–107, 2017, doi: 10.1016/j.jclepro.2017.01.069.
- [74] W. A. Tarpeh, K. M. Udert, and K. L. Nelson, “Comparing ion exchange adsorbents for nitrogen recovery from source-separated urine,” *Environ. Sci. Technol.*, vol. 51, no. 4, pp. 2373–2381, 2017, doi: 10.1021/acs.est.6b05816.
- [75] S. J. O’Connor, K. J. D. MacKenzie, M. E. Smith, and J. V. Hanna, “Ion exchange in the charge-balancing sites of aluminosilicate inorganic polymers,” *J. Mater. Chem.*, vol. 20, no. 45, pp. 10234–10240, 2010, doi: 10.1039/c0jm01254h.
- [76] T. Luukkonen, M. Sarkkinen, K. Kemppainen, J. Rämö, and U. Lassi, “Metakaolin geopolymer characterization and application for ammonium removal from model solutions and landfill leachate,” *Appl. Clay Sci.*, vol. 119, pp. 266–276, 2016, doi: 10.1016/j.clay.2015.10.027.
- [77] T. Samarina and E. Takaluoma, “Simultaneous removal of nutrients by geopolymers made from industrial by-products,” *Proc. World Congr. New Technol.*, vol. 0, no. November, pp. 4–9, 2019, doi: 10.11159/ICEPR19.169.
- [78] X. fei Tan *et al.*, “Biochar-based nano-composites for the decontamination of wastewater: A review,” *Bioresour. Technol.*, vol. 212, pp. 318–333, 2016, doi: 10.1016/j.biortech.2016.04.093.

## **APPENDICES**

### **APPENDIX A**

**Physicochemical Analysis of Virgin Adsorbents**

**Compressive Strength of Geopolymer Composites**

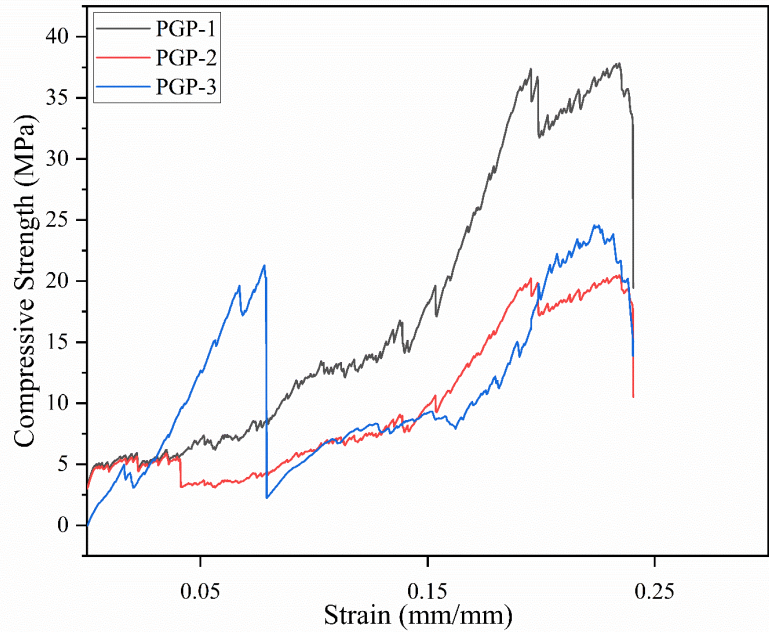


Figure A. 1. Compressive strength and strain diagram of pure geopolymer samples. Testing repeated three times with three separate samples. Compressive strength reported as 37.84 MPa at maximum and average is reported as 27.63 MPa

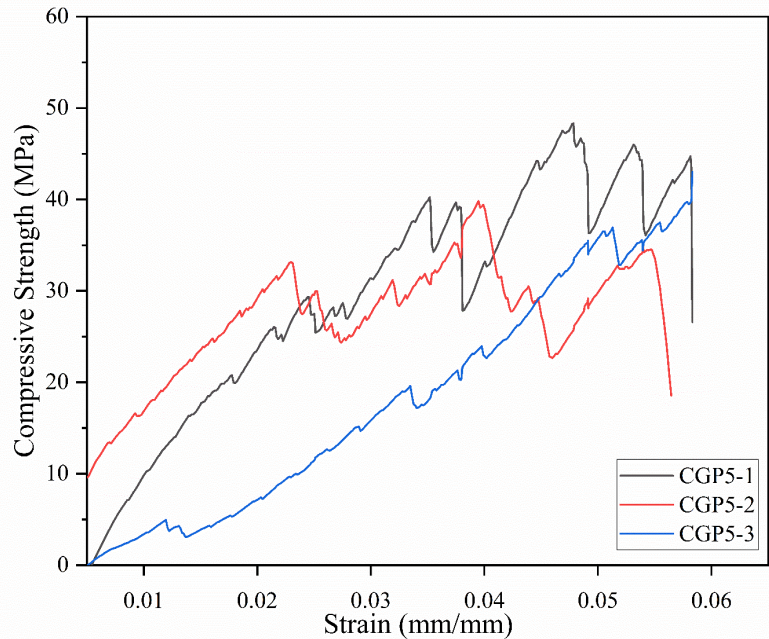


Figure A. 2. Compressive strength and strain diagram of clinoptilolite-geopolymer composite samples with 5% clinoptilolite by volume. Testing repeated three times with three separate samples with compressive strength reported as 55.73 MPa at maximum and average is reported as 47.96 MPa



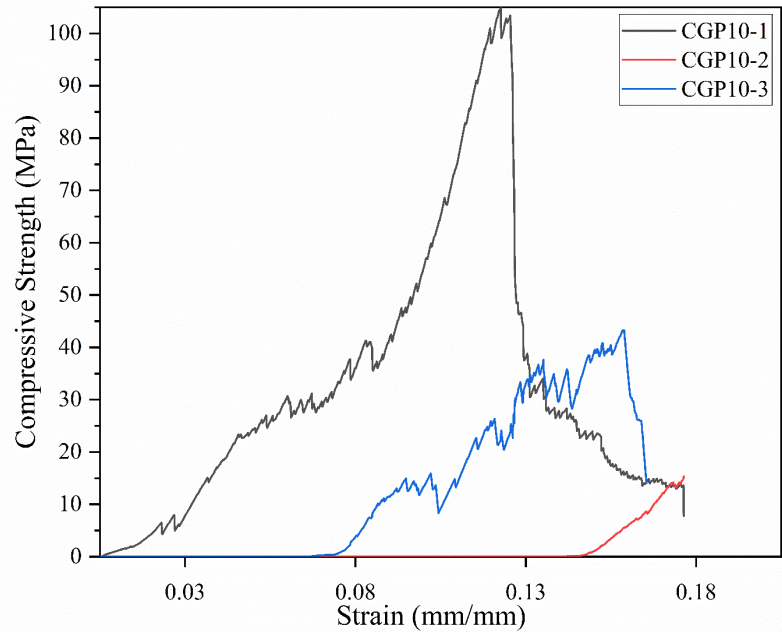


Figure A. 3. Compressive strength and strain diagram of clinoptilolite-geopolymer composite samples with 10% clinoptilolite by volume. Testing repeated three times with three separate samples with compressive strength reported as 104.96 MPa at maximum and average is reported as 66.36 MPa

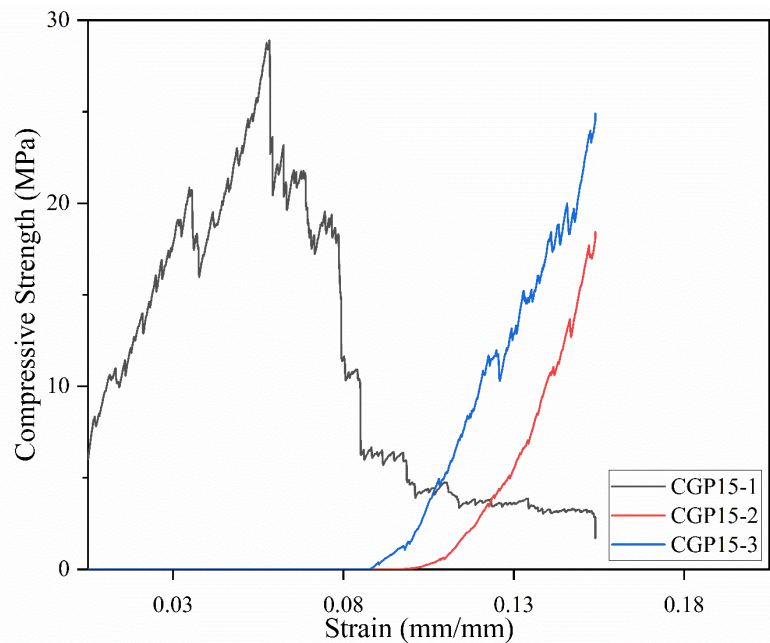


Figure A. 4. Compressive strength and strain diagram of clinoptilolite-geopolymer composite samples with 15% clinoptilolite by volume. Testing repeated three times with three separate samples with compressive strength reported as 30.52 MPa at maximum and average is reported as 28.54 MPa



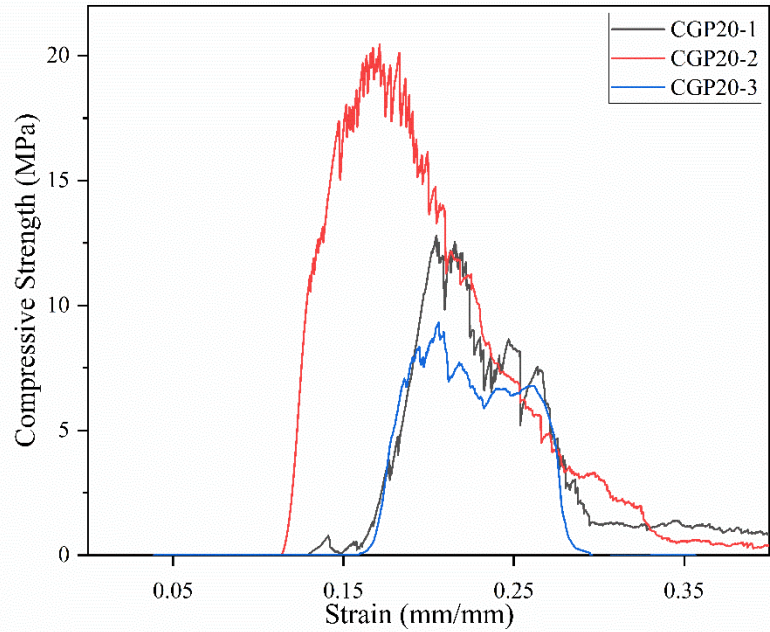


Figure A. 5. Compressive strength and strain diagram of clinoptilolite-geopolymer composite samples with 20% clinoptilolite by volume. Testing repeated three times with three separate samples with compressive strength reported as 20.46 MPa at maximum and average is reported as 14.19 MPa

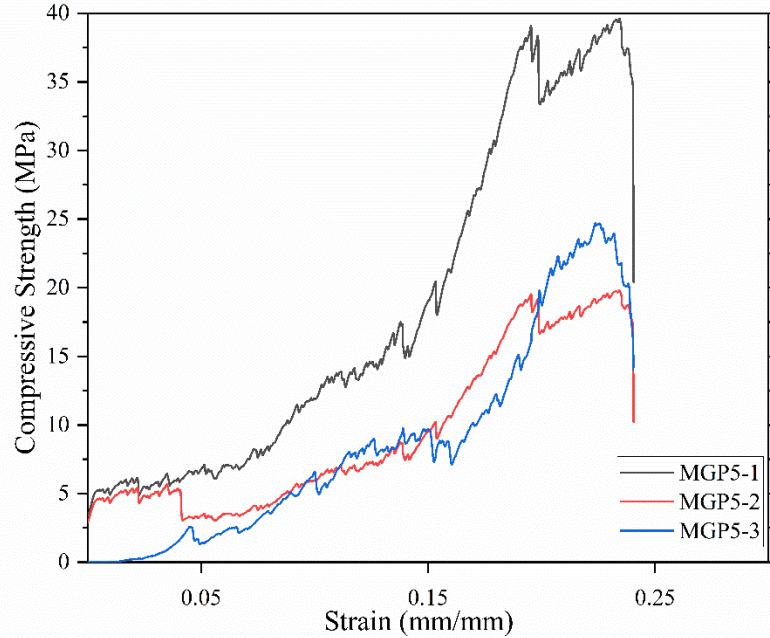


Figure A. 6. Compressive strength and strain diagram of clinoptilolite-geopolymer composite samples with 5% MgO by volume. Testing repeated three times with three separate samples with compressive strength reported as 39.69 MPa at maximum and average is reported as 32.23 MPa

## **APPENDIX B**

### **Physicochemical Analysis of Virgin Adsorbents**

#### **Porosity and Permeability Results of Geopolymers and Geopolymer Composites**

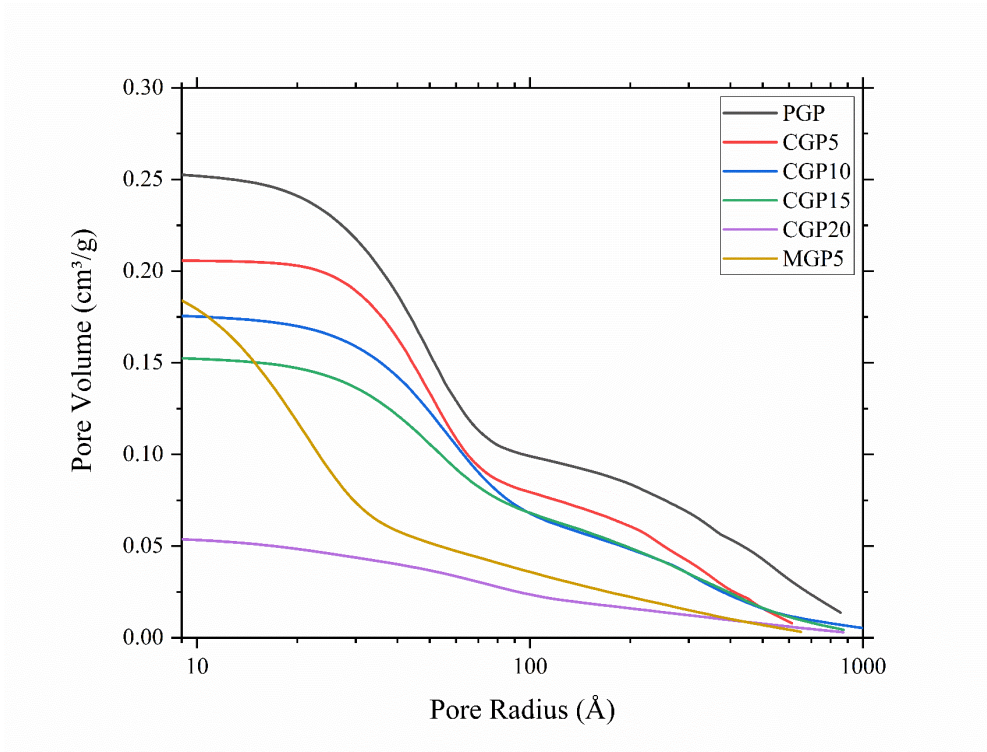


Figure B. 1. Cumulative adsorption graph of corresponding geopolymer composites obtained by gas adsorption (BJH analysis for pore size and volume distribution)

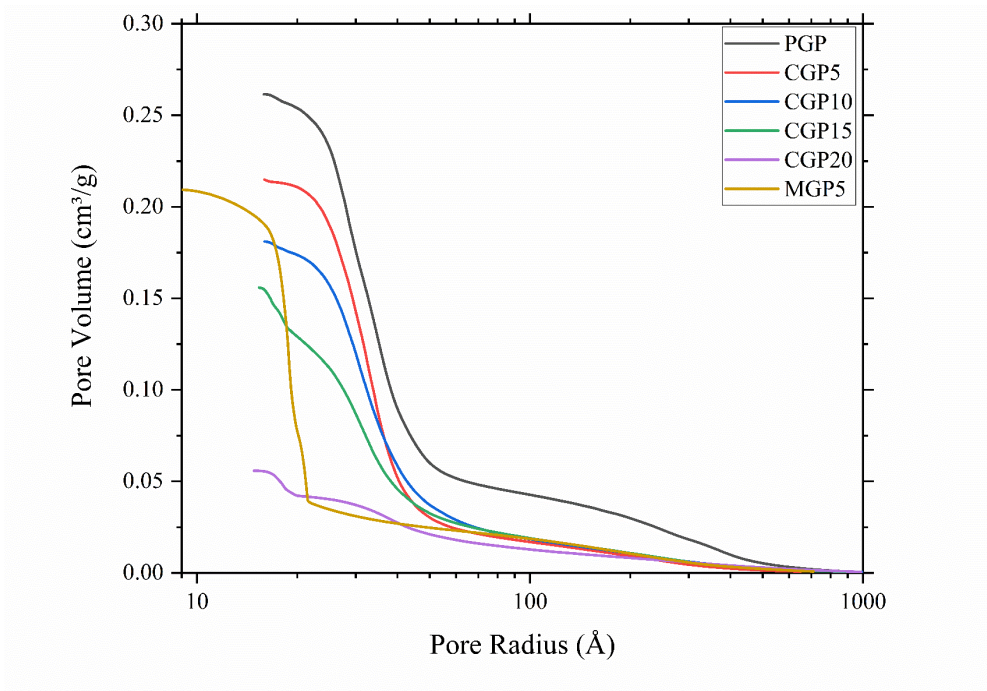


Figure B. 2. Cumulative desorption graph of corresponding geopolymer composites obtained by gas adsorption (BJH analysis for pore size and volume distribution)

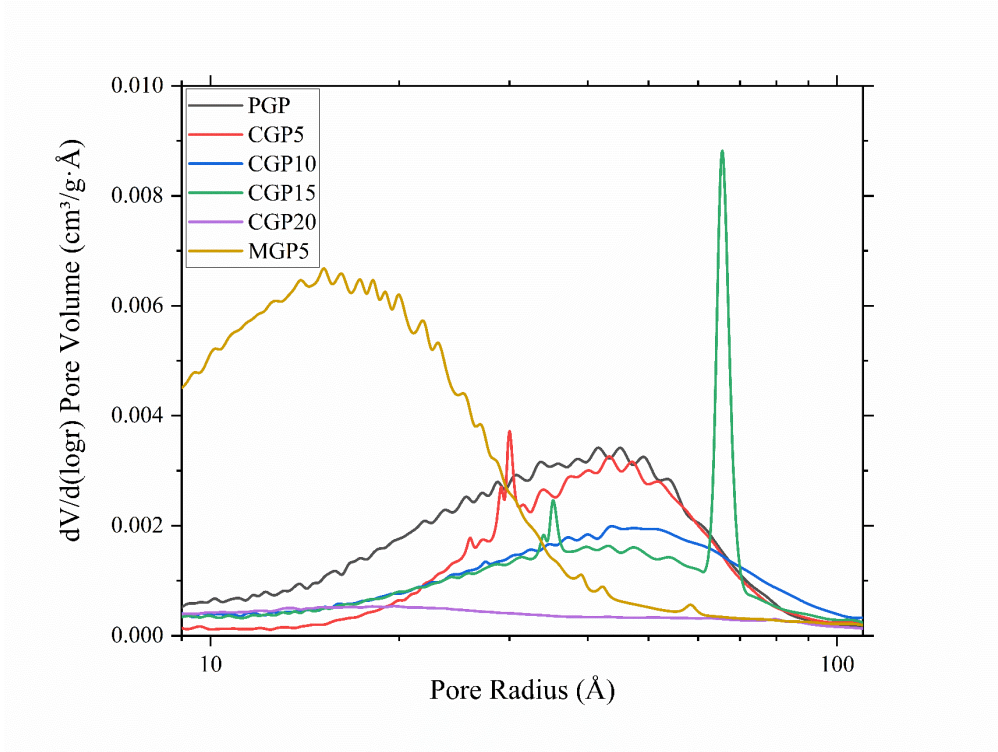


Figure B. 3. Cumulative adsorption graph of corresponding geopolymer composites obtained by gas adsorption (BJH analysis for pore size and volume distribution)

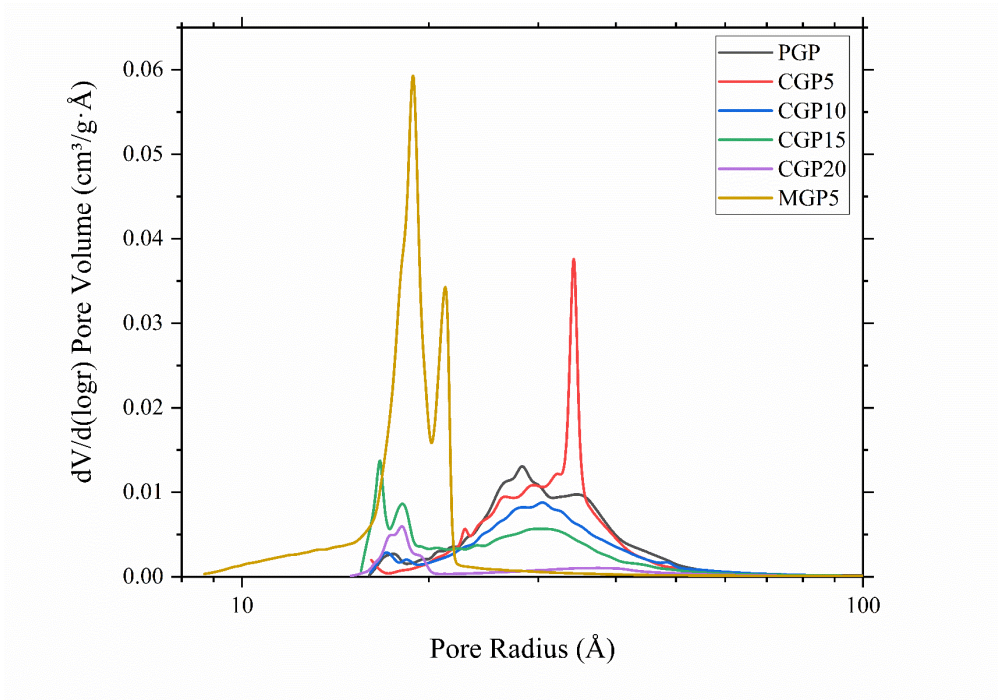


Figure B. 4. Cumulative desorption graph of corresponding geopolymer composites obtained by gas adsorption (BJH analysis for pore size and volume distribution)



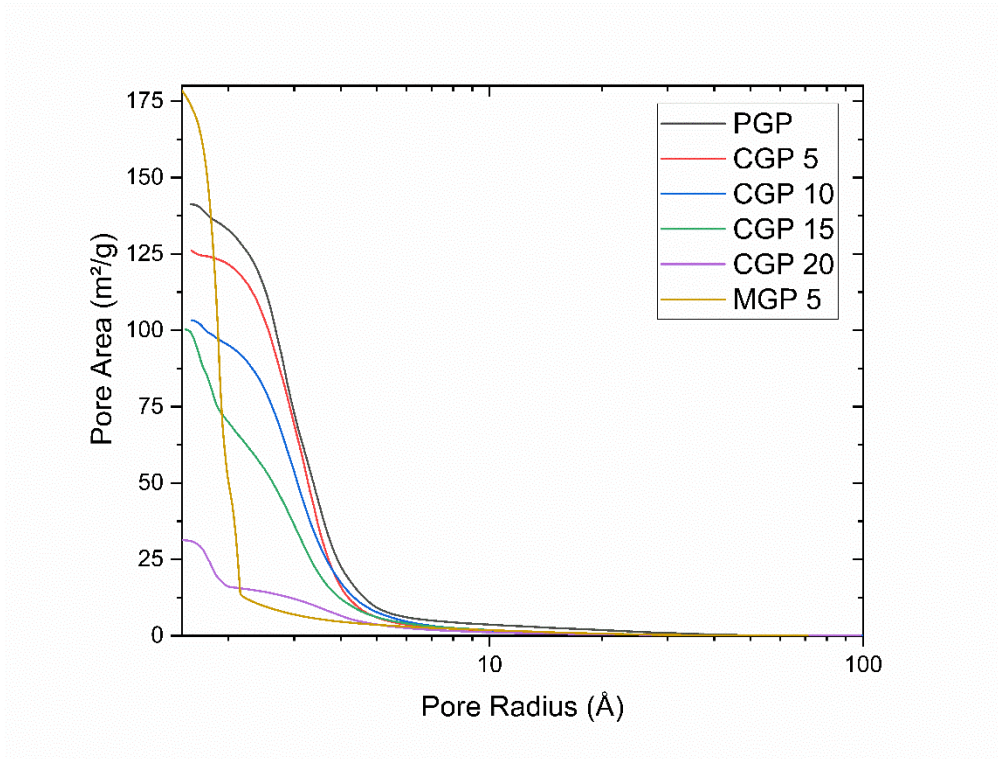


Figure B. 5. Pore area corresponding to pore radius obtained by gas adsorption for geopolymer and geopolymer composites.

## **APPENDIX C**

### **Physicochemical Analysis of Virgin Adsorbents**

#### **Water Quality Parameters and Results Obtained During Experiment Period**

Table C. 1. Water quality testing results for pure geopolymer on phosphorus removal

	10 min					20 min				
	pH	T	Ionic S.	TDS	Cond	pH	T	Ionic S.	TDS	Cond
<b>P1</b>	4.9	25.1	114.2	158.0	315.0	5.0	24.7	105.4	160.0	319.0
<b>P2</b>	4.9	25.5	113.8	170.0	337.0	5.0	25.1	105.6	171.0	342.0
<b>P3</b>	5.1	25.7	103.5	162.0	324.0	5.2	24.5	98.5	165.0	330.0
	30 min					45 min				
	pH	T	Ionic S.	TDS	Cond	pH	T	Ionic S.	TDS	Cond
<b>P1</b>	5.2	24.5	98.8	161.0	363.0	4.3	25.3	148.1	162.0	324.0
<b>P2</b>	5.2	25.1	99.5	171.0	341.0	5.3	25.1	91.7	172.0	344.0
<b>P3</b>	5.2	25.1	95.2	164.0	329.0	5.3	24.6	89.1	162.0	332.0
	60 min					120 min				
	pH	T	Ionic S.	TDS	Cond	pH	T	Ionic S.	TDS	Cond
<b>P1</b>	5.6	23.6	76.6	165.0	331.0	5.6	23.6	71.9	167.0	333.0
<b>P2</b>	5.6	23.7	76.2	174.0	349.0	5.6	23.5	72.4	174.0	348.0
<b>P3</b>	5.6	23.8	75.6	168.0	337.0	5.6	23.6	72.3	170.0	339.0
	180 min					240 min				
	pH	T	Ionic S.	TDS	Cond	pH	T	Ionic S.	TDS	Cond
<b>P1</b>	5.7	23.3	69.5	168.0	336.0	5.7	23.8	66.2	169.0	338.0
<b>P2</b>	5.7	23.4	69.7	176.0	354.0	5.8	23.8	65.9	177.0	354.0
<b>P3</b>	5.8	23.5	64.7	171.0	342.0	5.8	23.9	65.1	171.0	342.0
	300 min					360 min				
	pH	T	Ionic S.	TDS	Cond	pH	T	Ionic S.	TDS	Cond
<b>P1</b>	5.8	23.9	64.2	170.0	340.0	5.8	23.7	62.3	172.0	345.0
<b>P2</b>	5.8	23.9	65.7	177.0	354.0	5.9	23.8	60.1	180.0	361.0
<b>P3</b>	5.8	23.9	65.3	173.0	346.0	5.8	23.8	60.6	174.0	349.0
	420 min					480 min				
	pH	T	Ionic S.	TDS	Cond	pH	T	Ionic S.	TDS	Cond
<b>P1</b>	6.1	21.9	43.7	184.0	367.0	6.2	23.3	39.4	195.0	389.0
<b>P2</b>	6.2	22.0	43.0	190.0	380.0	6.3	23.4	33.5	202.0	404.0
<b>P3</b>	6.1	22.1	43.7	184.0	368.0	6.3	23.4	34.4	196.0	391.0

Table C. 2. Water quality testing results for pure geopolymer on nitrogen removal

	10 min					20 min				
	pH	T	Ionic S.	TDS	Cond	pH	T	Ionic S.	TDS	Cond
N1	4.3	25.7	148.3	140.0	279.0	4.4	25.5	140.7	141.0	282.0
N2	3.9	25.8	172.3	145.0	291.0	3.9	25.5	168.5	147.0	293.0
N3	4.1	25.8	160.6	143.0	286.0	4.2	25.5	154.4	145.0	289.0
	30 min					45 min				
	pH	T	Ionic S.	TDS	Cond	pH	T	Ionic S.	TDS	Cond
N1	4.4	25.1	131.8	141.0	281.0	4.8	24.7	118.1	141.0	283.0
N2	4.0	25.2	163.6	145.0	291.0	4.2	24.7	153.5	146.0	292.0
N3	4.3	25.3	148.1	144.0	288.0	4.5	24.8	135.2	144.0	289.0
	60 min					120 min				
	pH	T	Ionic S.	TDS	Cond	pH	T	Ionic S.	TDS	Cond
N1	5.3	23.9	91.3	145.0	289.0	5.4	23.6	84.6	145.0	290.0
N2	4.9	23.9	112.3	147.0	294.0	5.1	23.6	101.6	148.0	295.0
N3	5.1	24.0	100.6	146.0	292.0	5.3	23.7	92.0	147.0	294.0
	180 min					240 min				
	pH	T	Ionic S.	TDS	Cond	pH	T	Ionic S.	TDS	Cond
N1	5.6	24.1	72.8	149.0	297.0	5.7	23.9	68.4	149.0	297.0
N2	5.5	24.0	79.6	150.0	301.0	5.5	23.9	77.9	151.0	303.0
N3	5.6	24.1	74.0	150.0	300.0	5.6	24.0	72.0	151.0	302.0
	300 min					360 min				
	pH	T	Ionic S.	TDS	Cond	pH	T	Ionic S.	TDS	Cond
N1	5.8	23.9	64.2	170.0	340.0	5.8	23.7	62.3	172.0	345.0
N2	5.8	23.9	65.7	177.0	354.0	5.9	23.8	60.1	180.0	361.0
N3	5.8	23.9	65.3	173.0	346.0	5.8	23.8	60.6	174.0	349.0
	420 min					480 min				
	pH	T	Ionic S.	TDS	Cond	pH	T	Ionic S.	TDS	Cond
N1	6.1	22.1	47.0	158.0	316.0	6.3	23.5	37.3	169.0	338.0
N2	6.0	22.1	52.6	160.0	320.0	6.2	23.5	38.9	170.0	341.0
N3	6.0	22.1	49.2	160.0	320.0	6.3	23.6	35.5	171.0	340.0



Table C. 3. Water quality testing results of CPG5 on nitrogen removal.

	10 min					20 min				
	pH	T	Ionic S.	TDS	Cond	pH	T	Ionic S.	TDS	Cond
N1	4.7	26.9	110.0	139.0	279.0	4.8	26.6	104.7	140.0	281.0
N2	4.7	27.3	108.8	140.0	281.0	4.8	27.1	104.8	141.0	281.0
N3	4.7	27.6	110.1	139.0	277.0	4.8	27.2	107.5	139.0	278.0
	30 min					45 min				
	pH	T	Ionic S.	TDS	Cond	pH	T	Ionic S.	TDS	Cond
N1	4.9	26.5	100.6	141.0	282.0	5.0	25.7	94.6	141.0	181.0
N2	4.9	26.5	100.3	141.0	282.0	5.0	25.9	94.0	143.0	284.0
N3	4.8	26.8	102.1	139.0	279.0	4.9	26.2	96.6	140.0	281.0
	60 min					120 min				
	pH	T	Ionic S.	TDS	Cond	pH	T	Ionic S.	TDS	Cond
N1	5.0	25.3	90.5	142.0	283.0	5.2	24.6	80.4	143.0	286.0
N2	5.0	25.6	90.0	143.0	285.0	5.2	24.7	80.2	144.0	288.0
N3	5.0	25.8	92.8	141.0	282.0	5.2	24.9	82.6	142.0	285.0
	180 min					240 min				
	pH	T	Ionic S.	TDS	Cond	pH	T	Ionic S.	TDS	Cond
N1	5.3	24.3	74.3	144.0	288.0	5.4	24.0	70.0	145.0	290.0
N2	5.3	24.3	74.8	145.0	291.0	5.4	24.1	69.5	147.0	293.0
N3	5.3	24.5	76.7	144.0	286.0	5.4	24.4	71.6	144.0	289.0
	300 min					360 min				
	pH	T	Ionic S.	TDS	Cond	pH	T	Ionic S.	TDS	Cond
N1	5.5	23.9	65.3	147.0	292.0	5.5	23.8	64.0	148.0	295.0
N2	5.5	23.8	65.3	148.0	295.0	5.5	24.0	63.9	148.0	296.0
N3	5.5	24.1	67.4	145.0	290.0	5.5	24.1	66.0	146.0	292.0
	420 min					480 min				
	pH	T	Ionic S.	TDS	Cond	pH	T	Ionic S.	TDS	Cond
N1	5.6	23.8	62.7	148.0	296.0	5.6	23.7	61.1	149.0	298.0
N2	5.6	23.9	62.4	149.0	299.0	5.6	23.9	60.6	150.0	300.0
N3	5.5	24.1	64.0	147.0	293.0	5.6	24.0	61.9	147.0	295.0

Table C. 4. Water quality testing results for CGP10 on nitrogen removal

	<b>10 min</b>					<b>20 min</b>				
	<b>pH</b>	<b>T</b>	<b>Ionic S.</b>	<b>TDS</b>	<b>Cond</b>	<b>pH</b>	<b>T</b>	<b>Ionic S.</b>	<b>TDS</b>	<b>Cond</b>
<b>N1</b>	3.4	27.3	176.9	151.0	301.0	3.4	26.5	177.7	150.0	300.0
<b>N2</b>	3.3	27.5	185.8	152.0	304.0	3.3	27.2	184.8	152.0	303.0
<b>N3</b>	4.6	27.0	112.4	136.0	273.0	4.8	26.9	107.6	137.0	274.0
	<b>30 min</b>					<b>45 min</b>				
	<b>pH</b>	<b>T</b>	<b>Ionic S.</b>	<b>TDS</b>	<b>Cond</b>	<b>pH</b>	<b>T</b>	<b>Ionic S.</b>	<b>TDS</b>	<b>Cond</b>
<b>N1</b>	3.5	25.8	171.5	150.0	300.0	3.6	25.3	163.6	150.0	300.0
<b>N2</b>	3.4	26.5	180.0	151.0	303.0	3.5	25.1	174.1	151.0	303.0
<b>N3</b>	4.8	26.3	101.4	137.0	275.0	4.9	25.8	96.8	137.0	275.0
	<b>60 min</b>					<b>120 min</b>				
	<b>pH</b>	<b>T</b>	<b>Ionic S.</b>	<b>TDS</b>	<b>Cond</b>	<b>pH</b>	<b>T</b>	<b>Ionic S.</b>	<b>TDS</b>	<b>Cond</b>
<b>N1</b>	3.8	25.6	156.7	150.0	299.0	4.2	24.2	134.5	151.0	301.0
<b>N2</b>	3.6	25.5	168.9	151.0	303.0	3.9	24.5	148.7	151.0	302.0
<b>N3</b>	5.0	25.4	93.4	138.0	276.0	5.2	24.6	82.8	139.0	280.0
	<b>180 min</b>					<b>240 min</b>				
	<b>pH</b>	<b>T</b>	<b>Ionic S.</b>	<b>TDS</b>	<b>Cond</b>	<b>pH</b>	<b>T</b>	<b>Ionic S.</b>	<b>TDS</b>	<b>Cond</b>
<b>N1</b>	4.5	23.8	115.9	151.0	302.0	4.8	23.7	102.7	152.0	304.0
<b>N2</b>	4.3	24.1	130.1	151.0	302.0	4.6	23.9	115.1	152.0	303.0
<b>N3</b>	5.3	24.2	75.8	141.0	282.0	5.4	24.1	71.8	142.0	284.0
	<b>300 min</b>					<b>360 min</b>				
	<b>pH</b>	<b>T</b>	<b>Ionic S.</b>	<b>TDS</b>	<b>Cond</b>	<b>pH</b>	<b>T</b>	<b>Ionic S.</b>	<b>TDS</b>	<b>Cond</b>
<b>N1</b>	4.9	23.6	92.4	153.0	306.0	5.1	23.5	87.5	155.0	309.0
<b>N2</b>	4.9	23.7	101.4	153.0	306.0	5.0	23.8	95.8	154.0	307.0
<b>N3</b>	5.5	23.8	67.5	144.0	286.0	5.5	23.8	65.9	144.0	287.0
	<b>420 min</b>					<b>480 min</b>				
	<b>pH</b>	<b>T</b>	<b>Ionic S.</b>	<b>TDS</b>	<b>Cond</b>	<b>pH</b>	<b>T</b>	<b>Ionic S.</b>	<b>TDS</b>	<b>Cond</b>
<b>N1</b>	5.2	23.4	82.4	155.0	310.0	5.2	23.5	83.8	155.0	311.0
<b>N2</b>	5.0	23.6	90.6	154.0	308.0	5.1	23.5	88.6	155.0	310.0
<b>N3</b>	5.5	23.7	65.5	145.0	290.0	5.5	23.7	64.8	145.0	290.0

Table C. 5. Water quality testing results for CGP15 on nitrogen removal

	10 min					20 min				
	pH	T	Ionic S.	TDS	Cond	pH	T	Ionic S.	TDS	Cond
N1	4.8	27.3	105.5	145.0	290.0	4.9	26.9	98.7	146.0	292.0
N2	4.8	27.3	105.1	139.0	277.0	4.9	26.9	98.7	141.0	281.0
N3	5.0	27.2	93.7	138.0	275.0	5.0	26.8	90.9	140.0	281.0
	30 min					45 min				
	pH	T	Ionic S.	TDS	Cond	pH	T	Ionic S.	TDS	Cond
N1	4.9	26.5	99.4	146.0	295.0	5.0	25.9	92.0	147.0	294.0
N2	4.9	26.5	99.4	141.0	282.0	5.0	25.9	93.0	141.0	282.0
N3	5.0	26.5	92.5	140.0	280.0	5.1	25.9	86.9	140.0	280.0
	60 min					120 min				
	pH	T	Ionic S.	TDS	Cond	pH	T	Ionic S.	TDS	Cond
N1	5.0	25.5	91.3	143.0	296.0	5.2	25.0	79.6	150.0	299.0
N2	5.0	89.9	25.6	142.0	285.0	5.2	24.8	81.5	144.0	287.0
N3	5.2	84.3	25.6	141.0	282.0	5.3	24.9	77.4	142.0	285.0
	180 min					240 min				
	pH	T	Ionic S.	TDS	Cond	pH	T	Ionic S.	TDS	Cond
N1	5.3	24.5	75.8	151.0	302.0	5.4	24.4	73.5	151.0	302.0
N2	5.3	24.5	75.2	145.0	289.0	5.4	24.4	73.3	145.0	289.0
N3	5.3	24.7	73.7	143.0	287.0	5.4	24.5	71.8	144.0	288.0
	300 min					360 min				
	pH	T	Ionic S.	TDS	Cond	pH	T	Ionic S.	TDS	Cond
N1	5.4	24.3	70.1	152.0	304.0	5.5	24.2	64.8	153.0	305.0
N2	5.4	24.4	71.7	146.0	292.0	5.5	24.3	66.6	147.0	294.0
N3	5.4	24.5	68.9	144.0	289.0	5.5	24.5	65.0	145.0	290.0
	420 min					480 min				
	pH	T	Ionic S.	TDS	Cond	pH	T	Ionic S.	TDS	Cond
N1	5.5	24.1	64.2	154.0	308.0	5.6	24.1	62.0	155.0	309.0
N2	5.5	24.3	65.5	148.0	296.0	5.5	24.3	63.2	148.0	307.0
N3	5.5	24.3	63.5	146.0	292.0	5.6	24.4	61.5	146.0	291.0

Table C. 6. Water quality testing results for CGP20 on nitrogen removal

	10 min					20 min				
	pH	T	Ionic S.	TDS	Cond	pH	T	Ionic S.	TDS	Cond
<b>N1</b>	4.9	26.7	99.3	143.0	286.0	4.8	26.6	101.2	143.0	288.0
<b>N2</b>	4.8	27.1	105.3	144.0	287.0	4.9	26.5	99.5	143.0	285.0
<b>N3</b>	4.8	27.2	105.4	147.0	293.0	4.9	26.8	98.1	147.0	294.0
	30 min					45 min				
	pH	T	Ionic S.	TDS	Cond	pH	T	Ionic S.	TDS	Cond
<b>N1</b>	4.9	25.9	97.0	143.0	288.0	5.1	25.1	89.5	144.0	286.0
<b>N2</b>	4.9	26.2	97.6	143.0	288.0	5.0	25.6	91.1	144.0	289.0
<b>N3</b>	4.9	26.3	97.7	148.0	295.0	5.0	25.7	90.7	149.0	296.0
	60 min					120 min				
	pH	T	Ionic S.	TDS	Cond	pH	T	Ionic S.	TDS	Cond
<b>N1</b>	5.1	25.3	86.2	144.0	291.0	5.3	24.4	74.1	149.0	297.0
<b>N2</b>	5.1	25.4	87.6	145.0	290.0	5.3	24.5	75.9	147.0	294.0
<b>N3</b>	5.1	25.5	88.5	149.0	298.0	5.3	24.6	75.2	151.0	301.0
	180 min					240 min				
	pH	T	Ionic S.	TDS	Cond	pH	T	Ionic S.	TDS	Cond
<b>N1</b>	5.4	25.0	68.8	151.0	302.0	5.5	23.7	68.0	152.0	304.0
<b>N2</b>	5.4	24.3	70.2	148.0	298.0	5.4	24.1	70.9	149.0	299.0
<b>N3</b>	5.4	24.3	71.7	153.0	305.0	5.4	24.2	70.9	154.0	307.0
	300 min					360 min				
	pH	T	Ionic S.	TDS	Cond	pH	T	Ionic S.	TDS	Cond
<b>N1</b>	5.5	24.2	64.9	149.0	300.0	5.6	23.9	61.5	152.0	303.0
<b>N2</b>	5.5	24.2	66.1	150.0	300.0	5.6	24.0	62.9	151.0	302.0
<b>N3</b>	5.5	24.2	67.2	155.0	310.0	5.6	24.1	61.8	156.0	312.0
	420 min					480 min				
	pH	T	Ionic S.	TDS	Cond	pH	T	Ionic S.	TDS	Cond
<b>N1</b>	5.5	23.8	63.7	155.0	309.0	5.7	23.9	55.6	154.0	309.0
<b>N2</b>	5.6	24.0	60.7	152.0	305.0	5.7	24.0	57.0	153.0	306.0
<b>N3</b>	5.6	24.1	60.7	157.0	313.0	5.6	24.0	58.5	158.0	315.0

Table C. 7. Water quality testing results for CGP5 on phosphorus removal

	10 min					20 min				
	pH	T	Ionic S.	TDS	Cond	pH	T	Ionic S.	TDS	Cond
<b>P1</b>	4.8	27.5	102.0	169.0	338.0	5.1	26.9	88.3	168.0	336.0
<b>P2</b>	5.0	27.8	94.0	163.0	326.0	5.1	27.2	88.9	165.0	330.0
<b>P3</b>	5.0	27.8	90.8	163.0	327.0	5.2	27.3	84.5	165.0	331.0
	30 min					45 min				
	pH	T	Ionic S.	TDS	Cond	pH	T	Ionic S.	TDS	Cond
<b>P1</b>	5.4	26.6	72.8	169.0	336.0	5.5	25.8	67.8	170.0	339.0
<b>P2</b>	5.3	26.9	75.0	165.0	332.0	5.4	26.4	69.8	167.0	333.0
<b>P3</b>	5.4	26.8	74.0	166.0	333.0	5.5	26.4	68.3	167.0	335.0
	60 min					120 min				
	pH	T	Ionic S.	TDS	Cond	pH	T	Ionic S.	TDS	Cond
<b>P1</b>	5.5	25.3	64.1	171.0	343.0	5.8	24.9	51.0	175.0	351.0
<b>P2</b>	5.5	25.1	65.1	169.0	337.0	5.4	25.1	52.0	171.0	342.0
<b>P3</b>	5.5	26.0	65.0	169.0	338.0	5.8	25.2	51.2	172.0	344.0
	180 min					240 min				
	pH	T	Ionic S.	TDS	Cond	pH	T	Ionic S.	TDS	Cond
<b>P1</b>	5.8	24.4	47.3	178.0	357.0	6.0	24.8	42.0	181.0	360.0
<b>P2</b>	5.8	24.9	48.7	175.0	348.0	6.0	24.8	43.8	176.0	353.0
<b>P3</b>	5.9	25.0	46.9	175.0	349.0	5.9	24.9	42.8	177.0	354.0
	300 min					360 min				
	pH	T	Ionic S.	TDS	Cond	pH	T	Ionic S.	TDS	Cond
<b>P1</b>	6.0	24.8	38.3	182.0	365.0	6.1	24.6	36.0	185.0	368.0
<b>P2</b>	6.0	24.8	41.0	178.0	356.0	6.0	24.8	38.5	179.0	360.0
<b>P3</b>	6.0	24.8	40.8	179.0	357.0	6.0	24.8	38.2	180.0	361.0
	420 min					480 min				
	pH	T	Ionic S.	TDS	Cond	pH	T	Ionic S.	TDS	Cond
<b>P1</b>	6.1	24.4	35.1	186.0	372.0	6.1	24.3	34.2	187.0	375.0
<b>P2</b>	6.0	24.7	36.9	181.0	362.0	6.1	24.7	36.5	182.0	364.0
<b>P3</b>	6.1	24.8	36.7	182.0	364.0	6.1	24.8	35.5	183.0	366.0

Table C. 8. Water quality testing results for CGP20 on phosphorus removal

	10 min					20 min				
	pH	T	Ionic S.	TDS	Cond	pH	T	Ionic S.	TDS	Cond
<b>P1</b>	5.3	27.8	76.2	170.0	340.0	5.5	27.3	65.9	173.0	346.0
<b>P2</b>	5.3	27.8	76.4	165.0	331.0	5.6	27.3	60.9	168.0	338.0
<b>P3</b>	5.4	27.7	70.0	169.0	337.0	5.6	27.1	62.3	172.0	343.0
	30 min					45 min				
	pH	T	Ionic S.	TDS	Cond	pH	T	Ionic S.	TDS	Cond
<b>P1</b>	5.8	26.8	51.8	175.0	351.0	5.9	26.4	47.6	178.0	355.0
<b>P2</b>	5.8	26.7	53.1	170.0	342.0	5.8	26.4	48.3	173.0	346.0
<b>P3</b>	5.7	26.7	54.2	174.0	348.0	5.8	26.4	48.2	176.0	352.0
	60 min					120 min				
	pH	T	Ionic S.	TDS	Cond	pH	T	Ionic S.	TDS	Cond
<b>P1</b>	5.9	26.1	44.4	181.0	361.0	6.2	25.2	29.8	190.0	389.0
<b>P2</b>	5.9	26.0	45.6	175.0	350.0	6.1	25.2	32.0	184.0	367.0
<b>P3</b>	5.9	26.1	46.4	179.0	357.0	6.1	25.4	33.1	187.0	372.0
	180 min					240 min				
	pH	T	Ionic S.	TDS	Cond	pH	T	Ionic S.	TDS	Cond
<b>P1</b>	6.9	25.1	24.1	194.0	387.0	6.4	25.0	20.8	198.0	397.0
<b>P2</b>	6.2	25.1	26.4	187.0	375.0	6.3	25.1	23.5	192.0	383.0
<b>P3</b>	6.2	25.2	27.4	190.0	380.0	6.3	25.2	24.8	195.0	389.0
	300 min					360 min				
	pH	T	Ionic S.	TDS	Cond	pH	T	Ionic S.	TDS	Cond
<b>P1</b>	6.4	25.0	17.5	202.0	404.0	6.5	24.9	15.2	206.0	413.0
<b>P2</b>	6.4	25.0	20.5	195.0	391.0	6.4	25.0	18.4	199.0	397.0
<b>P3</b>	6.4	25.1	21.0	198.0	395.0	6.4	25.2	19.5	201.0	404.0
	420 min					480 min				
	pH	T	Ionic S.	TDS	Cond	pH	T	Ionic S.	TDS	Cond
<b>P1</b>	6.5	24.9	14.5	209.0	418.0	6.5	24.9	11.7	212.0	425.0
<b>P2</b>	6.4	25.0	16.9	201.0	402.0	6.5	25.0	15.4	205.0	409.0
<b>P3</b>	6.4	25.2	18.3	204.0	407.0	6.4	25.1	16.2	207.0	414.0

Table C. 9. Water quality testing results for pure geopolymer on simultaneous removal of nitrogen and phosphorus

	10 min					20 min				
	pH	T	Ionic S.	TDS	Cond	pH	T	Ionic S.	TDS	Cond
<b>PGP-Sim-1</b>	4.3	24.5	130.8	281.0	561.0	4.7	24.4	108.0	276.0	551.0
<b>PGP-Sim-2</b>	4.3	24.6	127.2	278.0	555.0	4.6	24.4	112.1	279.0	556.0
<b>PGP-Sim-3</b>	4.3	24.5	126.4	279.0	560.0	4.6	24.4	111.3	262.0	583.0
	30 min					45 min				
	pH	T	Ionic S.	TDS	Cond	pH	T	Ionic S.	TDS	Cond
<b>PGP-Sim-1</b>	4.8	24.2	102.5	275.0	550.0	4.9	24.2	99.6	274.0	547.0
<b>PGP-Sim-2</b>	4.8	24.3	103.1	278.0	556.0	4.9	24.2	99.3	279.0	558.0
<b>PGP-Sim-3</b>	4.8	24.2	104.3	283.0	565.0	4.8	24.2	100.7	283.0	563.0
	60 min					120 min				
	pH	T	Ionic S.	TDS	Cond	pH	T	Ionic S.	TDS	Cond
<b>PGP-Sim-1</b>	4.9	24.0	97.9	277.0	97.9	5.1	23.7	88.6	280.0	560.0
<b>PGP-Sim-2</b>	4.9	24.0	95.8	279.0	95.8	5.1	23.8	86.2	281.0	564.0
<b>PGP-Sim-3</b>	4.9	24.0	96.4	284.0	96.4	5.1	23.8	85.9	280.0	563.0
	180 min					240 min				
	pH	T	Ionic S.	TDS	Cond	pH	T	Ionic S.	TDS	Cond
<b>PGP-Sim-1</b>	5.2	23.7	81.2	280.0	559.0	5.3	23.6	75.4	280.0	561.0
<b>PGP-Sim-2</b>	5.2	23.7	81.2	282.0	565.0	5.3	23.7	75.3	283.0	563.0
<b>PGP-Sim-3</b>	5.2	23.8	91.4	285.0	571.0	5.3	23.7	76.2	287.0	572.0
	300 min					360 min				
	pH	T	Ionic S.	TDS	Cond	pH	T	Ionic S.	TDS	Cond
<b>PGP-Sim-1</b>	5.3	23.7	74.2	278.0	568.0	5.4	23.7	71.9	280.0	562.0
<b>PGP-Sim-2</b>	5.4	23.8	73.4	284.0	568.0	5.4	23.8	70.7	285.0	570.0
<b>PGP-Sim-3</b>	5.3	23.9	73.7	287.0	574.0	5.4	23.8	71.7	288.0	578.0
	420 min					480 min				
	pH	T	Ionic S.	TDS	Cond	pH	T	Ionic S.	TDS	Cond
<b>PGP-Sim-1</b>	5.4	23.7	68.6	282.0	566.0	5.5	23.1	62.9	282.0	565.0
<b>PGP-Sim-2</b>	5.4	23.7	68.5	286.0	572.0	5.5	23.1	64.1	287.0	573.0
<b>PGP-Sim-3</b>	5.4	23.8	69.2	289.0	577.0	5.5	23.7	65.3	291.0	582.0

Table C. 10. Water quality testing results for CGP5 on simultaneous removal of nitrogen and phosphorus

	10 min					20 min				
	pH	T	Ionic S.	TDS	Cond	pH	T	Ionic S.	TDS	Cond
<b>CGP5-Sim-1</b>	4.4	22.0	120.0	280.0	561.0	4.7	22.0	108.0	284.0	567.0
<b>CGP5-Sim-2</b>	4.5	22.0	116.4	282.0	565.0	4.7	22.0	107.6	285.0	569.0
<b>CGP5-Sim-3</b>	4.6	23.7	114.3	267.0	534.0	4.7	23.5	105.0	269.0	539.0
	30 min					45 min				
	pH	T	Ionic S.	TDS	Cond	pH	T	Ionic S.	TDS	Cond
<b>CGP5-Sim-1</b>	4.8	22.1	103.4	284.0	568.0	4.8	22.0	99.2	279.0	558.0
<b>CGP5-Sim-2</b>	4.8	22.1	103.9	284.0	569.0	4.9	22.1	98.5	285.0	571.0
<b>CGP5-Sim-3</b>	4.8	23.3	101.4	270.0	540.0	4.9	23.1	96.1	271.0	540.0
	60 min					120 min				
	pH	T	Ionic S.	TDS	Cond	pH	T	Ionic S.	TDS	Cond
<b>CGP5-Sim-1</b>	4.9	22.0	95.2	284.0	568.0	5.1	22.3	87.3	287.0	575.0
<b>CGP5-Sim-2</b>	4.9	22.2	95.1	285.0	571.0	5.1	22.4	87.0	287.0	574.0
<b>CGP5-Sim-3</b>	5.0	23.0	93.2	271.0	541.0	5.1	22.8	84.5	273.0	574.0
	180 min					240 min				
	pH	T	Ionic S.	TDS	Cond	pH	T	Ionic S.	TDS	Cond
<b>CGP5-Sim-1</b>	5.2	22.3	82.5	289.0	578.0	5.3	22.6	78.0	291.0	582.0
<b>CGP5-Sim-2</b>	5.2	22.5	82.0	289.0	578.0	5.3	22.7	78.0	291.0	581.0
<b>CGP5-Sim-3</b>	5.2	22.8	80.3	274.0	550.0	5.3	22.9	76.0	276.0	553.0
	300 min					360 min				
	pH	T	Ionic S.	TDS	Cond	pH	T	Ionic S.	TDS	Cond
<b>CGP5-Sim-1</b>	5.3	22.8	75.3	291.0	582.0	5.6	22.9	57.7	293.0	587.0
<b>CGP5-Sim-2</b>	5.3	22.8	75.0	291.0	582.0	5.3	22.9	73.3	292.0	584.0
<b>CGP5-Sim-3</b>	5.3	22.9	73.4	277.0	554.0	5.4	23.0	71.6	278.0	557.0
	420 min					480 min				
	pH	T	Ionic S.	TDS	Cond	pH	T	Ionic S.	TDS	Cond
<b>CGP5-Sim-1</b>	5.4	22.6	71.5	294.0	588.0	5.4	22.8	70.0	295.0	590.0
<b>CGP5-Sim-2</b>	5.4	22.9	71.4	293.0	586.0	5.4	22.8	69.7	294.0	588.0
<b>CGP5-Sim-3</b>	5.4	23.0	69.7	279.0	559.0	5.5	23.0	67.5	280.0	561.0



Table C. 11. Water quality testing results for CGP20 on simultaneous removal of nitrogen and phosphorus

	10 min					20 min				
	pH	T	Ionic S.	TDS	Cond	pH	T	Ionic S.	TDS	Cond
<b>CGP20-Sim-1</b>	4.8	25.2	103.6	277.0	505.0	5.0	24.7	99.5	279.0	559.0
<b>CGP20-Sim-2</b>	4.8	26.0	103.0	284.0	568.0	5.0	25.4	94.8	287.0	574.0
<b>CGP20-Sim-3</b>	4.8	26.3	102.1	293.0	586.0	5.0	25.7	94.5	294.0	590.0
	30 min					45 min				
	pH	T	Ionic S.	TDS	Cond	pH	T	Ionic S.	TDS	Cond
<b>CGP20-Sim-1</b>	5.0	24.3	90.8	281.0	561.0	5.1	24.0	85.5	282.0	564.0
<b>CGP20-Sim-2</b>	5.0	25.0	91.3	287.0	575.0	5.1	24.4	86.0	289.0	579.0
<b>CGP20-Sim-3</b>	5.0	25.2	91.3	296.0	591.0	5.1	24.6	85.9	297.0	593.0
	60 min					120 min				
	pH	T	Ionic S.	TDS	Cond	pH	T	Ionic S.	TDS	Cond
<b>CGP20-Sim-1</b>	5.2	23.7	82.4	283.0	567.0	5.3	23.1	74.3	288.0	576.0
<b>CGP20-Sim-2</b>	5.2	24.1	83.0	290.0	581.0	5.3	23.3	74.1	295.0	590.0
<b>CGP20-Sim-3</b>	5.2	24.3	82.5	299.0	596.0	5.3	23.4	74.0	302.0	604.0
	180 min					240 min				
	pH	T	Ionic S.	TDS	Cond	pH	T	Ionic S.	TDS	Cond
<b>CGP20-Sim-1</b>	5.4	23.0	62.5	291.0	582.0	5.5	23.1	64.8	294.0	578.0
<b>CGP20-Sim-2</b>	5.4	23.1	69.9	298.0	595.0	5.5	23.1	65.8	300.0	599.0
<b>CGP20-Sim-3</b>	5.4	23.2	68.9	305.0	611.0	5.5	23.1	65.4	208.0	616.0
	300 min					360 min				
	pH	T	Ionic S.	TDS	Cond	pH	T	Ionic S.	TDS	Cond
<b>CGP20-Sim-1</b>	5.5	23.0	62.8	295.0	590.0	5.6	23.1	60.9	297.0	594.0
<b>CGP20-Sim-2</b>	5.6	23.1	58.1	303.0	604.0	5.6	23.1	59.8	305.0	610.0
<b>CGP20-Sim-3</b>	5.6	23.1	57.7	311.0	621.0	5.6	23.1	59.0	312.0	625.0
	420 min					480 min				
	pH	T	Ionic S.	TDS	Cond	pH	T	Ionic S.	TDS	Cond
<b>CGP20-Sim-1</b>	5.6	23.1	59.4	299.0	599.0	5.6	23.1	57.6	302.0	603.0
<b>CGP20-Sim-2</b>	5.6	23.1	59.9	307.0	614.0	5.6	23.1	58.5	308.0	617.0
<b>CGP20-Sim-3</b>	5.6	23.2	58.8	315.0	630.0	5.6	23.2	57.6	316.0	633.0

Table C. 12. Water quality testing results for MGP5 on simultaneous removal of nitrogen and phosphorus

	10 min					20 min				
	pH	T	Ionic S.	TDS	Cond	pH	T	Ionic S.	TDS	Cond
MGP5-Sim-1	4.6	24.6	111.3	272.0	544.0	4.7	23.6	108.6	278.0	555.0
MGP5-Sim-2	4.6	24.8	114.6	286.0	572.0	4.7	24.4	108.1	288.0	575.0
MGP5-Sim-3	4.5	24.9	116.6	278.0	555.0	4.7	24.5	109.0	278.0	557.0
	30 min					45 min				
	pH	T	Ionic S.	TDS	Cond	pH	T	Ionic S.	TDS	Cond
MGP5-Sim-1	4.8	23.6	104.4	279.0	557.0	4.9	23.2	99.1	279.0	557.0
MGP5-Sim-2	4.8	24.1	104.2	287.0	572.0	4.8	23.7	99.8	288.0	577.0
MGP5-Sim-3	4.7	24.2	105.4	279.0	559.0	4.8	23.8	101.0	279.0	559.0
	60 min					120 min				
	pH	T	Ionic S.	TDS	Cond	pH	T	Ionic S.	TDS	Cond
MGP5-Sim-1	4.9	23.1	94.9	279.0	558.0	5.1	22.7	87.8	283.0	564.0
MGP5-Sim-2	4.9	23.4	95.5	290.0	579.0	5.1	22.8	87.8	291.0	581.0
MGP5-Sim-3	4.9	23.6	97.1	279.0	559.0	5.0	23.0	89.9	282.0	563.0
	180 min					240 min				
	pH	T	Ionic S.	TDS	Cond	pH	T	Ionic S.	TDS	Cond
MGP5-Sim-1	5.1	22.6	83.6	283.0	567.0	5.2	22.5	79.8	285.0	568.0
MGP5-Sim-2	5.2	22.8	83.2	293.0	584.0	5.2	22.7	79.5	293.0	586.0
MGP5-Sim-3	5.1	22.8	85.1	282.0	565.0	5.2	22.8	81.9	284.0	567.0
	300 min					360 min				
	pH	T	Ionic S.	TDS	Cond	pH	T	Ionic S.	TDS	Cond
MGP5-Sim-1	5.3	22.7	77.1	286.0	570.0	5.3	22.7	74.0	286.0	571.0
MGP5-Sim-2	5.3	22.7	76.7	294.0	588.0	5.3	22.8	74.8	295.0	590.0
MGP5-Sim-3	5.2	22.9	78.6	284.0	570.0	5.3	22.9	76.8	286.0	571.0
	420 min					480 min				
	pH	T	Ionic S.	TDS	Cond	pH	T	Ionic S.	TDS	Cond
MGP5-Sim-1	5.3	22.8	73.9	286.0	573.0	5.4	22.6	70.9	288.0	574.0
MGP5-Sim-2	5.4	22.9	73.1	295.0	590.0	5.4	22.9	71.8	296.0	591.0
MGP5-Sim-3	5.3	23.0	74.8	287.0	572.0	5.4	23.0	72.9	287.0	573.0

## VITA

Gizem Gul Topal

Candidate for the Degree of

Master of Science

Thesis: A STUDY ON THE USE OF GEOPOLYMER COMPOSITES FOR NITROGEN AND PHOSPHORUS REMOVAL FROM POULTRY LITTER

Major Field: Material Science and Engineering

### Biographical:

#### Education:

Completed the requirements for the Master of Science in Materials Science and Engineering at Oklahoma State University, Stillwater, Oklahoma in December, 2020.

Completed the requirements for the Bachelor of Science in Environmental Engineering at Middle East Technical University, Ankara, Turkey in 2014

#### Experience:

Graduate Teaching Assistant, Oklahoma State University, Stillwater/Tulsa, Oklahoma (2018-2020)

Graduate Research Assistant, Oklahoma State University, Tulsa, Oklahoma (2019-2020)

Water Engineer, ALTER International Engineering and Consultancy, Ankara, Turkey (2015-2018)

#### Professional Memberships:

Member, Materials Research Society

Member, American Ceramic Society